



GEO-3900

MASTER'S THESIS IN GEOLOGY

**DEVELOPMENT OF THE LATE PALEOZOIC, MESOZOIC AND CENOZOIC
SEDIMENTARY SUCCESSION IN SW BARENTS SEA AND THEIR ROLE IN
FLUID LEAKAGE PROCESS**

SYED YASIR HASSAN

JUNE, 2012

FACULTY OF SCIENCE AND TECHNOLOGY

Department of Geology

University of Tromsø

GEO-3900
MASTER'S THESIS IN GEOLOGY

DEVELOPMENT OF THE LATE PALEOZOIC, MESOZOIC AND CENOZOIC
SEDIMENTARY SUCCESSION IN SW BARENTS SEA AND THEIR ROLE IN
FLUID LEAKAGE PROCESS

SYED YASIR HASSAN
JUNE, 2012

Abstract

2D seismic and well data have been used to understand the geological evolution of the SW Barents Sea by interpreting different seismic units and to evaluate their role in distribution of fluid migration system. Eight seismic unit including seafloor are identified in the study area based on well tie with seismic data. Torsk and Kolmule formation show western progradational pattern suggesting deposition during relative sea level fall. Stappen High and Loppa High appear to act as main sediment source area in western margin of SW Barents Sea. The distributions of fluid flow features are significantly higher in western part than in the eastern part of study area. The distribution of fluid flow show direct relationship with structural elements of SW Barents Sea although net erosion might have had added effect on fluid migration process. The late Jurassic Hekkingen formation, are considered as the widespread source rock in western Barents Sea. In addition to this, lower Cretaceous unit and Snadd formation are potential source rock in the study area. Among the various observed fluid flow features were gas chimneys, leakage along faults and high amplitude anomalies. Gas chimneys were most abundant fluid flow features in the study area. The location of chimney structures are associated with major fault complexes in the study area suggesting close relation between the fault and fractures. The inferred gas leakages are closely related to the Cenozoic evolution of the Barents Sea, and are possible caused by gas expansion due to removal of overburden of sediments from the Barents Sea.

Preface

This master thesis completes a two year master program in Petroleum Geology and Petroleum Geophysics at the Institute of Geologi, University of Tromsø. The master thesis have been supervised by Associate Professor Dr.Stefan Buenz.

Acknowledgements

I would like to express my special gratitude to Associate Professor Dr.Stefan Buenz for his guidance, constructive comments, encouragement and interesting discussions during the period of writing this thesis. I would like the entire member of Geophysics Group and especially thanks to my co-supervisor Professor Dr.Jürgen Mienert who also helped me a lot during Geophysics Group meetings. I also need to thanks Alexandros Tasianas and Sunil Vadakkepuliambatta for their technical support.

I would like to thanks all students who I had the pleasure to meet during the course of two years especially to all my friends here in Tromsø. I would also like to thanks my working boss Olav for his kind support in my difficult time during my thesis work.

Last but the least, I would to thanks my family and my close friends back home for their encouragement and financial support during these years in Tromsø.

Contents

1 Introduction	1
1.1 Objectives	1
1.2 Geological Framework of Barents Sea	2
1.2.1 Regional Geological evolution of Barents Sea	2
1.2.2 Geological setting	6
1.3 Structural Geology of the Barents Sea	10
1.4 Hydrocarbon fluid flow	16
1.5 General stratigraphy of Western Barents Sea	27
1.6 Source rock of SW Barents Sea	35
1.7 Reservoir rock of SW Barents Sea	37
2. Data and Methods	38
2.1 Data	38
2.2 2D seismic lines and 3D seismic cubes	38
2.3 Well data	41
2.4 Methods	46
2.5 Seismic interpretation	52
3. Results	57
3.1 Interpreting seismic horizons	57
3.1.1 Sea floor	58
3.1.2 Torsk formation	61
3.1.3 Kolmule formation	64
3.1.4 Hekkingen formation	67
3.1.5 Snadd formation	69
3.1.6 Ørn formation	72
3.1.7 Bottom Tertiary unit	74
3.1.8 Bottom Cretaceous unit	76
3.2 Fluid leakage features	77

3.2.1 Gas chimneys	78
3.2.2 Fault related fluid leakage	85
3.2.3 Small pipe like structures	94
3.3.4 Salt diapirs structures	95
3.3.5 Distribution of fluid flow features	96
4 Discussion	98
4.1 Stratigraphic development	98
4.2 Distribution of fluid flow features	106
4.3 Upper termination of fluid flow features	108
4.4 Source of fluid flow	110
4.5 Mechanism and geological process leading to the formation of fluid flow feature	111
5 Conclusion	118
6 Reference	120

1. Introduction:

Objective:

The objective of this master thesis is to contribute to a better understanding of the stratigraphic development of the late Paleozoic, Mesozoic and Cenozoic sedimentary succession in the SW Barents Sea and their underlying geological processes and mechanisms. The large stratigraphic framework chosen herein does allow for a general overview of geologic evolution and its impact on fluid flow. It is not within the scope of the thesis to study every stratigraphic formation and fluid flow feature in detail. The study is based on two dimensional (2D) seismic data and a total of 64 wells have been integrated in the study for better understanding of lithostratigraphy, physical properties and depositional environmental of the subsurface environment.

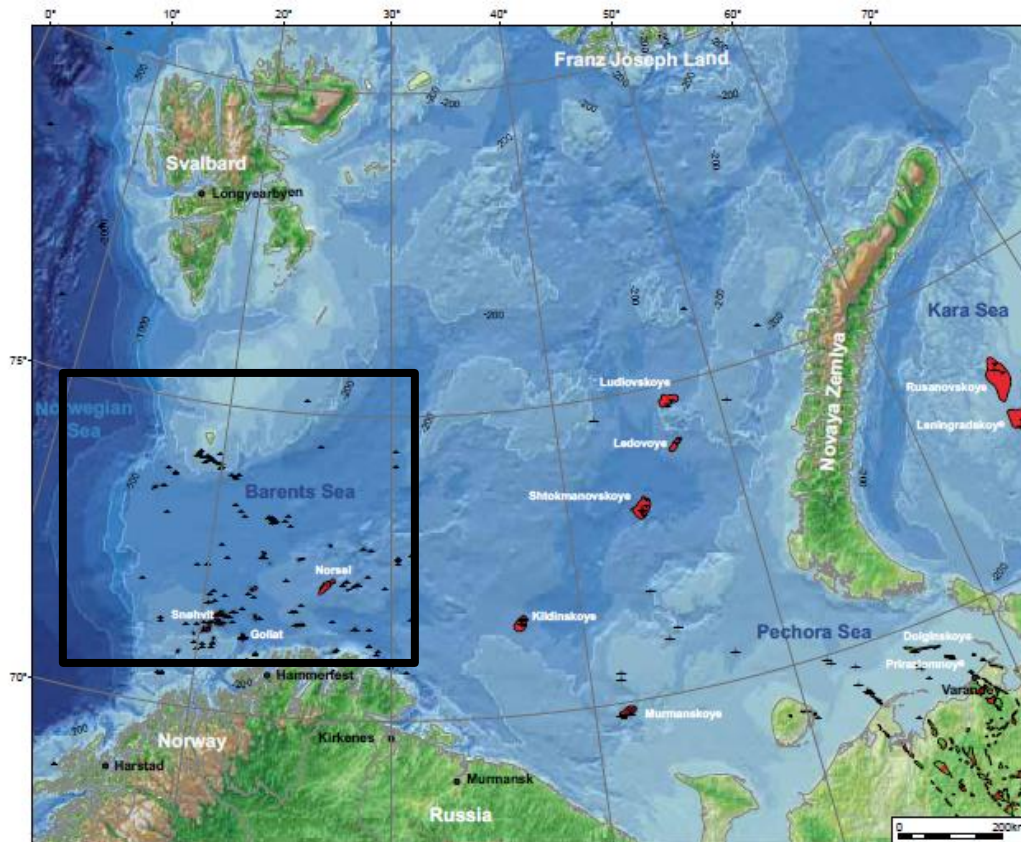


Fig1: Bathymetric map of the Barents Sea with black square indicating location of study area (modified from Henriksen et al., 2011b)

1.2 Geological Framework of Barents Sea:

1.2.1 Regional Geological evolution of Barents Sea:

The main tectonic phases setting the Geological framework of the Barents Shelf are the Timanian, Caledonides and Ural Orogenies, Proto-Atlantic rifting in the west, the opening of the Euramerican basin in the north and the subsequent breakup and opening of the Northern North Atlantic Ocean along the western margin of the Barents Shelf. (Smelror et al., 2009)

The Barents Shelf comprises a wide range of deep sedimentary basins that formed in response to different geological processes during a complex geological history. In some places the sedimentary succession exceeds 15 km in thickness. The eastern Barents Sea is underlain by a wide and deep sedimentary basin that extends for more than 1000 km in a north-south direction. (Faleide et al., 1993a,b; Gudlaugsson et al., 1998)

The post-coledonian geological history of western Barents Sea has undergone three major rift phases from late Devonian-Carboniferous, middle Jurassic-early Cretaceous and early Tertiary (Faleide et al. 1993, 2008). The Barents Sea continental shelf is dominated by ENE-WSE to NE-SW and NNE-SSW to NNW-SSE structural trends. The eastern part of the Barents Sea has been relatively stable since late Carboniferous, while the western part of the Barents Sea has been tectonically active from Late Paleozoic (Gabrielsen et al., 1990).

Most of the part of Barents Sea has affected by crustal extension during late Paleozoic time characterized by westward migration of the rifting, formation of well-defined rift and pull-apart basin in the southwest and development of strike-slip faults in the north. The Atlantic and Arctic regions are linked by transcurrent-transform zone separating the Barents Sea and Greenland shelves during late Mesozoic and Cenozoic times. (Faleide et al., 1984)

A series of sedimentary basin from the Rockall Trough and northward (Faeroe-Møre-Vøring basins) formed as a result of subsidence due to Jurassic-Cretaceous rifting. The SW Barents Sea was located in a region of rift shear interaction having affinities to both the North Atlantic and Arctic region. (Faleide et al., 1984)

During late Paleozoic times, 300 km wide rift zone, extending at least 600km in a north-easterly direction was formed. The rift zone was a direct continuation of north east Atlantic rift between Greenland and Norway. The rift zone had a fan shaped array of rift basin and intrabasinal high with orientation ranging from north easterly in the main rift zone to northerly at the present western continental margin. From the beginning of late Carboniferous the tectonic development was dominated by regional subsidence. This development was interrupted by a Permian to early Triassic rifting phase and the formation of North trending structures in the western part of the rift zone. The late Devonian-middle Carboniferous rift phase results in the formation of several interconnected extensional basin filled with syn-rift deposits and separated by fault-bounded highs. SW Barents Sea is dominated by structural trends striking from north-east to north (Gudlaugsson et al., 1998). Since middle Jurassic time SW Barents Sea comprises of two main stages including late Mesozoic rifting and basin formation and early Tertiary rifting and opening of the Norwegian-Greenland Sea. (Faleide et al., 1993a,b)

The SW Barents Sea province developed within the De Geer Zone having affinities to both the North Atlantic and Arctic regions initially as an area of oblique extension linking the Arctic and North Atlantic rift system (middle Jurassic-early Cretaceous), then in a continental mega shear setting (late Cretaceous-Paleocene) and finally a combined sheared-rifted margin setting during opening of Norwegian-Greenland Sea (Eocene-Present) (Faleide et al., 1984)

The western part of the Barents Sea has been the tectonically most active sector throughout Mesozoic and Cenozoic times whereas eastern and northeastern parts have relatively stable platform with less pronounced tectonic activity. (Smelror et al., 2009)

Various structural elements can be recognized in Barents Sea on the basis of sedimentary fill, tectonic style and crustal structure includes; Lofoten Basin formed during the Cenozoic opening of Norwegian-Greenland Sea and the Vestbakken Volcanic province. Various Cretaceous and Early Tertiary basin (Harstad,Tromsø, Bjørnøya and Sørvestsnaget Basin) separated by Intrabasinal Highs (Senja Ridge, Veslemøy High and Stappen High) and Mesozoic basin including Hammerfest Basin, Loppa High, Fingerdjupet subbasin.(Faleide et al., (1993; 2008)

The western Barents Sea sediments is underlain by late Silurian to early Devonian metamorphic basement (Faleide et al., 1984, Smelror et al., 2009). The basement was formed when the Laurentian and Baltican plates collided and sutured into the Laurasian plate. The collision led to the Caledonian Orogeny (Smelror et al., 2009). Caledonian structures visible onshore have a north-eastern trend in northern Norway and a north-western trend in Svalbard. (Ritsmen and Faleidi., 2007; Faleide et al., 1984)

Following the mountain creating processes in late Silurian to early Devonian is a time of exhumation and extensive erosion of hinterland in middle Devonian to early Carboniferous. Gradually the Caledonian Orogeny was eroded and the western Barents Sea was peneplaned in Frasnian times. This led to accumulation of Old Red Sandstones in western Barents Sea basins (Smelror et al., 2009).

In late Devonian, the Caledonian compressional regime changed into left lateral shear regime accompanied by large scale strike slip movement leads to folded and graben structures. Rift basin may have been formed along the axis from the Tromsø to the Nordkapp basin. During late Devonian-early Carboniferous there is a change in stress regime and the area went from compressional tectonics to extensional tectonics. Rift basins is formed on the continental shelf and filled up with continental clastics, carbonates and evaporites (Faleide et al., 1984). Late Devonian-middle Carboniferous rift phase resulted in several interconnected rift basins filled with syn-rift deposits (Faleide et al., 1984). Stemmerik (2000) stated that sedimentation in this period is characterized by non-marine deposits in narrow, isolated halfgrabens. This is documented in East Greenland, Spitsbergen and Bjørnøya (Stemmerik, 2000).

The oldest extensional event that can be mapped out in the western Barents Sea occurred in late Devonian-early Carboniferous and was due to the initial rifting between Norway and Greenland. This event establishes the fundamental basement architecture of half grabens and inter-basinal highs, which controls the younger basins later deposited. The basins are a result from the combined effects of sinistral strike-slip faulting in the western Barents Sea and a conjugate dextral strike-slip fault in the central Barents Sea (Dengo and Røssland, 1992). Tromsø, Bjørnøya, Nordkapp, Fingerdjupet, Maud and Ottar are basins formed at this time in addition Hammerfest Basin may also have been initiated at this time (Gudlaugsson et al., 1998). The Barents Sea and Svalbard undergone further rifting during

the carboniferous resulting in fan-shaped array of half-graben and highs that are influenced by zones of weakness in the basement.(Henriksen et al., 2011b)

In regional view crustal extension ceased in late Carboniferous and a period of basin subsidence and calm tectonic environment followed through to mid Jurassic (Dengo and Røssland 1992, Gudlaugsson et al., 1998).The Carboniferous rifting was replaced by a quiet tectonic period in most of the Barents Sea in middle Carboniferous. Regional subsidence and accumulation of sediments accumulated in a regional sag-basin (Gudlaugsson et al., 1998). A widespread carbonate shelf covering the areas from Sverdrup Basin to the Pechora Basin was established. Carbonates of various facies, evaporites and some clastics were deposited in layers of relatively even thickness (Faleide et al., 1984). From late Permian through early Triassic the Ural mountain chain in east supplied the western Barents Sea with clastic sediments (Dengo and Røssland, 1992).The region apparently passed from the humid tropical zone in the early Carboniferous through the northern arid zone in the mid- Carboniferous to early Permian, before entering more temperate conditions in the mid- Permian (Steel & Worsley, 1984; Worsley et al.,1986; Stemmerik & Worsley 1989).Triassic in general was a quiet tectonic period, characterized by regional subsidence leading to onlap on the local highs (Faleide et al., 1984). The calm tectonic environment followed through to mid Jurassic (Dengo and Røssland 1992, Gudlaugsson et al., 1998), interrupted only by renewed rifting in Permian-Triassic in the N-S striking structural elements of the Western Barents Sea (Gudlaugsson et al., 1998).

Late Permian-early Triassic tectonic movements led to normal faulting, uplift, tilting and erosion. East-west crossing seismic profiles show clear evidence of syn-tectonic sedimentation. Late Permian-early Triassic fault movements can be tracked in north-south trending structures of the Western Barents Sea, evidence of fault movement is found along the western Loppa High and as far north as the Fingerdjupet basin (Gudlaugsson et al., 1998).From Carboniferous to Permian times Loppa High experienced a total of eight identified tectonic events, two of these might be Triassic in age (Johansen et al., 1994).

Mid-late Jurassic to early Cretaceous renewed crustal extension occurred from Loppa High and westward. Deformation created a series of pull-apart basins, and tilted fault blocks. The north eastern structural trends inherited from late Devonian-early Carboniferous deformation is still current, and controls the tectonic patterns across the western Barents

Sea (Dengo and Røssland 1992). A number of highs became positive features in this period as a result of faulting and differential subsidence (Faleide et al., 1993a,b).

Middle to late Jurassic rifting splits the Barents Sea through the Hammerfest and Bjørnøya Basins, and decouples the northeastern Barents Sea from the western margin (Smelror et al., 2009). The rifting event leads to block faulting and deposition of late Jurassic shales between the faulted blocks. At the transition from late Jurassic to early Cretaceous major rifting probably led to a lowstand in sea-level, this resulted in a major erosional surface visible in the entire North Atlantic, known as the Base Cretaceous unconformity. During early Cretaceous Bjørnøya, Tromsø and Harstad Basins become deep basins and main depocenters in the western Barents Sea (Faleide et al., 1993a,b). In middle Cretaceous times the northeastern part of the Barents Sea was uplifted and eroded. This resulted in large amounts of sediments being transported into the rapidly subsiding basins along the western margin. The uplift possibly coincides with the increased volcanic activity on Franz Josef Land, Kong Karls Land and adjacent offshore areas (Smelror et al., 2009).

Successive rifting throughout Cretaceous further enhanced the deep basins; Tromsø, Harstad and Bjørnøya on the western margin of the Barents Sea. The rifting developed into a dextral stress field along the Senja-Hornsund lineament during Paleogene. This led to the formation of pull-apart basins in the westernmost part of the Barents Sea (e.g. Sørvestsnaget Basin and Vestbakken Volcanic Province) (Smelror et al., 2009).

During Paleogene sea-floor spreading started and the final continental breakup of the North Atlantic was a fact. The Norwegian-Greenland Sea was set around the transition from Paleocene to Eocene, 55 Ma years ago (Faleide et al., 2008, Smelror et al., 2009).

Regional uplift and erosion of the Barents Sea shelf was initiated some time during the Oligocene-Miocene time interval, prior to the Plio-Pleistocene Northern Hemisphere glaciation (Faleide et al., 1996, Dimakis et al., 1998).

1.2.2 Geological Setting:

The Barents Sea, an epicontinental sea covers the north western corner of the Eurasian continental shelf bounded by young passive margin to the west and north that developed as a result of Cenozoic opening of the Norwegian-Greenland Sea and the Eurasia Basin,

respectively. It is bordered by Svalbard archipelago to the northwest, Franz Josef Land to the northeast, Novaya Zemlya to the east (fig 1.2; fig 1.4). This defines an area of about 1.3 million km² with an average water depth of about 300m (Breivik et al., 1995; Faleide et al., 1984). The continental shelf of the Barents Sea reaches about 1000 km both in north-south and east-west direction and exhibits a more or less continuous sedimentary succession from the Carboniferous to Quaternary; many structural elements reflect Jurassic and later tectonics: not least a Tertiary phase of differential uplift had a profound effect on the final sculpting of the province (Faleide et al., 1993a,b; Gudlaugsson et al., 1998; Nylandet al., 1992). In a Barents Sea region, the top basement usually lies deeper than 10 km but there is large difference that can be observed between eastern and western part of Barents Sea. In the western part of Barents Sea, the top basement has a depth of 14km with series of narrow basin whereas the top basement of the eastern part of the Barents Sea has a depth of upto 20 km reflecting the presence of two, broad mega scale basin. (Smelror et al., 2009).

The Barents Shelf has two major and highly disparate provinces monoclinial in structure trending north-south separating the eastern from western region of Barents Sea. The eastern province of the Barents Shelf are characterized by the complex tectonic histories of Novaya Zemlya and the Timian-Pechora Basin and by the Uralian Orogeny whereas the western province was mostly controlled by major, post Caledonian rifting phases as well as by later rifting episodes related to continental breakup along the northwestern margin of the Eurasian plate. (Smelror et al., 2009).

Both the North and South Barents Sea formed in the fore deep zone to the Novaya Zemlya tectonic belt. (Smelror et al., 2009).

The western part of Barents Sea can further be subdivided into three geological province separated by major fault zone including 1) the Svalbard platform is covered by a relatively flat lying succession of upper Paleozoic and Mesozoic, mainly Triassic, sediment, 2) Basin province between the Svalbard Platform and the Norwegian coast characterized by a number of subbasin and highs with an increasingly accentuated structural relief westward. The basin consists of Jurassic –Cretaceous sediment and Paleocene-Eocene sediments in the west, 3) The continental margin consists of three main segments (a) a southern sheared margin along the Senja Fracture zone, (b) a central rifted complex southwest of Bjørnøya associated with volcanism and (c) a northern, initially sheared and later rifted margin along

the Hornsund Fault Zone. The continent-ocean transition occurs over a narrow zone along the line of Early Tertiary breakup and the margin is covered by a thick upper Cenozoic sedimentary wedge. (Faleide et al., 1993a,b)

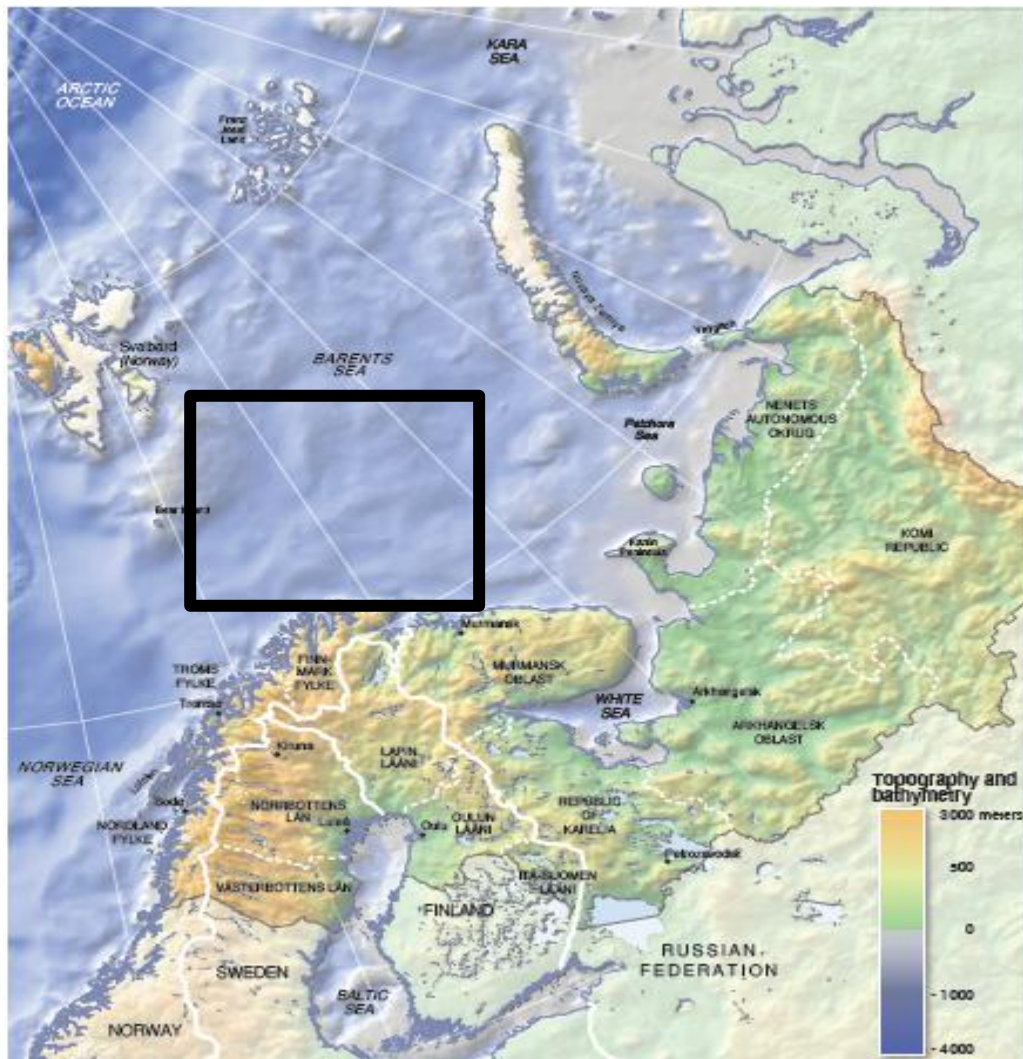


Fig1-2: showing the bathymetric and topographic map of the Barents Sea and square box shows the location of study area. (Ref : Hugo Ahlenius, UNEP/GRID-Arendal)

At least five phases of basin development recognized widely throughout the Barents Sea including 1) Late Devonian- middle Carboniferous rifting, 2) Late Carboniferous- Permian carbonate platform development, 3) Triassic- Cretaceous siliciclastic shelf development, 4) Early Cenozoic crustal break-up and 5) Late Cenozoic passive margin development. (Faleide et al., 1984)

The Barents Sea comprises of numerous basins and structural highs. Regionally structures are dominated by major basin west of Novaya Zemla including Pechora Basin and the North and South Barents Basin. Towards the eastern direction the Southern Barents basin forms a depocenter for Paleozoic and Mesozoic strata between Novaya Zemlya and Central Barents Arch. Following the western direction, the platform areas shows thick Paleozoic-early Cretaceous strata disassembled by several small basins and structural highs between the Central Barents Arch and the faulted, deeply subsided western (Atlantic) margin. (Henriksen et al., 2011b)

Nordkapp Basin is characterized by its deeply spaced Paleozoic salt structures whereas Bjørnøya Basin and others are recognized by its thick Cretaceous strata. (Henriksen et al., 2011b)

In the western Barents Sea, the Caledonian Orogeny causes the closure of Lapetus Ocean, which separated the Eurasia from Laurentia. Deformation begun during the middle Ordovician reached to its climax at Silurian. The trend of the Caledonides (Barents Sea Caledonides) follows the general northeast axis of the Scandinavian-Greenland Caledonides covering the most of the SW Barents Sea and continued towards the northeast. The separated northerly oriented Svalbard Caledonides, underlies the north-western Barents Sea had undergone a final late Devonian compressive phase. Later on late Paleozoic crustal extension led to the development of half grabben structures and regional sag basins. During Devonian and Carboniferous time, the uplifting phenomenon occurs to the east induced by the onset of Uralide Orogeny and as a result of the Permian plate collision led to the a pronounced change in basin physiography during late Paleozoic to early Triassic time. Post Permian subsidence was primarily focused on the basins flanking Novaya Zemlya and in Nordkapp Basin locally. (Henriksen et al., 2011b)

Through Geological time, the focus of extensional tectonic has shifted westward towards the Atlantic rift system and as a result of that middle to late Jurassic rifting is prominent in the Hammerfest Basin and along the western margin. Cretaceous basins are prominent in basin lies within western margin whereas Cenozoic subsidence is dominated further to the west in Sørvestsnaget Basin and Vestbakken Volcanic Province. (Henriksen et al., 2011b)

Barents Sea region have been subjected to different magnitude of uplift and erosion that has affected the petroleum system including reservoir quality, source rock maturity/ migration

and reservoir pressure. Net erosion values vary from 0 to more than 3000m. Svalbard, Novaya Zemlya and the Norwegian mainland have been much affected by uplift and net erosion. Certain areas on Spitsbergen may have been buried more than 3000m deeper than present. The deeper basins are less eroded. The southern Barents Basin may have undergone less than 500m of net erosion whereas in the Norwegian sector, the net erosion values in sedimentary basins ranges from 900- 1400m. Late Neogene isostatic uplift affected the whole Barents Sea region. Different areas in the Barents Sea achieved maximum burial at different times. Higher areas affected by Paleogene uplift and erosion might not have seen deeper burial after the Paleogene tectonics, while in basin areas continuous sedimentation may have occurred until glacial erosion in Plio-Pleistocene times. (Henriksen et al., 2011b)

1.3 Structural Geology of Barents Sea:

The Barents Sea region has an intracratonic setting that has been affected by several phases of tectonism since the Caledonian Orogeny in early Devonian time. The Barents Sea continental shelf is dominated by ENE-WSW to NE-SW and NNE-SSW to NNW structural trend. Southern part of the Barents Sea dominated by ENE-WSW trend is defined by the major fault complexes bordering the Hammerfest and Nordkapp Basin. This trend is subparallel to another major zone to the north by Veslemøy High and fault complexes separating the Loppa High from the Bjørnøya Basin. (Faleide et al., 1993a,b; NPD 6)

The western part of the Barents Sea and Svalbard continental margin consists of three main structural segments including 1) southern sheared margin along the Senja Fracture zone ($70^{\circ} - 72^{\circ} 30' N$), 2) a central rift complex associated with volcanism ($72^{\circ} 30' - 75^{\circ} N$), and 3) a northern initially sheared and later rifted margin along the Homsund fault zone ($75 - 80^{\circ} N$). (NPD 6)

There are several fault complex of Jurassic-Cretaceous in age that creates the boundary of deep sedimentary basin including are Troms-Finnmark Fault Complex south of $71^{\circ} N$, the Ringvassøy-Loppa Fault Complex, Bjørnøyrenna Fault Complex and Leirdjupet Fault Complex. (Faleide et al., 1993a, b)

The SW Barents Sea may be divided into three main geological province separated by major fault zone including 1) The Oceanic Lofoten basin and Vestbakken volcanic province in the west, 2) the SW Barents Sea basin province of deep cretaceous and early Tertiary basin (Harstad, Tromsø, Bjørnøya and Sørvestsnaget Basins) and 3) Mesozoic basins and highs further east between 20 and 25°E that have not experienced the Cretaceous-Tertiary subsidence (Finnmark Platform, Hammerfest Basin, Loppa High, Fingerdjupet subbasin). (Faleide et al., 1993a, b).

The basin of the SW Barents Sea developed in time from oldest in east to youngest in west (fig1.3).In east, three main basin of late Paleozoic in age are present (Nordkapp Basin, Ottar Basin and Svalis Dome) (Faleide et al., 1998).The central part of the SW Barents Sea hold three structure of interest of late Jurassic age. The Hammerfest Basin is classified as a late Jurassic Basin. In north, Hammerfest Basin bounds the Loppa High by the Asterias Fault Complex and has evidence of syn-tectonic sedimentation of pre-Permian age towards these faults (Faleide et al., 1998).The Loppa High is a result of late Jurassic to early Cretaceous and late Cretaceous-Tertiary tectonism (Gabrielsen et al., 1990). The Fingerdjupet Subbasin is situated north of Loppa High. Late Jurassic tectonism generated the dominate fault trend, although it was formed in early Cretaceous as a shallower part of the Bjørnøya basin (Gabrielsen et al. 1990).

Further west two basins of late Jurassic-early Cretaceous age is located .The Tromsø Basin evolved mainly due to extension in this time period, but contains salt diapirs from salt deposition in late Paleozoic times The Bjørnøya Basin is located north of the Tromsø Basin. The two basins merged post late Paleozoic times and separated in late Cretaceous by the Bjørnøyrenna Fault Complex. Most sediments in the Bjørnøya Basin is of early Cretaceous age(Faleide et al. 1993a,b).In west, Sørvestsnaget Basin holds very thick succession of Cretaceous and Tertiary sediments which is limited by Vestbakken Volcanic province in the north (Gabrielsen et al., 1990)

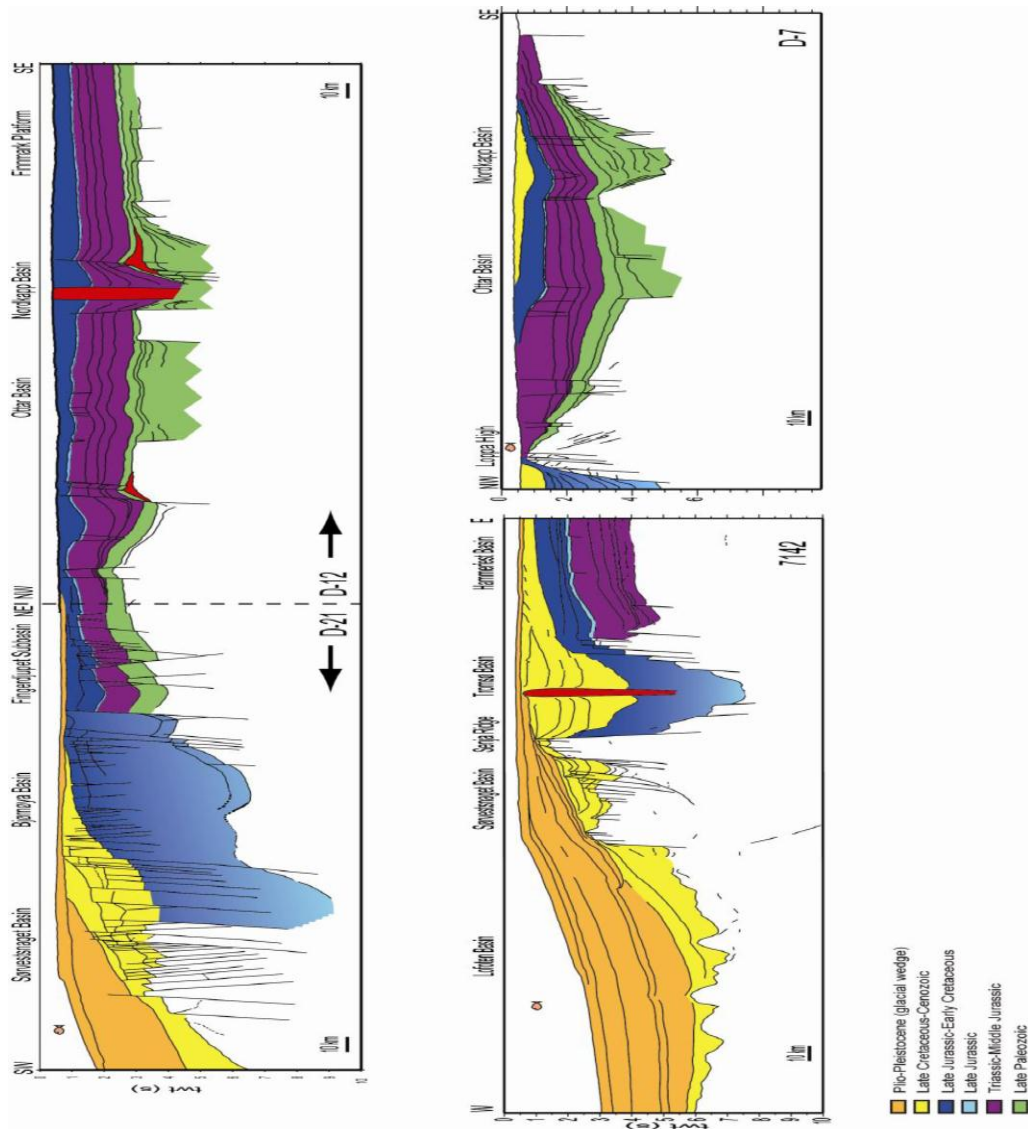


Fig1-3: showing regional profile across the SW Barents Sea (Faleide et al., 2009)

1.3.1 Major Structural Elements of South Western Barents Sea:

The major structural elements of SW Barents Sea are as follows: (fig 1.4)

1.3.1.1 Hammerfest Basin:

The Hammerfest Basin is relatively shallow and has a ENE-WSW structural trend and is situated between 70°50'N, 20°E, 71°15'N, 20° E, 72°15'N, 23°15'E and 71°40'N, 24°10'E. It is separated from the Finnmark Platform to the south by the Troms-Finnmark Fault complex and from the Loppa High to the north by the Asterias Fault complex. The

Hammerfest Basin is subdivided into a western and eastern subbasin by the extension of the Trollfjord-Komagelv fault trend. It is characterized by a gentle central dome paralleling the basin axis and has an internal fault system trending E-W, ENE-WSW and WNW-ESE. The Hammerfest Basin has been interpreted as a failed rift in triple junction and as a remnant of an older rift system. (NPD 6)

1.3.1.2 Finnmark Platform:

Finnmark Platform is bounded to the south by coledonides of the Norwegian Mainland. Its western and northwestern boundaries are defined by the Troms-Finnmark Fault Complex and the Norkapp Basin. The Platform is underlain by Paleozoic and Precambrian rocks that has been affected by Coledonian Orogeny. (NPD 6)

1.3.1.3 Harstad Basin:

The Harstad Basin located north of Anøya, between 69°20' and 71°N and 16°30' and 17°45'E, close to the Shelf edge and having NNE-SSW striking trend. Its eastern boundary is defined by the southernmost part of the Troms-Finnmark Fault Complex whereas the western limit coincides with the transition to oceanic crust. (NPD 6)

1.3.1.4 Loppa High:

The Loppa High is situated north of the Hammerfest Basin and southeast of the Bjørnøya Basin, between 71°50'N, 20°E and 71°55'N, 22°40'E, and 72°55'N, 24°10'E and 73°20'N, 23°E. Loppa High is bounded on the south by the Asterias Fault Complex, and on the east and southeast by a monocline towards the Hammerfest Basin and the Bjarmeland Platform. It is bounded by Ringvassøy-Loppa and Bjørnøyrenna Fault Complex. A major salt structure, the Svalis Dome and its associated rim syncline, the Maud Basin marks the north-eastern limit of High. (NPD 6)

1.3.1.5 Maud Basin:

The Maud Basin is situated east of the Svalis Dome, between 72°50' and 73°30'N, and 23°15' and 24°30'E. It is interpreted as part of primary rim syncline of the Svalis Dome. (NPD 6)

1.3.1.6 Svalis Dome:

The Svalis Dome is located at the north-eastern margin of the Loppa High, between 73°15'N and 23°20'E. It has a sub circular cross-section in map view with a diameter of

approximately 35 km and appears as a salt pillow and interpreted to be of Late Carboniferous age. (NPD 6)

1.3.1.7 Nordkapp Basin:

The Nordkapp Basin is situated between 71°30'N, 25°E and 73° 30'N, 34°E. It is a deep Paleozoic basin with a general NE-SW trend but central part of the basin has an E-W orientation and is more than 300 km long and 30-80 km in wide. It is associated with gravity low and its central part is deformed by numerous salt structures. (NPD 6)

1.3.1.8 Stappen High:

The Stappen High is situated between 73°30'N and 75°30'N trending N-S. It is bounded to the west by Knølegga Fault, to the south by the Bjørnøya Basin and to the east by the Sørkapp Basin. The southern part of the High is strongly affected by NNE-SSW trending faults. (NPD 6)

1.3.1.9 Sørvestsnaget Basin:

The Sørvestsnaget Basin is situated between 71° and 73° N and between the oceanic crust and 18°E and composed of thick succession of Cretaceous and Tertiary sediments. The Sørvestsnaget Basin represents structural continuation of the Bjornøya Basin and is separated from Bjørnøya Basin by a normal fault system of Tertiary age. The Northern limit of the basin is defined by the lavas of the Vestbakken volcanic province and by the NE-SW trending fault complexes on the southern part of the Stappen High. The basin is bounded by the Senja Ridge and Veslemøy High in the Southeast direction. (NPD 6)

1.3.1.10 Troms-Finnmark Fault Complex:

The Troms-Finnmark Fault Complex is situated between 69°20'N, 16°E and 71°40'N, 23°40'E. It comprises of individual faults trending NNW-SSW, NE-SW and ENE-WSW. It represents major structural division between Finnmark Platform in the south and southeast and the basinal area (Harstad Basin, Tromsø Basin and Hammerfest Basin) to the north and northwest. It is characterized by listric normal faults accompanied by hanging wall roll over anticlines and antithetic faults. (NPD 6)

1.3.1.11 Tromsø Basin:

The Tromsø Basin is situated north of Tromsø Town from 71° to 72°15'N and 17°30' to 19°50'E and is bordered by the Senja Ridge to the west and the Ringvassøy-Loppa Fault complex to the east. To the southeast, it terminates against the Troms-Finnmark Fault

complex. In the north, it is separated from the Bjørnøya Basin by the Veslemøy High. The Tromsø Basin has a NNE-SSW trending axis enhanced by a series of salt diapirs and associated with a system of detached faults. (NPD 6)

1.3.1.12 Veslemøy High:

The Veslemøy High is situated between 72°N, 18°E to 72°30'N, 19°E and extends in a NE-SW direction. The Veslemøy High is bounded by the deep Bjørnøya Basin and the Sørvestsnaget Basin to the north and northwest and the Tromsø to the south. (NPD 6)

1.3.1.13 Bjørnøya Basin:

The Bjørnøya Basin is situated between 72°30' and 74°N and between 18° and 22°E and is divided by the Leirdjupet Fault Complex into deeper westerly and a shallow easterly part (the Fingerdjupet Subbasin). The basin is bounded to the southeast by the Bjørnøyrenna Fault Complex and the northwestern boundary is a faulted slope dipping down from the Stappen High towards the basin. It has a characteristic of half graben. (NPD 6)

1.3.1.14 Bjørnøyrenna Fault Complex:

It is situated between 72°N, 19°E and 73°15'N, 22°E and trending NE-SW direction. It defines the boundary between the Loppa High and the deep Bjørnøya Basin in the southwest and in the northeast it separates the Loppa High from the Shallow Fingerdjupet subbasin. In general the complex is characterized by normal faults with large throws. (NPD 6)

1.3.1.15 Vestbakken Volcanic province:

It is situated south and west of Bjørnøya between 73°30' and 74°30'N and between the oceanic crust and approximately 17°E. (NPD 6)

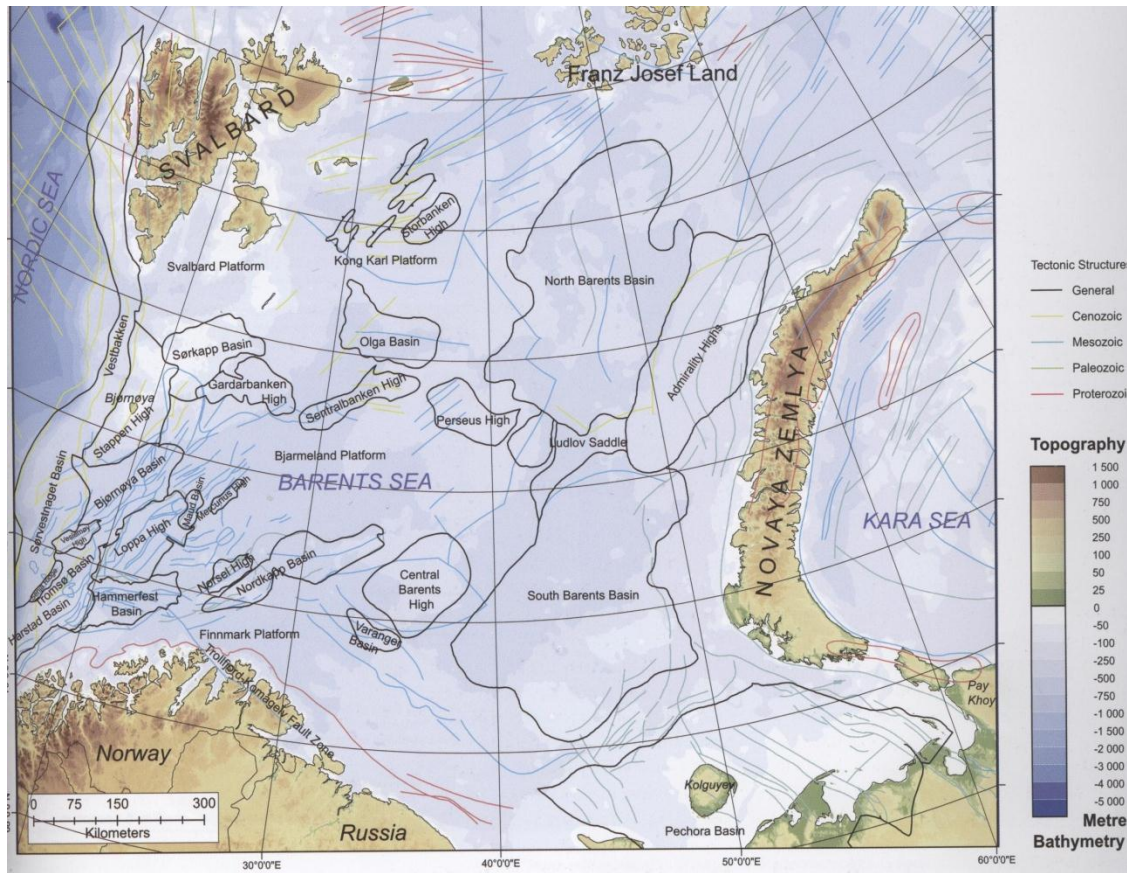


Fig 1-4: Major structural elements of Barents Sea (Smelror et al., 2009)

1.4 Hydrocarbon Fluid Flow:

Subsurface hydrocarbon (HC) migration and accumulation is of great interest to petroleum geologists and engineers for several reasons: (1) Fluids are an inherent part of sediments and rocks. They are generally present in the sediments from their deposition to their very deepest burial depth, though being gradually reduced by compaction processes (Andreassen et al., 2007b), (2) its presence and associated features may point towards deeper prospective reservoir (Heggland, 1998), (3) Shallow gas accumulation may reduce the shear strength of the sediments and pose a hazard to hydrocarbon exploration and development (Andreassen et al., 2007b), (4) Shallow gas accumulation may be of commercial interest in the future (Carstens, 2005). Technological development during recent years led to the discovery of numerous focused fluid flow system and morphological expression of seabed. Mapping of

these fluid flow systems is important for understanding their spatial and temporal resolution.

Hydrocarbon migration is divided into three main categories also illustrated in the (fig 1.5)

Primary Hydrocarbon Migration: is the movement of hydrocarbon from mature organic rich source rock into the adjacent reservoir rock. (Aydin, 2000)

Secondary Hydrocarbon Migration: is the movement of hydrocarbon through the conduits rock into the trap.

Tertiary Hydrocarbon Migration: Involves the leakage, dissipation and alteration of hydrocarbon as it migrated from reservoir rock into the surface. (Gluyas and Swarbrick, 2004)

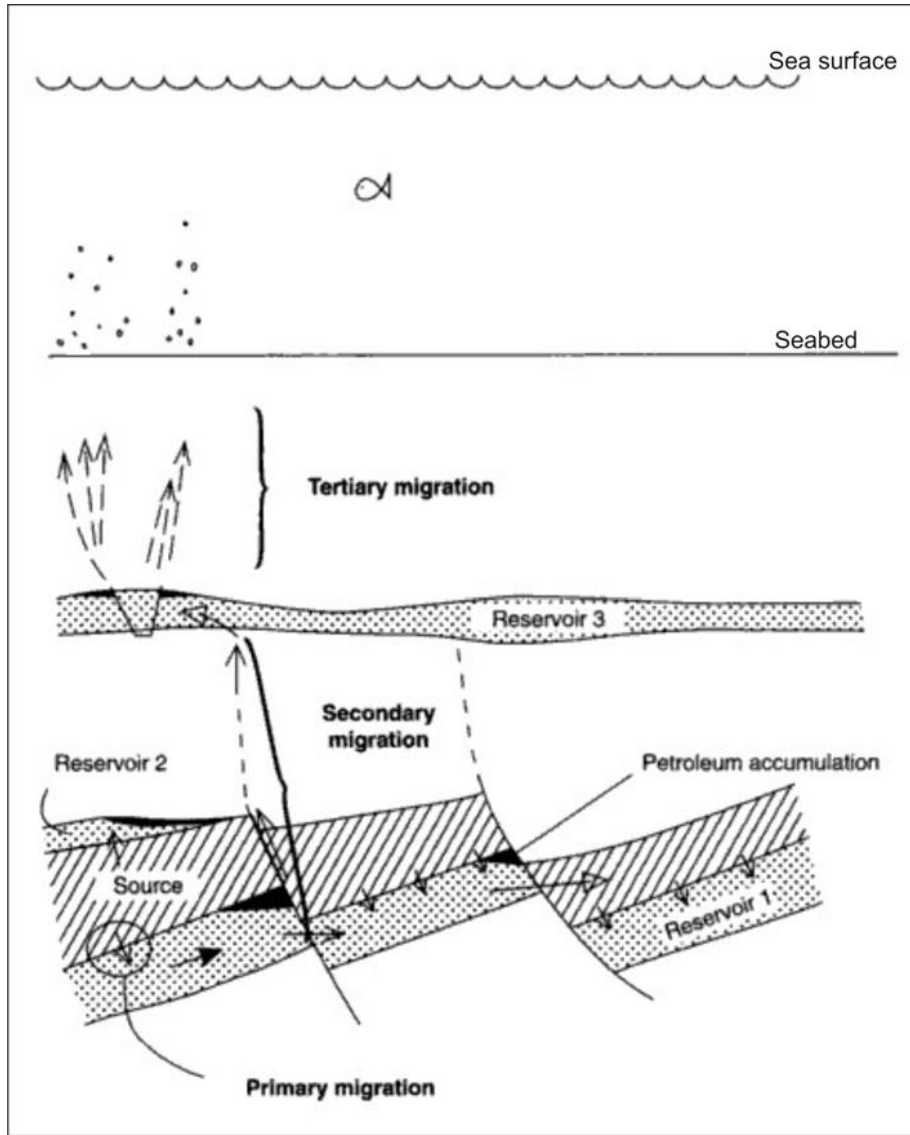


Fig1-5: showing the migration pattern of hydrocarbon. Indicating three stages of migration: primary migration out of the source rock, secondary migration through the carrier bed and into the reservoir and tertiary migration from reservoir into the surface. (Fig modified from Gluyas and Swarbrick (2004)).

Fluid flow is a long-term and complex geological process. It is part of a system where fluid generation, migration, accumulation and seabed seepage all may occur at different times (Selley, 1998). There are several processes involved in formation and migration of Hydrocarbon which are briefly described as:

- a) With increasing temperature the organic matter in source rock produces hydrocarbon and this increase in temperatures results from the overburden of the overlying rock.
- b) Once Hydrocarbon generated in the source rock the gas and liquid plus remaining content of organic matter occupy more space than original organic content of the rock and as a result there is increase in pressure within the rock.
- c) This internal pressure kept on increasing as generation of hydrocarbon imposes pressure on the fluids that occurs in the pore spaces called as pore fluid pressure
- d) Once Hydrocarbon generated then it is migrated to adjacent porous and permeable reservoir rock due to buoyant force as it is less dense than formation water.
- e) However, hydrocarbon migration through a reservoir rock is not enough to form an oil or gas pocket. Unless the hydrocarbon molecules are prevented from rising, they will only pass through the reservoir rock instead of accumulating within it. To form a hydrocarbon reserve, an impermeable rock - called a seal or cap rock - is needed to form a barrier above the reservoir rock. The best cap rocks are the most impermeable, which are clay or layer of crystalline salts.

Hydrocarbon reservoirs are increasingly recognized spatially in terms of pore fluid content, pore fluid saturation, porosity, permeability, lithology and structural geometry of the rocks. (Lumley, 1995). Knowledge of these reservoir rocks parameters is very important in estimating the total volume of hydrocarbon reserves in place. (Lumley, 1995).

Some rocks are well suited to aid migration because of their hydro-mechanical properties, low capillary pressure and high permeability (Abrams, 2005). Fluids either flow predominantly along major stratal surfaces or they cross stratal surfaces via faults, diapirs, or major fracture systems. Fluids can be migrated along strata or across strata but migration across strata requires sufficient pore pressures to overcome capillary entry pressure in lowered capillary pressures zones. (Abrams, 2005)

Fractures and faults play an important role in controlling the hydraulic properties of rock by providing the permeable conduits for fluids (Cartwright et al., 2007; Zhang et al., 2011). And they also plays an intricate role in hydrocarbon migration and accumulation as they serves either as seal or conduits (Zhang et al., 2011).Conversely, the presence of fluids strongly influence deformation and rupture of rock by controlling fluid pressure and geochemical properties within fracture and faults. So the study of orientation and

distribution of fractures and faults and their relation to the current stress field along with their importance to fluid flow is of great interest. (Zhang et al., 2011)

In general fracture-enhanced permeability depends upon fracture density, orientation and the most important hydraulic conductivity of individual faults and fracture (Aydin, 2000). This is specially very critical in hydrocarbon reservoir with low matrix permeability where fractures are the primary pathway for oil and gas migrating from source rock into the reservoir rock therefore it is important to discriminate hydraulically conductive from hydraulically non-conductive fractures and faults in order to increase the efficiency of oil production and reservoir development. Hydrofractures and faults can provide the driving mechanism of primary migration of hydrocarbon fluids-High fluid pressure which is the prominent features of hydrocarbon source rock and shearing leads to development of open fractures and dilatant faults at all depth of interest to hydrocarbon exploration and production. (Aydin. 2000)

Fluid flow is controlled by rock physical properties such as capillary entry pressure, hydraulic conductivity and wettability, and by seal bypass systems (Cartwright et al., 2007). Fractured driven flow is often considered the most common bypass mechanism. (Cartwright et al., 2007)

1.4.1 Fluid Flow dynamics:

The dynamics of fluid flow can be explained by Darcy's law which describes that flow of fluid along a hydrodynamic gradient i.e. from higher to lower pressure. From the Darcy law equation, we can conclude that fluid flow increases with pressure gradient and decreases with increasing viscosity of fluid.

$$Q = K A [\Delta P]/\mu \quad \text{(Darcy law equation)}$$

Q= Fluid flow rate; K= permeability constant; A= cross sectional area;
 ΔP = Pressure gradient; μ = Viscosity of fluid.

Fluid can be present in the sediment either in the form of gaseous or liquidous phase. Within the liquids we can find both oil and water are immiscible, while the natural gases can be dissolved in the liquid or present in gaseous phase. Oil and gas can migrate within rock due to driving mechanism run by a combination of buoyancy and hydrodynamics (Selley, 1998). Since buoyance depends upon density difference between the liquids so the

gaseous phase with less density migrated to the top of the liquid as it is less denser than oil and water (fig 1-6). The migration pathway can be lateral or vertical depends upon relationship with stratigraphy of reservoir rock.

Fluid migration within the reservoir rock can also be governed by hydrodynamic nature of the fluid as hydrodynamic gradient within the reservoir rock works against seepage.

Hydrodynamic is more important for oil and water than for gases

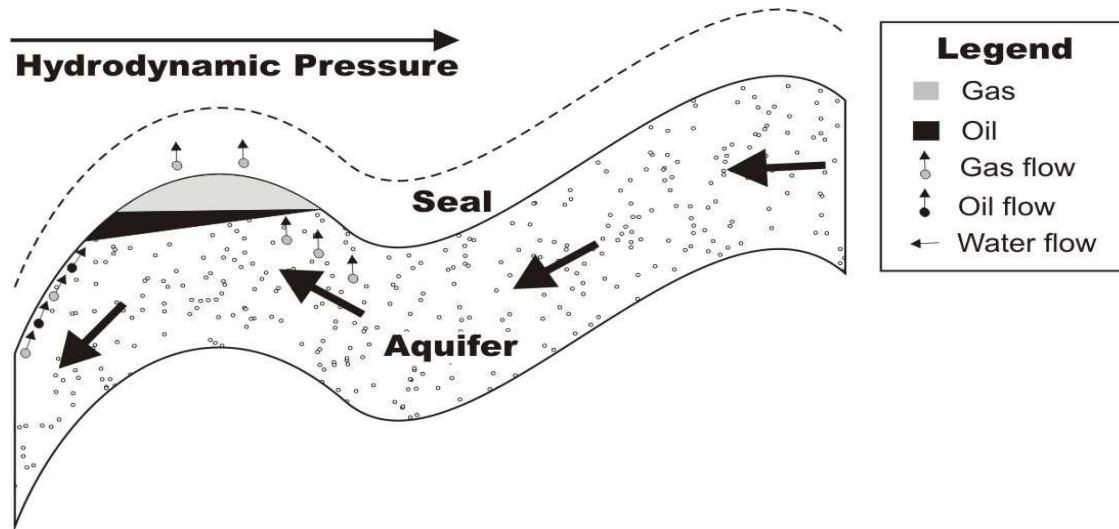


Fig 1-6: Conceptual model of fluid flow dynamics where aquifer movement is controlled by the pressure potential movement, due to which gas and oil moves up dip because of the buoyancy factor. (Perrodon, 1983)

1.4.2 Seismic Indication of Gas and fluid migration:

Seismic method can be used to determine fluid flow pathway and fluid accumulation areas. Fluid flow features are commonly subdivided into two categories: (Løseth et al. 2009)

1. Fluid flow feature that permanently deformed the primary bedding or created new syn-leakage features. (Løseth et al., 2009)
2. Changes in seismic expression caused by change in formation fluid from formation water to oil or gas. (Løseth et al., 2009)

1.4.2.1 Permanent deformation

Fluid flow can cause post depositional deformation of primary layering; mud mobilization and sand injection, permanent alteration of rocks (Løseth et al., 2009). These deformation can either takes place as soft sediment deformation or as brittle deformation. Fluid flow

may also be nutrient as it may contains nutrient fluids which can helps in creation of local algal mats, shell banks and carbonate buildup. (Løseth et al., 2009)

Pockmarks are shallow seabed depression from a few meters to tens of meters deep with the diameters varies from less than 5 meters to several hundreds of meters (fig 1.7).(Løseth et al., 2009). They generally formed in soft, fine grained sediment by the escape of fluid into the water column. On seismic section, it can express as minor depression of the seafloor which may be circular or elliptical in shape. Pockmarks are often characterized by vertical zone of degraded signal beneath or above high amplitude anomalies. (Løseth et al., 2009)

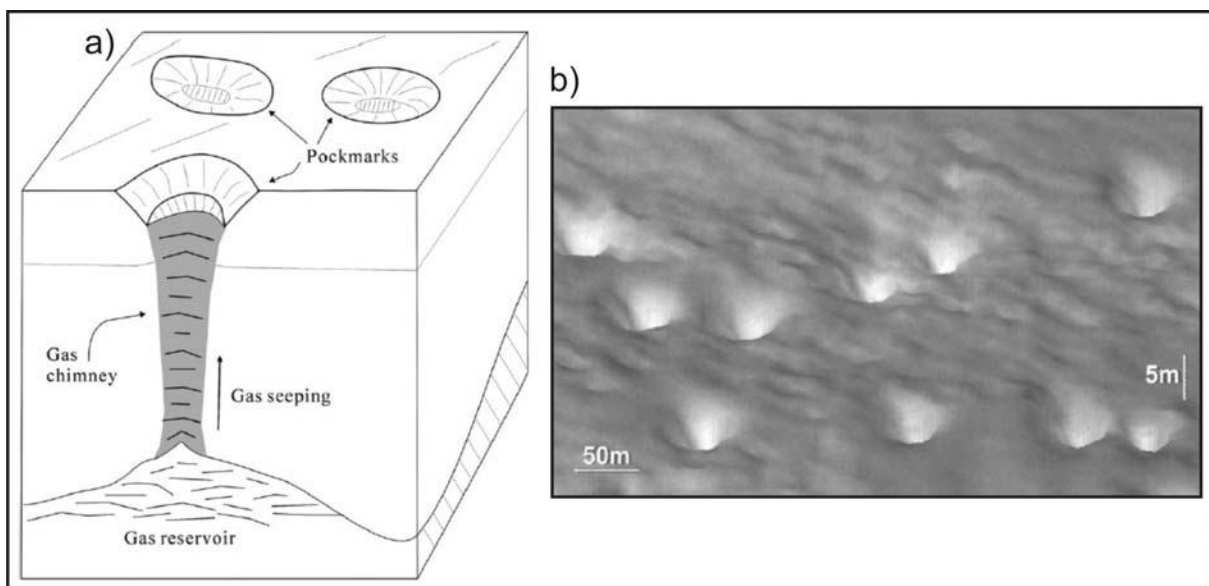


Fig1-7: a) Pockmarks located on top of gas chimneys b) Pockmarks on the seafloor. (Hovland (2003)

1.4.2.2 Acoustic changes due to fluid leakage

Seismic reflection results from the change in acoustic impedance of the rock which is the product of density and compressional wave velocity (P-wave velocity, V_p). It has been observed that the presence of free gas in sediment pore space causes a dramatic reduction in P-wave velocity. The change in P-wave velocity together with density difference can be observed in seismic data in different ways including Bright spots, dim spots, flat spots, phase reversal, acoustic masking, acoustic pipes, and high amplitude anomalies, fault zone, Leakage zone (Andreassen et al., 2007b) are shown in fig (1.8;1.9;1.10)

Bright Spot is the anomalously high amplitude reflection that arises from unlithified and porous sediment indicating presence of gas in the sediment. The reflection normally gives negative reflection coefficient. (Andreassen et al., 2007b)

Dim Spot is an area on a seismic section that lies above hydrocarbon accumulation where the reflections from the stratigraphic layers are visible but weaker than in adjacent areas and where reflection continuity and amplitude are reduced. (Andreassen et al., 2007b)

Flat Spot is the reflection from the base of the gas zone when there is acoustic impedance contrast between the gas and underlying sediments with fluids in the pore spaces and it represents positive reflection coefficient. (Andreassen et al., 2007b)

Phase reversal occurs when a reflection changes laterally from a positive polarity to a negative polarity which gives an indication of hydrocarbon as sediments containing hydrocarbon have a significant lower acoustic impedance. (Andreassen et al., 2007b)

Acoustic Masking refers to an area of the seismic profile with low seismic reflectivity or where seismic reflections are highly distorted or disturbed. (Løseth et al., 2009)

Gas Chimneys are the vertical zones of acoustic masking and are interpreted to represent either tectonically or hydro-fractured low-permeable cap rock shale that contains many irregularly distributed low-velocity gas-charged zones. (Løseth et al., 2009)

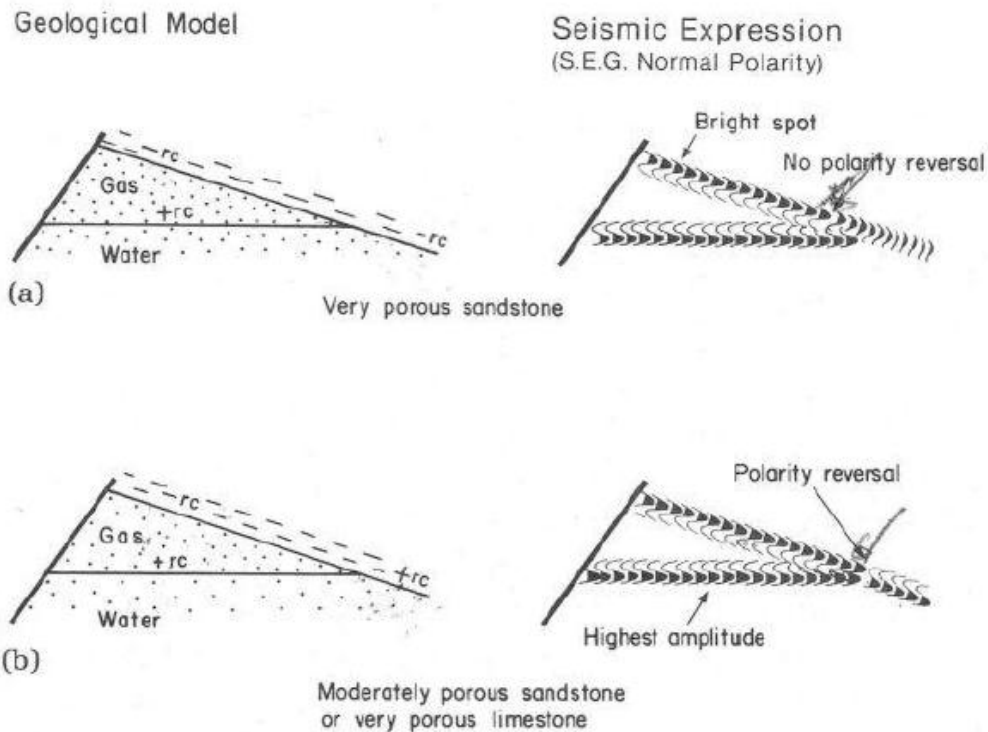


Fig 1-8: illustrating the basic theory behind Bright spot, Phase reversal, flat spot based on polarity convention (Andreassen , 2009)

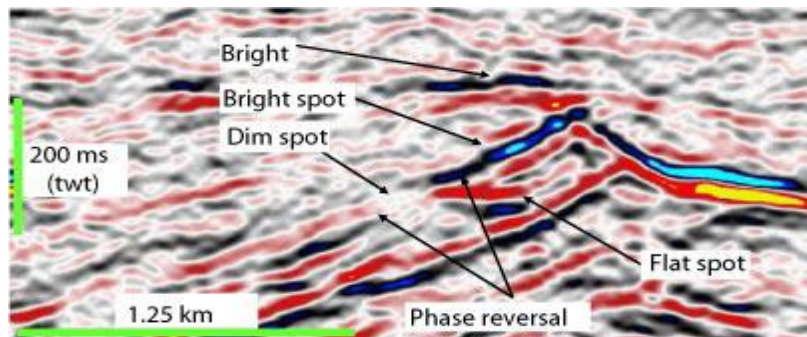


Fig1-9: showing various seismic indication of hydrocarbon such as Bright spot, dim spot, flat spot (Løseth et al., 2009)

Wipeout zone can also be interpreted as gas chimneys but on a smaller scale. (Løseth et al., 2009)

Acoustic pipes are sub-vertical, circular, narrow zones of acoustic masking where the continuity of reflections is disrupted over a long vertical extent representing vertical pathway for fluid flow at the time of their formation. They can be subdivided into blowout,

seepage, hydrothermal and dissolution pipes. (Cartwright et al., 2007). Blowout pipes are cylindrical or steeply conical zones of intense disruption of stratal reflection typically developed directly above the localized breached points of underlying fluid source interval, linked to pockmarks (Cartwright et al., 2007). Seepage pipes are defined as for blowout pipes but have no links to pockmarks. Pipes and chimneys can be associated with both push-down and or pull-up effects. (Cartwright et al., 2007)

High amplitude anomalies can be observed above hydrocarbon accumulation zones (Løseth et al., 2009). The anomalies lie several hundred meters above the top reservoir and lateral extent of these anomalies are related to the lateral extent of the underlying gas cap. This type of high amplitude anomaly is located above normally pressured hydrocarbon accumulations where no significant tectonic deformation of the cap rock can be observed. (Løseth et al., 2009)

Fault zones may contain numerous interconnected fractures or faults representing conduits for hydrocarbon fluid flow (Løseth et al., 2009). It may be filled with ductile clay or cement and be sealing or leaking when the fluid pressure increases above a threshold value. Open or pressure dependent open faults may be important vertical migration routes. The fault zone can easily be identified as line-ups of reflection discontinuities on vertical seismic sections. Under some conditions seismic data can reveal faults acting as vertical conduits for fluid flow. (Løseth et al., 2009)

Leakage zone can be recognized on seismic data and it is defined as volume of seismic anomalies caused by hydrocarbon leaving a trap through the cap rock (Løseth et al., 2009). The leakage zone comprises all types of leakage processes involving migration from one reservoir to the next or from the reservoir to the surface. The leakage zone has a unique shape as it comprises of a root where the leakage starts, a body or the zone itself where vertical movements of hydrocarbons take place and a top where the leakage terminates. The top of leakage zone can be a tight cap rock or salt layers. (Løseth et al., 2009)

Fault bypass is the larger group of Seal bypass system. Faults together with small fractures acts as main conduits for fluid flow (Cartwright et al., 2007). Fault bypass can be subdivided into two families: trap defining or supratrap, based on whether the faults define and delimit the trap with a lateral seal component, or whether they are embedded within the sealing sequence. (Cartwright et al., 2007)

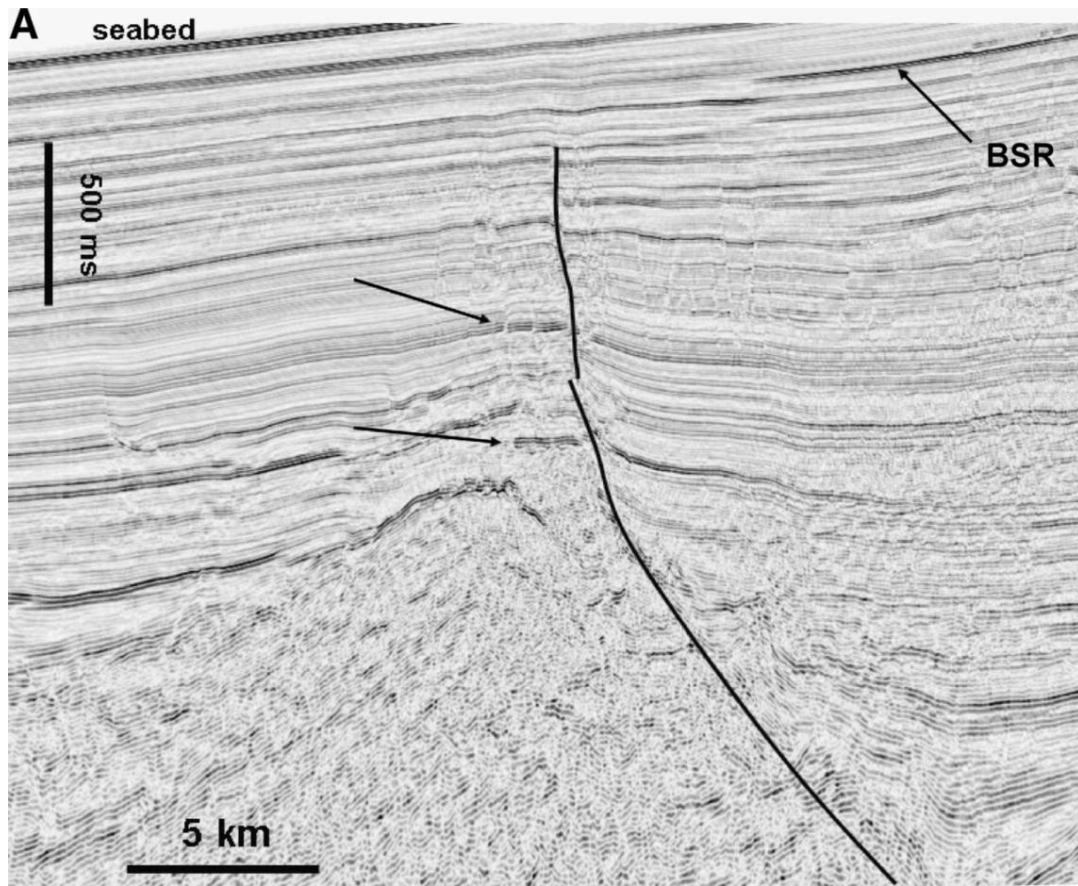


Fig1-10: Seismic section of large tilted fault block where arrows indicate different vertically distributed amplitude anomalies acted as a hydrocarbon leakage zone. There is also indicated bottom simulation reflector (BSR) relevant for hydrocarbon leakage. (modified from Cartwright et al., 2007)

Intrusive bypass are group of intrusive structures that breach the integrity of seal in three distinctive ways (Cartwright et al., 2007). First the intrusion itself may contain the fluids and involves in puncturing of the seal for example when mud volcanoes formed. Second, the intruded material has a much higher permeability than the sealing sequence acting as a bypass, for example sandstone intrusion. Third, the intrusive event results in intense fracturing and deformation of the sealing sequence, for example sheath zone around salt diapirs or metamorphic aureoles around igneous intrusion. (Cartwright et al. 2007)

Mud Volcano is applied to more or less violent eruption or surface extrusion of watery mud or clay accompanied by natural gases and has a more or less conical or volcano like shape

and are commonly related along the line of fracture, faulting or sharp folding (Brown, 1990). The source of mud volcanoes may be diapir of high plastic and under compacted mud or shale. Mud volcanoes and mud diapirs are closely related to one another (Brown, 1990). Mud diapirs and diastremes are characterized by episodic intrusion and extrusion of mud across the impermeable sediments.(Brown, 1990)

Salt diapirs results from gravitational (Rayleigh- Taylor) instability due to dense fluid overburden overlying a less dense fluid salt. The thicker the overburden the unstable the salt to be and more likely to rise upward (Al-Zoubi & Brink 2001). Salt diapirism influence fluid flow through the development of fractures and faults that are formed during the process of salt diapirism. (Al-Zoubi & Brink 2001).

Pipe bypass are columnar zones of disturbed reflection that may or may not be associated with sub vertically stacked amplitude anomalies (Cartwright et al., 2007). Pipes tend to exhibit vertical to sub vertical geometry on seismic data and commonly seen to originate from crestal regions, e.g., tilted fault block crest, fold crest, or crest of sand bodies with positive topography. Pipes are commonly circular to sub circular in planar form and in some cases it composed of zones of deformed reflection related to minor folding and faulting while in others they appears as stacked pockmarks craters or stacked localized amplitude anomalies. (Cartwright et al., 2007)

1.5 General Stratigraphy of Western Barents Sea:

A dominant feature of Barents Sea stratigraphy is major unconformity at the base of the Quaternary (Henriksen et al., 2011b). The unconformity is due to the Paleogene-Recent uplift and erosion of the entire Barents Sea to the east of the western margin, with erosion products being re-deposited to the west, particularly during the late Pliocene-Pleistocene. (Henriksen et al., 2011b; NPD)

The generalized Stratigraphy of western Barents Sea is:

1.5.1 Paleozoic Succession:

1.5.1.1 Billefjorden Group:

It is well-developed lower Carboniferous stratigraphic unit in southern Barents Sea dominated by continental and shallow marine siliciclastics with partly coaly material in it.

Three formations are assigned to Billefjorden group are Soldogg formation, Blærerot formation and Tettegras formation. (NPD bulletin 4)

a) Soldogg Formation

It composed of sandstone and conglomeratic sandstone with thin beds of carbonaceous siltstone, shale and coal and is deposited in braided river fluvial environment. Age is assigned to be of middle Viséan. (NPD 4)

b) Blærerot Formation

It composed of intensely bioturbated grey to yellowish brown limestone and sandy dolomite and are interpreted as coastal plain deposits. Age assigned to be of late Viséan to early Serpukhovian. (NPD 4)

c) Tettegras Formation

It comprises of alternating bed of fine grained sandstone, siltstone, claystone and coal and are interpreted to be deposited in flood plain or delta plain. Age assigned to be of Viséan. (NPD 4)

1.5.1.2 Gipsdalen Group:

It covers the offshore mid-Carboniferous to early Permian succession in the southern Barents Sea dominated by red coloured siliciclastics and warm water often dolomitized carbonates with significant amount of evaporates in the basinal areas. Three formation assigned to Gipsdalen Group are Ugle formation, Falk formation and Ørn formation. (NPD 4)

a) Ugle Formation:

Ugle formation is characterized by reddish brown to brown conglomerates, coarse grained sandstone and minor siltstone and is interpreted to be deposited in semi- arid terrestrial environment. Age assigned to be of late Serpukhovian to early Bashkirian. (NPD 4)

b) Falk Formation

This formation composed of a mixture of shallow marine sandstone, siltstone and shallow marine carbonated and are interpreted to be deposited in shallow marine shelf environment. Age assigned to be of late Bashkirian to early-middle Gzelian. (NPD 4)

c) Ørn Formation

This formation is mostly dominated by shallow marine carbonates and interbedded carbonates and evaporites and is deposited in shallow marine carbonate environment as a

result of high frequency and high amplitude fluctuation of sea level changes. Age assigned to be of late Gzelian to early Sakmarian. (NPD 4)

1.5.1.3 Tempelfjorden Group:

It is well established middle to late Permian age lithostratigraphic unit characterized by dark to light grey spiculites, spiculitic cherts, silicified skeletal limestones and fine-grained siliciclastic including marls, calcareous claystones, shales and siltstones. Two formation assigned to Tempelfjorden Group are Røye formation and Ørret formation. (NPD 4)

a) Røye Formation

The Røye formation is dominated by silicified sediment that is resulted from silicification processes of abundant silica sponge spicules. In addition to this it also composed of dark grey to black, silicified calcareous claystone with minor amount of pyrite and organic material. The formation is interpreted to be deposited in distal marine, low energy deep shelf to basinal environment. Age assigned to this formation is still debatable but suggested as ?Kungurian to Kazanian or Tatarian? (NPD 4)

b) Ørret Formation

Ørret formation is dominated by siliciclastic sediments of sandstone, siltstone and shales. The formation is interpreted to be deposited from deltaic -lower coastal plain environment to deep shelf environment. Age suggested to this formation are ?Kungurian to ?Tatarian. (NPD 4)

1.5.2 Mesozoic Succession:

1.5.2.1 Ingøydjupet Group:

It composed of grey to black shales and claystone with subordinate amount of grey siltstone and sandstone and having approximately 1700 m thickness in type locality. Minor interbeds of carbonate and coal are also present. Four formation are assigned to this this Group are Havert, Klappmyss, Kobbe and Snadd formation. It is Griesbachian to early Norian in age. (NPD 4)

a) Havert Formation:

It composed of medium to dark greyish shale interbedded with pale grey siltstone and sandstone reflecting coarsening upward sequences and it is interpreted to be deposited in

marginal marine to open marine environment. It is of Griesbachian to Dienerian in age. (NPD 4)

b) Klappmyss Formation:

It comprises of medium to dark grey shale interbedded with siltstone and sandstone. It is interpreted to be deposited in marginal to open marine environment with age assigned to be of Smithian to Spathian. (NPD 4)

c) Kobbe Formation:

It comprises of thick shale units that passes upward into interbedded shale, siltstone and carbonate cemented sandstone and are deposited in marginal marine environment. It is of Anisian age. (NPD 4)

d) Snadd Formation:

It composed of grey shale that are coarsening upward into shale interbedded with grey siltstone and sandstone. Limestone and calcareous interbed with thin coaly lens can be recognized in the lower and middle part of formation. It is interpreted to be deposited in distal marine environment with age assigned to be of Ladinian to early Norian. (NPD 4)

1.5.2.2 Realgrunnen Group:

It composed of Pale grey sandstone It is approximately with minor amount of shale and coal. It comprises of four formation including Fruholmen, Tubaen, Nordmela and Stø formation. The group is present throughout Hammerfest Basin and thickens into the Tromsø Basin of SW Barents Sea. It is approximately 450 to 500 m in thickness and is of early Norian to Bajocian in age. (NPD 4)

a) Fruholmen Formation:

It comprises of grey to dark grey shale with interbedded sandstone, shale and coal. It is deposited in fluviodeltaic environment with age assigned to be early Norian for the basal part and Triassic/Jurassic for the top part of the formation. (NPD 4)

b) Tubåen Formation:

It is dominated by sandstone with subordinate shale and minor coals. The sandy unit in the formation represents stacked series of high energy marginal marine environment while coals and shale in the formation represents lagoonal environment. (NPD 4)

c) Nordmela Formation:

It comprises of interbedded siltstone, sandstone, shales and claystones with minor amount of coal and it is interpreted to be deposited in tidal flat to flood plain environment. Age assigned to be of Sinemurian to late Pliensbachian. (NPD 4)

d) Stø Formation:

The formation is dominated by moderately to well sorted sandstone with thin units of shale and siltstone are also present. And in some well phosphatic lag conglomerates are also identified. The sandy unit in the formation is interpreted to be deposited in prograding coastal regimes environments. Age assigned to this formation is late Pliensbachian to Bajocian. (NPD 4)

1.5.2.3 Teitengrunnen Group:

It composed of shales and claystone with minor interbeds of marly dolomitic limestone with rare siltstone or sandstone. It varies in thickness from over 300 m to the north of Troms-Finnmark Fault Complex to approximately 60 m on the structural high in the Hammerfest Basin. It is of late Callovian to Ryazanian in age. Two formation are assigned to this Group are Fuglen and Hekkingen formation. (NPD 4)

a) Fuglen Formation:

It composed of pyritic mudstone with interbedded thin whit to brownish limestone and dark brown shale. It is interpreted to be deposited in marine environment with age assigned to be of late Callovian to Oxfordian. (NPD 4)

b) Hekkingen Formation:

It consists of brownish grey to dark grey shale and claystone with thin interbeds of limestone, dolomite, siltstone and sandstone. It is assumed to be deposited in deep marine water under anoxic condition. It is of late Oxfordian/early Kimmeridgian to Ryazanian. (NPD 4)

1.5.2.4 Nordvestbanken Group:

It composed of Dark grey to grey brown shales and claystone with thin interbeds of grey to grey brown siltstone, limestone and dolomite. The group is laterally extended throughout the Ringvassøy-Loppa Fault Complex and Hammerfest Basin. It is approximately varies in thickness from 1440 m in the type well to 918m in the reference well and is of Valanginian

to Cenomanian in age. Three formation are assigned to this Group are Knurr, Kolje and Kolmule formation. (NPD 4)

a) knurr Formation:

It composed of dark grey to greyish brown claystone with thin interbeds of limestone and dolomite. Thin sandstone units can also be recognized in the formation .The formation is assumed to be deposited in open and generally distal marine environment with local restricted bottom condition. It is of Ryanzanian/Valanginian to early Barremuan in age. (NPD 4)

b) Kolje Formation:

It composed of dark brown to dark grey shale and claystone interbedded with pale limestone and dolomite. Thin interbeds of light grey-brown siltstone and sandstone can be recognized at the upper part of the formation. The formation is assumed to be deposited in distal open marine condition with good water circulation. It is of early Barremian to late Barremian/early Aptian in age. (NPD 4)

c) Kolmule Formation:

It composed of dark grey to green claystone and shale with thin siltstone interbeds and limestone and dolomite stringers. Traces of glauconite and pyrite can be recognized in the formation. It is interpreted to be deposited under open marine environment and is suggested to be of Aptian to mid-Cenomanian. (NPD 4)

1.5.2.5 Nygrunnen Group:

It comprises of greenish grey to grey claystone with thin interval of limestone in some part. The group thins eastward in the Hammerfest Basin from approximately 250 m to less than 50 m near the southern margin of the Hammerfest Basin. Age assigned to this group is from late Cenomanian to Maastrichtian. Two formation assigned to this Group are Kviting and Kveite formation. (NPD 4)

a) Kviting Formation:

The formation comprises of calcareous sandstone interbedded with sandy and glauconitic mudstone. In some wells limestones interbedded with sandy claystone are recognized. The formation is supposed to be deposited under deep to shallow shelf environment. Age assigned to this formation is Campanian. (NPD 4)

b) Kveite Formation:

It composed of greenish grey to grey shales and claystone with thin interbeds of limestone and siltstone. It is interpreted to be deposited under deep open shelf environment and is of late Cenomanian to early Maastrichtian in age. (NPD 4)

1.5.2.6 Sotbakken Group:

The Sotbakken Group is dominated by claystone with minor amount of siltstone, tuffaceous and carbonate horizons. The basal contact of Sotbakken Group representing unconformity between the latest Cretaceous and early Paleocene throughout the Tromsøflaket area. The age of the Group is interpreted to be late Paleocene to early/middle Eocene. Torsk formation is recognized within this group. (NPD 4)

a) Torsk Formation:

The formation composed of light to medium grey or greenish grey non-calcareous claystone in some cases stringers of siltstone and limestone can be seen in the formation. Tuffaceous horizons can also be observed in the lower part of the unit. The formation is deposited under open to deep marine shelf environment and is interpreted to be of late Paleocene to Oligocene in age. (NPD 4)

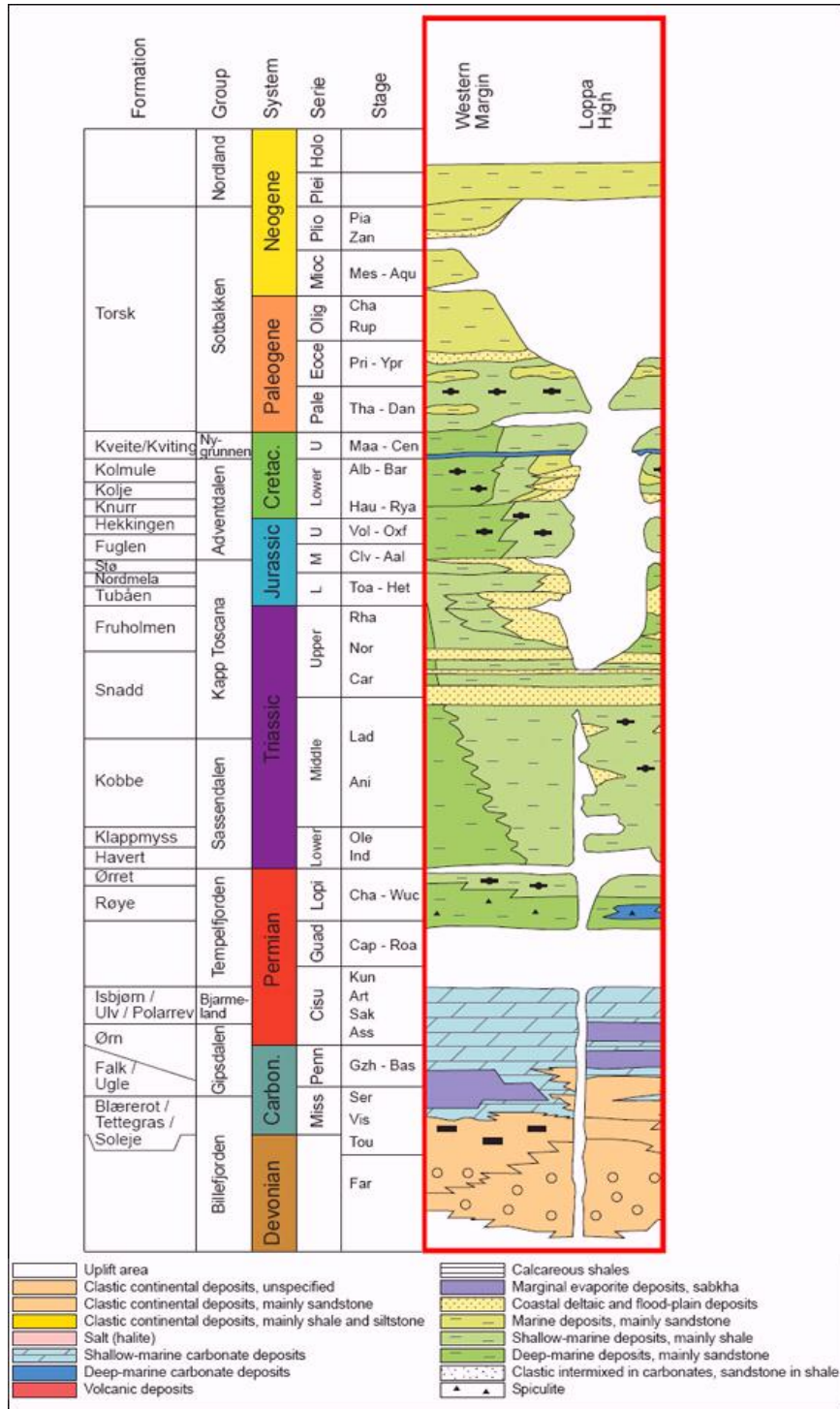


Fig1-11: Generalized lithostratigraphic chart of Western Barents Sea. (Elvebakk, 2008)

1.6 Source Rock of SW Barents Sea

Source rock refers to the rock from which hydrocarbon can be generated or is capable of being generated by thermal conductivity of organic matter (Kerogen)(Walter) It is an important elements of Petroleum system with total organic content of 1% . A petroleum system comprises an active source rock, the oil and natural gas it generates, and all of the essential elements and processes required for a petroleum accumulation to exist (Magoon and Dow, 1994)

Source rock ranging in age from Silurian to Cretaceous have been proven to found in Greater Barents Sea (fig 1.13) (Henriksen et al., 2011b).The western Barents Sea has been known to include source rock sedimentary facies and there has been in recent years proven that also accumulation of hydrocarbon exist in Snøhvit, Skrugard and Goliat (NPD 2012). (Ohm et al., 2008) described several possible source rocks (Fig 1.12).Numerous potential source rock of late Jurassic in age are widely distributed in Barents Sea. Petroleum systems related to the late Jurassic (Hekkingen formation) source rock are considered to be dominant in the SW Barents Sea. Despite of being widespread in Barents Sea, this Hekkingen shale have not been realized full generation due to maturity problem. The unit is thought to be mature for oil and gas generation in a narrow belt at the western margin of the Hammerfest Basin and along the western fringe of the Loppa High. Farther west it is too deeply buried, and farther east it is too shallow (Dore, 1995). The Hekkingen formation is the best source rock penetrated by the Snøhvit wells, and it has a very good potential for light oil, condensate, and gas (Linjordet and Olsen. 1992). Upper Triassic shale may also locally be of source quality in the Norwegian sector (Johansen et al., 1993).

There are three possible source rocks in Snøhvit field one already discussed and other two are, Nordmela formation, clay rich terrestrial deposited reservoir rock and has potential to generate hydrocarbon whereas the Triassic shales is gas prone source rock. Organic rich shales in the lower to middle Triassic may also be important source rocks (Linjordet and Olsen. 1992). The middle Jurassic shale of Bathonian member on Spitsbergen is thought to be a potential source rock for oil and gas. Drilling has identified equivalents of this unit in the southern Barents Sea, where it is believed to be widespread but of variable quality (Doré, 1995).

In Barents Sea, Ladinian marine and prodeltaic shale in the lowermost part of Snadd formation represent thin potential source rock with HI values of 400-500 mg/gTOC (Henriksen et al., 2011b).

Source rock in Barents Sea begun to generate oil by middle Triassic (Anisian) time and reached peak oil generation (Transformation ratio TR 0.4-0.6) in Ladinian time. (Henriksen et al., 2011b)

The Snadd, Kobbe, Klappmyss and Havert formation are potential Triassic source rocks.(NPD 2012)

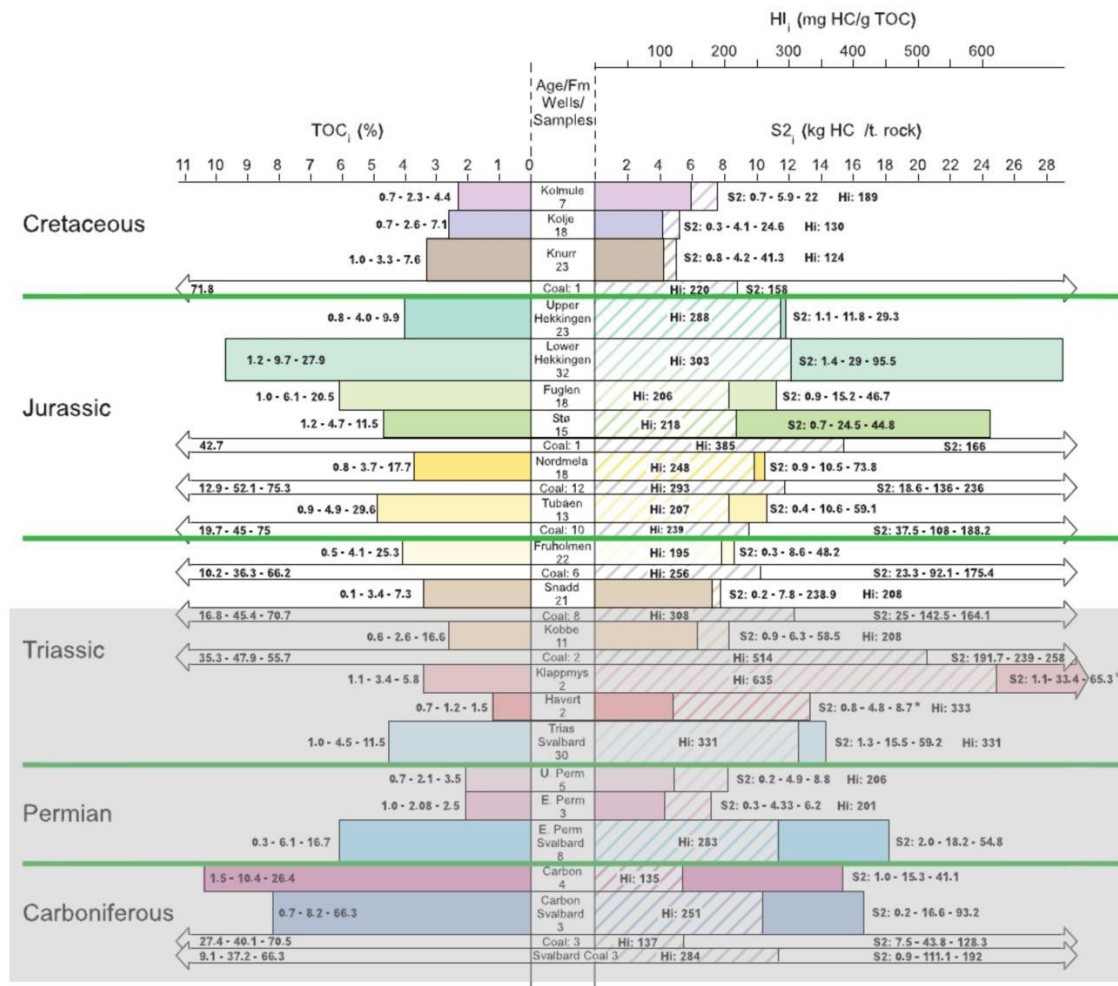


Fig1-12: Source rock in the western Barents Sea with characteristics indicating total organic carbon (TOC), S2 (hydrocarbon generative potential and hydrogen INDEX (HI). (Fig modified from Ohm et al., 2008)

1.7 Reservoir Rock of SW Barents Sea

Reservoir rocks are the porous and permeable units that are capable of holding hydrocarbon. The best reservoir rock includes porous sandstone, limestones and dolostones, some of which are the skeletal remains of ancient coral reefs, are other examples of reservoir rocks. The most significant proportion of the hydrocarbon resources in Barents Sea proved to be found within strata of Jurassic age includes Snøhvit, Albatross and Askeladden—all have a principal reservoir consisting of lower-middle Jurassic sandstone (Doré, 1995). The major portion of the hydrocarbons in Snøhvit field is encountered in the Stø Formation, with about 10% in the Nordmela formation (Linjordet and Olsen, 1992). According to Larsen et al. (1993), 85% of Norwegian Barents Sea resources lies within Stø, Fruholem and Knurr formation can also acts as potential reservoir rock.

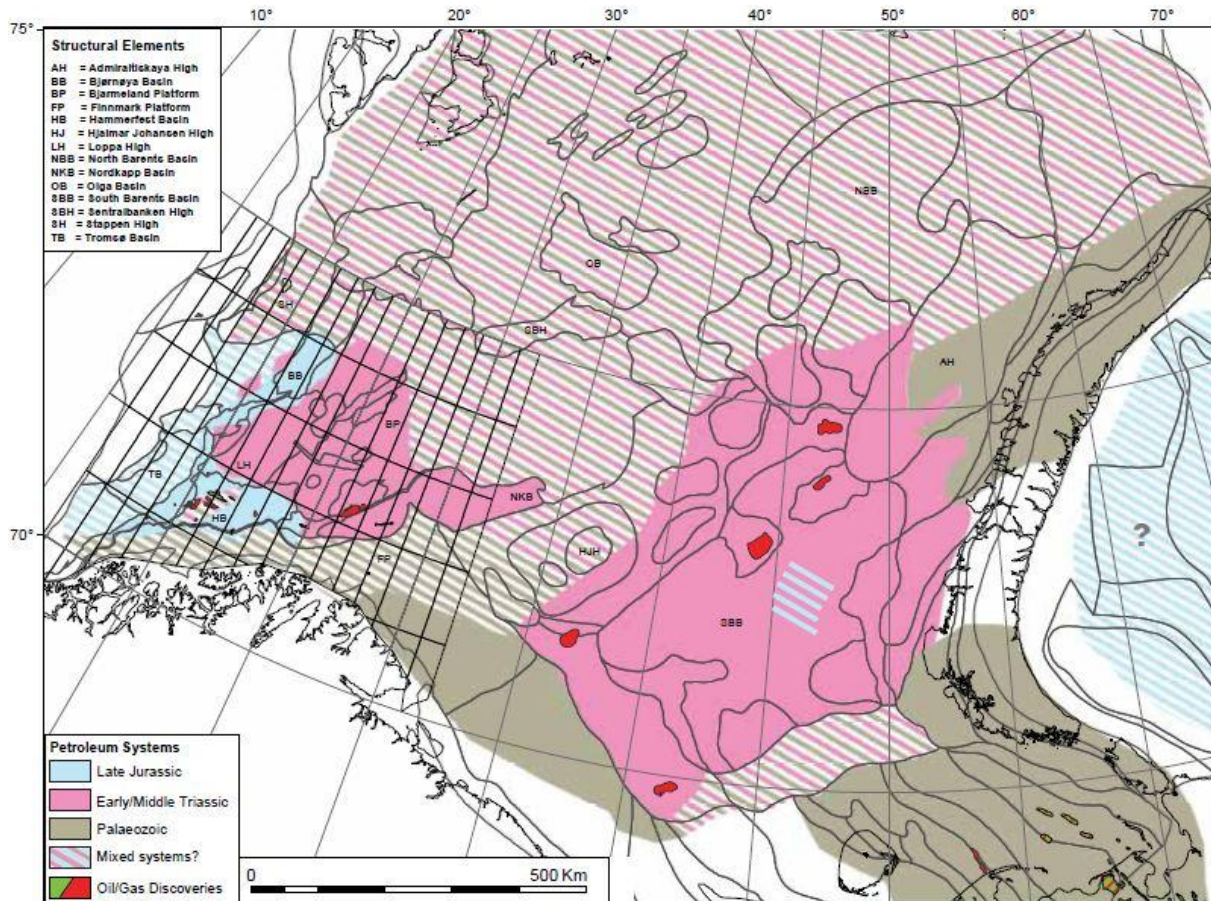


Fig1-13: Petroleum system of greater Barents Sea based on presence of source rock and modeled maturity calibrated to the distribution and geochemistry of hydrocarbon in the Norwegian Barents Sea. (Henriksen et al., 2011b)

2 Data and Methods:

2.1 Data

The data for this thesis are provided by NPD (Norwegian Petroleum Directorate) in collaboration with different exploration companies including Fugro, TGS, Det Norsk and others. The database consists of more than 3000 public and non public high quality 2D seismic line and well logs from more than 60 boreholes in SW Barents Sea. I also worked with three 3D cubes to fill up the gap in between the 2D seismic lines.

2.2 2D seismic lines and 3D seismic cube

The fundamental difference between 2D and 3D seismic method can be explained in two important aspects; the grid spacing in 2D seismic dataset reduced from km or so to 25 m or less in 3D seismic dataset results in dense concentrated data in lateral dimension as compared with the vertical resolution and secondly 3D seismic sampling in combination with the advanced 3D seismic migration algorithms allowing us to accurately image complex geological structures. The limitation in 2D seismic mapping is its spatial limitation as compared to 3D seismic map. Fig 2, an illustration from Cartwright and Huuse (2005), shows the significant difference in interpretation of the same area with 2D and 3D seismic dataset. 2D seismic data have much greater distance in between the seismic line due to which many features cannot be seen or only poorly mapped as compared to 3D dataset. The increased resolution of the 3D seismic data enables us to discover geological structures like mud diapirs feeders, thrust fault systems, gas blow-out pipes, giant pockmarks and sandstone intrusions (Cartwright & Huuse, 2005) because of all these reasons, 3D dataset is preferred over the 2D seismic dataset.

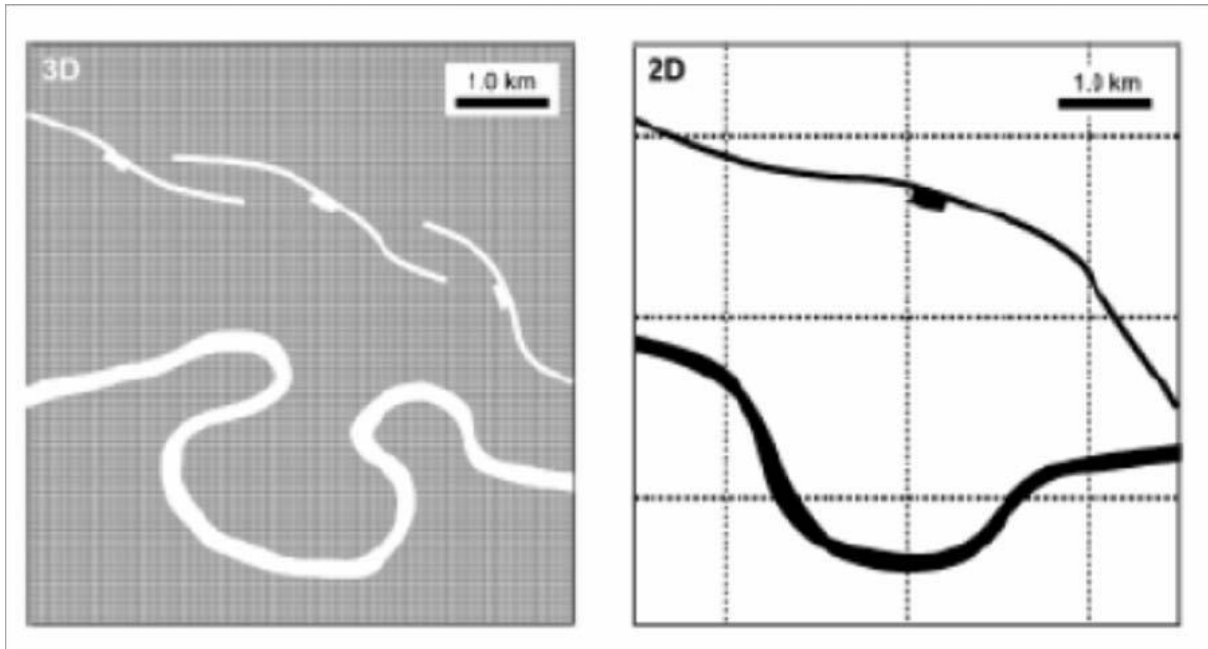


Fig2: Comparison of spatial resolution of 2D and 3D dataset. In 3D dataset with line spacing of 12.5m-50m we can identify faults and other structures like channel but on the right side of the fig, the map (using 2D seismic dataset) shows the same structures with line spacing of 2km (Cartwright & Huuse, 2005)

2.2.1 2D Seismic Data

The SW Barents Sea is covered by relatively dense grid of 2D seismic reflection data so as to carry out regional study and to map the regional stratigraphy of an area. The seismic data is of varying quality and there are significant problems with multiples in some areas. Data density is highest in southern part of the study area and somewhat restricted in the northern part. The 2D seismic data have generally spacing of 2 to 35 km line spacing. Fig 2.1 illustrates the overall distribution of 2D seismic data in SW Barents Sea.

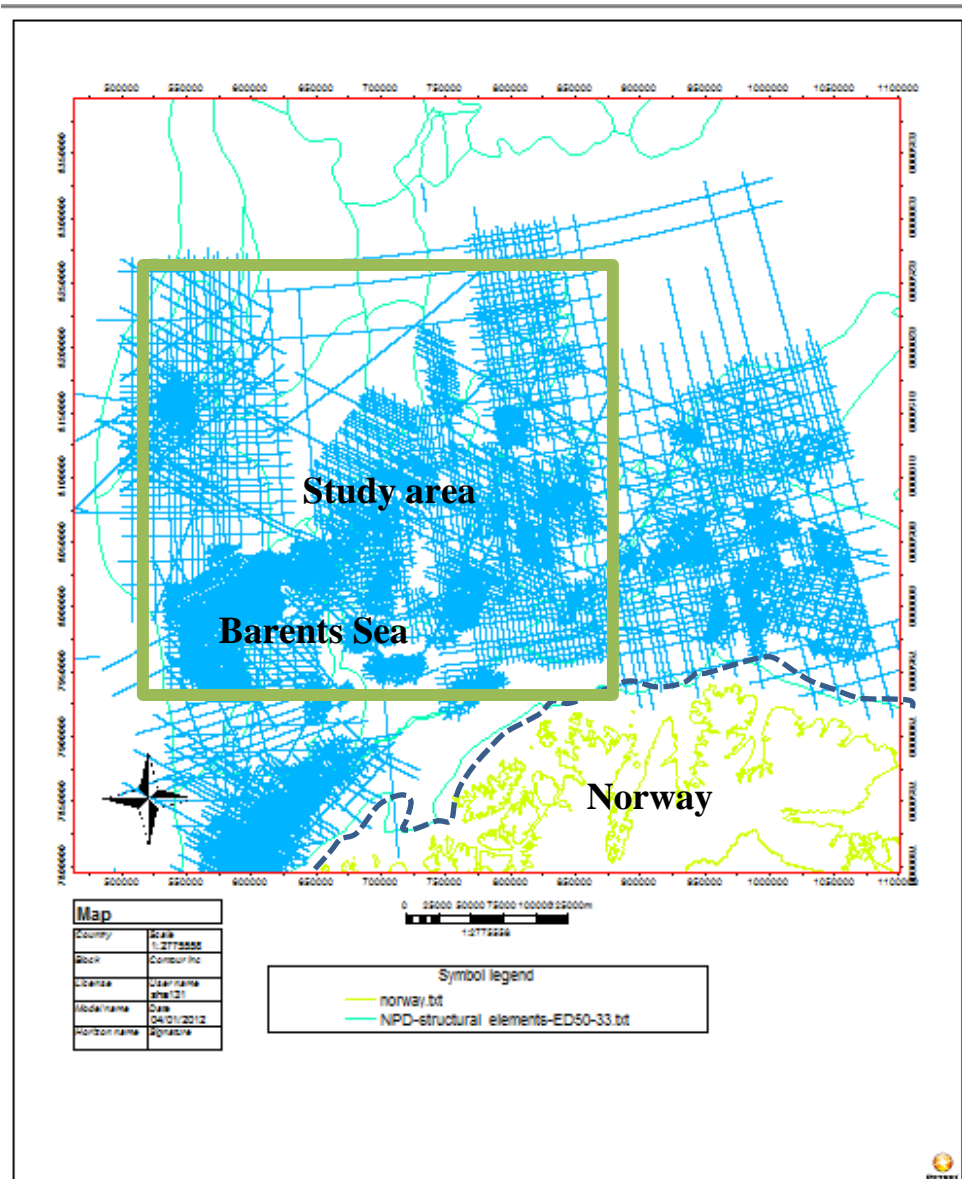


Fig 2-1: Map window showing study area and 2D seismic lines across Barents Sea.

2.2.2 3D Seismic Data

Three 3D seismic cubes have been used to cover the gap in between the 2D seismic data sets in order to extend the stratigraphic unit across the Hammerfest Basin. These cubes are located in Hammerfest Basin of Barents Sea. The 3D seismic cubes have Geodetic datum of ED50 UTM 34N with distance between inline and cross lines are 12.5mx 12.5m. The location of 3D cubes can be shown in fig 2.2.

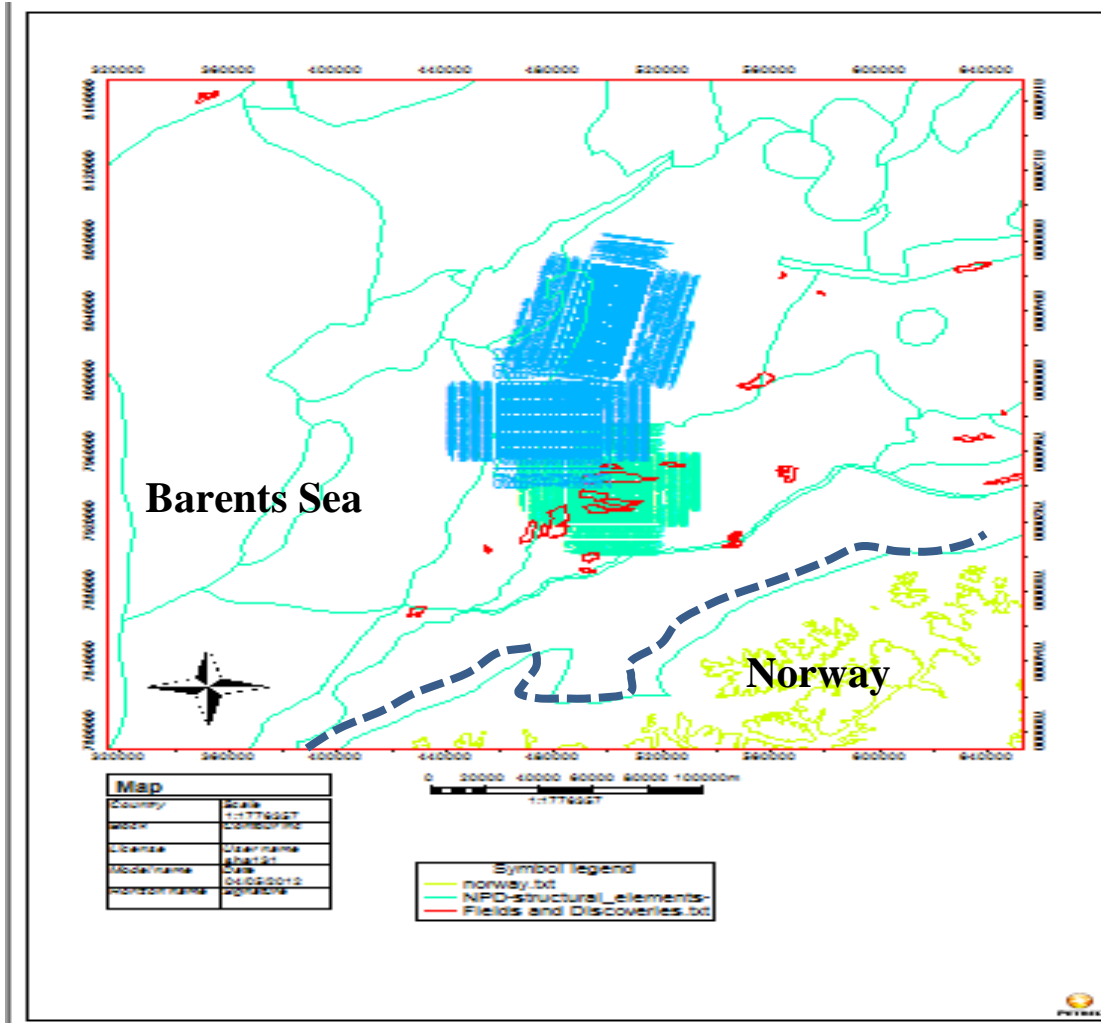


Fig 2-2: Map window showing location of 3D cube together with structural elements and discoveries in SW Barents Sea.

2.3 Well data

Different well logs were used to calibrate borehole depth to the two-way travel time of the seismic data and to understand lithostratigraphy, physical properties and depositional environmental of the subsurface. Well penetrated in SW Barents Sea are spaced large with up to 60-70 km in between the well. Since 1979, 87 exploration wells have been drilled in the south western Barents Sea and nearly half of those are inside the Hammerfest Basin. Thermal gradients are calculated from bottom hole temperature and maximum true vertical depth of the different wells. The average geothermal gradient of Barents Sea is around 30

°C /km (Laberg et al., 1998). The information of the different formations and their depositional environments stems from well information from NPD's fact pages, together with the use of additional literature. A number of important, representative wells are described below as shown in fig 2.3

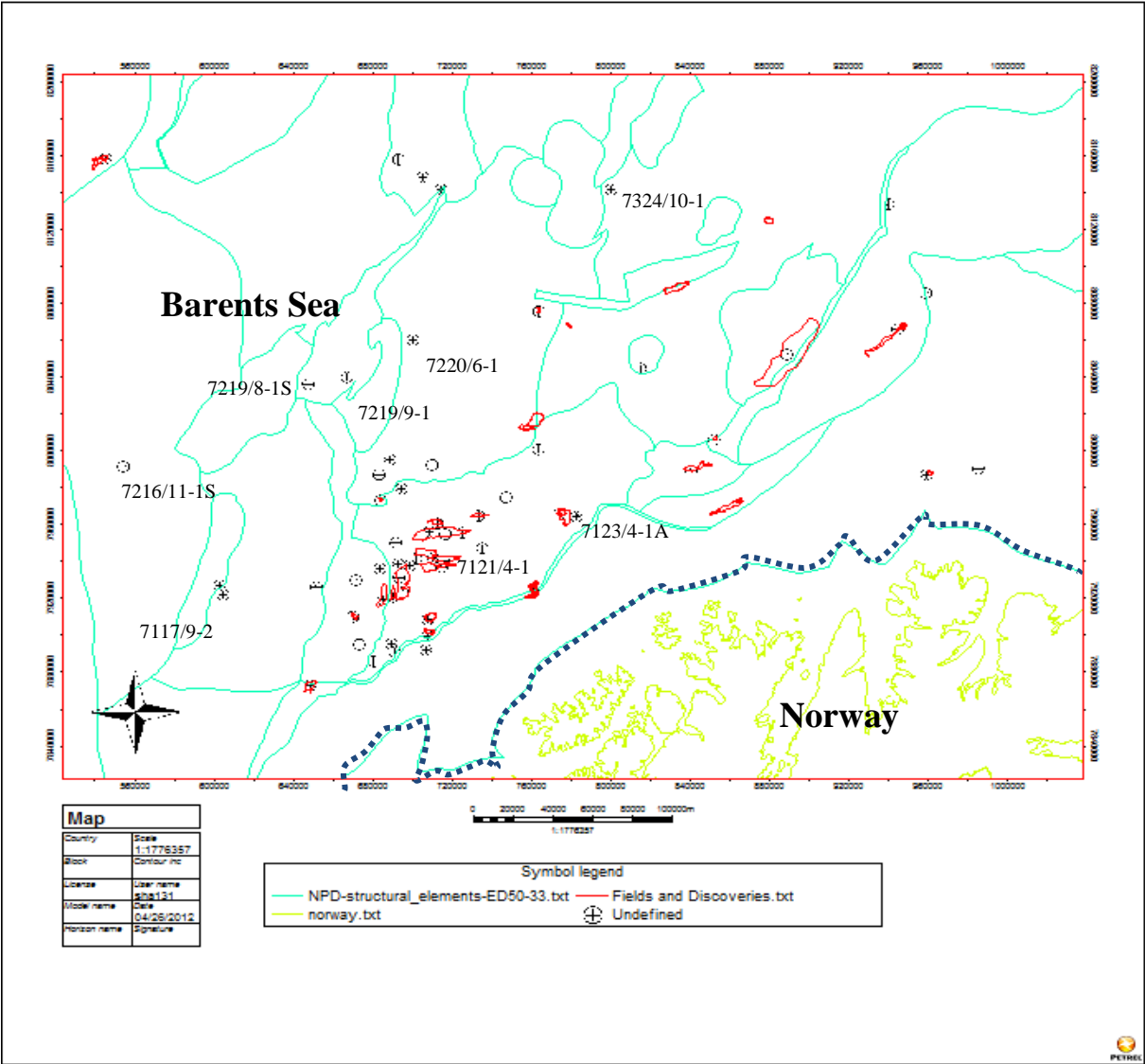


Fig 2-3: Map Window showing structural boundaries, Fields and location of wells in the SW Barents Sea.

2.3.1 Seismic Well Tie

The Seismic well tie is major task for interpretation and is used to correlate the well information (logs) to the 2D seismic line or 3D seismic cube which enables us to tie geological marker to seismic events.

Main steps of Seismic Well Tie workflow are:

1. Prepare well logs and checkshot data.
2. Calibrate sonic logs with checkshots.
3. Extract wavelet.
4. Visualize results.

2.3.2 Well Tops

Well Tops are also called as Formation top and can be used to identify the subsurface stratigraphy of the area. Fig 2-4 illustrates the seismic well tie process on 2D dataset which enables us to identify the formation top on seismic data.

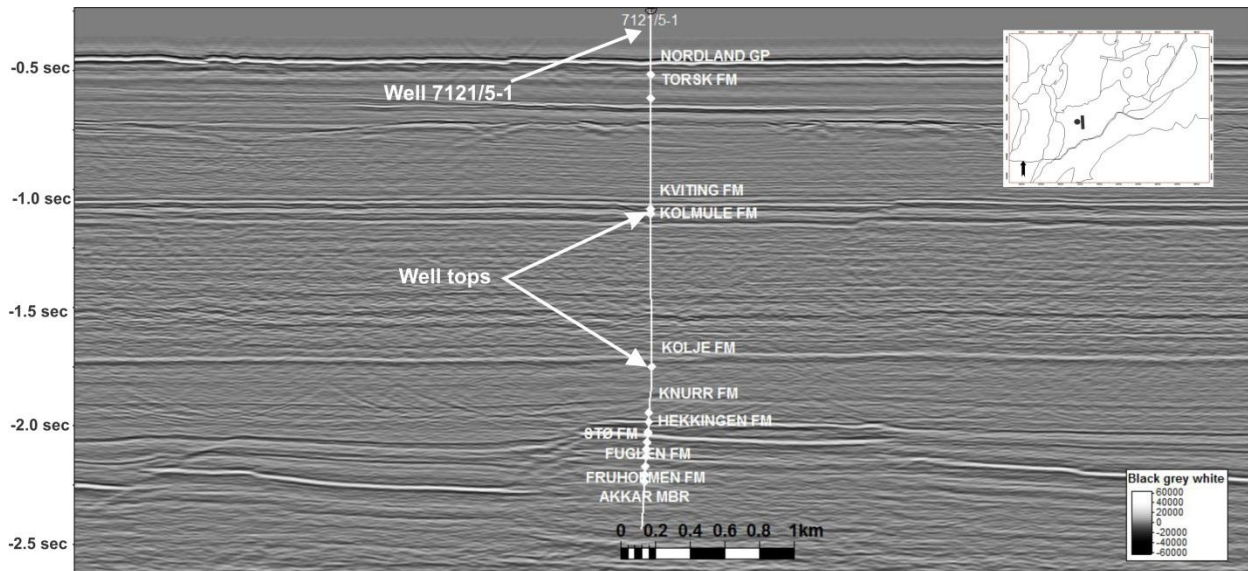


Fig 2-4: Well cross section showing the seismic well tie to seismic data. Map window in the small box showing the location of well and seismic line.

2.3.3 Well 7219/ 8-1 S (Bjørnøya Sør)

Well 7219/8-1S is located in the Bjørnøya Sør area of west of the Veslemøy High and was drilled by Saga Petroleum ASA in 1992. The main purpose to drill the well was to test the middle Jurassic Stø formation and to identify the possible sandstone in late Jurassic Hekkingen formation and in the early Cretaceous sequences. The Well 7219/ 8-1S has a total depth (MD) of 4611.0 and Bottom hole temperature of 165 °C. The well was spudded in water depth of 345 mMSL. At depth of 3319 mMSL TVD, the well penetrated claystone.

Traces of hydrocarbon seen in some silty parts in the Cretaceous from 2400 m to 2430 m in the knurr formation and from 2595 m to 2652 m in the knurr formation. (NPD)

2.3.4 Well 7216/11-1S (Sørvestsnaget Basin)

The exploration well is located in Sørvestsnaget Basin and was drilled by Norsk Hydro in 2000. The well was spudded in water depth of 361 mMSL (mean sea level) and terminated at a total depth of 4215 mMSL (true vertical depth is 3709 mMSL due to deviated well path. In rock of early Paleocene (Danian) age. The well have a bottom hole temperature of 114 °C and total depth of 4239.0. The well section comprised of two main units of Paleogene and Neogene related to Sotbakken and Nordland lithostratigraphic group .The well was dry but it proves the existence of significant sandstone reservoir rock of the Paleocene.(NPD; Ryseth et al., 2003)

2.3.5 Well 7219/9-1 (Bjørnøya Sør)

Well 7219/9-1 is located in the Bjørnøya Sør area between the Veslemøy High and the Polheim sub platform. The main purpose for drilling the well was to target the reservoir and hydrocarbon potential of early-middle Jurassic sandstone and late Triassic sandstone of the Snadd formation. The well has a total depth (MD) of 4300.0 m RKB and bottom hole temperature of 145 °C. (NPD)

During drilling, top reservoir, Stø formation was encountered from 1950.5 m to 2062m with 99 m net sand of 17.8 % average porosity. Nordmela formation was penetrated from 2062m to 225.5m, Tubåen formation from 2205.5m to 2305m, Top Snadd formation came in at 2876.5m.(NPD)

2.3.6 Well 7220/6-1 (Loppa High)

Well 7220/6-1 is located on the Loppa High in the Barents Sea and was drilled by Norsk Hydro Produksjon AS in 2005.. The main purpose for drilling the well was to test reservoir properties and migration pathway of hydrocarbon in the Permian and Carboniferous carbonates and to evaluate the Triassic interval in the area. The well has a total depth (MD) of 1540.0 m RKB and Bottom hole temperature of 46 °C .

During drilling, no significant amount of hydrocarbon were found from targeted reservoir rocks but residual amount of hydrocarbon were obtained from carbonates of the Gipsdalen Group, Ørn formation from 1138m and down to 1430 m. (NPD)

2.3.7 Well 7121/ 4-1 (Snøhvit Field)

Well 7121/4-1 is located in Snøhvit part of Hammerfest Basin in the Troms I area and was drilled by Den Norsk Stats Oljeselskap AS in 1984. The main objective to drill the well was to determine the hydrocarbon accumulation in sandstone of middle to early Jurassic rocks. The well has a total depth (MD) of 2609.0 m RKB and Bottom hole temperature of 88 °C. During drilling, hydrocarbon accumulation were discovered in uppermost sequence of Stø, Nordmela and Tubåen Formation from 2318m to 2442 m and in the lower sequence of Froholmen Formation was bearing gas between 2468.5 m and 2473m. (NPD)

2.3.8 Well 7123/4-1 A (East of Snøhvit Field)

Well 7123/4-1 A is located east of the Snøhvit field in the Hammerfest Basin of the Barents Sea and was operated by StatoilHydro ASA in 2008. The main purpose to drill the well was to prove the additional gas reserves in the Tornerose structure, east of the discovery wells 7122/6-1 and 7122/6-2. The well has a total depth (MD) of 2855.0 m RKB and Bottom hole temperature of 94 °C.

During drilling, the well penetrated rocks of Quarternary, Tertiary, Cretaceous, Jurassic and Triassic in age. Snadd reservoir were encountered at 2266.2 m. (NPD)

2.3.9 Well 7324/10-1 (Maud Basin)

Well 7324/10-1 is located in the Maud basin on the Bjarmeland Platform and was drilled by Den Norsk Stats Oljeselskap AS in 1989. The main objective for drilling the well was to evaluate the hydrocarbon potential at the base of Anisian level (Top Klappmyss Formation) and to test the sandstone below the Base Smithian level (Top Havert Formation). The well has a total depth (MD) of 8919.0 m RKB and Bottom hole temperature of 119 °C.

During drilling, minor gas was encountered in the Kobbe formation at the depth of 1607m and base Anisian/Klappmyss Formation at the depth of 1767m proved to be an intra Anisian seismic marker encountered at depth of 1822m. The top Havert formation were encountered at the depth of 2512 m. (NPD)

2.3.10 Well 7117/9-2 (Senja Ridge)

Well 7117/9-2 is located on the Senja Ridge west of the Tromsø Basin and was operated by Norsk Hydro Produksjon AS in 1983. The main objective to drill the well was to test

sandstone or limestone reservoir rocks of early Cretaceous age within the Senja Ridge. The well has a total depth (MD) of 5000.0 m RKB and Bottom hole temperature of 173 °C.

During drilling, the well encountered the Pliocene deposits down to 400 m which is underlain by Pliocene clay at the depth of 1092m and Paleocene rock continue to penetrate down to 1345 m which is then followed by sequence of Campanian and late Albian to early Cenomanian deposits at the depth of 1380-1396 m and 1400-1410 m respectively. The lower most strata penetrated by well comprises of thick, poorly defined sequence of claystones. (NPD)

2.4 Methods

The data analysis was carried out by using Petrel 2011 PC Schlumberger software.

Methods applied for the analysis of the data are listed below

- Correlation of well log into the 2D and 3D seismic line
- Seismic interpretation of main horizons unit in the study area.
- Visualization of these interpreted horizons unit.
- Interpretation of fluid leakage and gas accumulation features.

2.4.1 Basic Seismic Reflection Theory

The basic technique of seismic exploration is to map out subsurface geological structure by generating seismic waves with artificial sources. The pulses of seismic waves travel downward are partially reflected from the interface in the rock (reflector) and are recorded by receiver (geophone) on the surface while some of the waves are refracted through high velocity layer. Seismic reflection originated from acoustic impedance contrast in between the two interfaces of the rock (Andreassen, 2009). Each layer in the subsurface has its own acoustic impedance contrasts that are dependent upon density and velocity of individual layer a

$$\text{Acoustic Impedance} = \text{Density} \times \text{Velocity} \quad (\text{Andreassen, 2009})$$

The resolution between layers and the penetration into the sub-surface when performing a seismic survey is related to frequency. The higher the frequency the higher the resolution but lower the penetration and vice versa (Andreassen, 2009).

The energy reflected back and the energy transmitted into next substance is determined by Snell's law as shown in fig (2.5)

$$\sin_{\theta_{inc}} / V_1 = \sin_{\theta_{trans}} / V_2 = \sin_{\theta_{ref}} / V_1 \quad (\text{Andreassen, 2009})$$

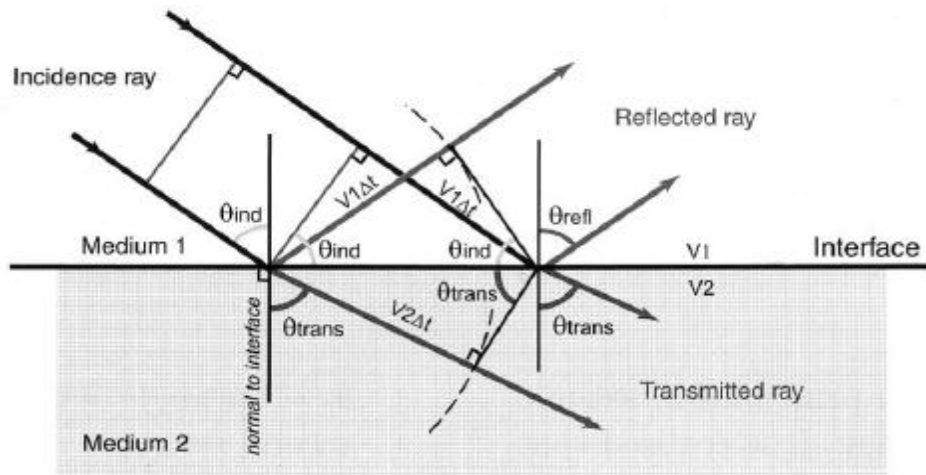


Fig 2-5: Acoustic sound waves are affected by an acoustic impedance contrast between the two layers. The reflected and transmitted plane wavefront are also shown as well. (Andreassen .2009)

The strength of reflection generated at the interface in the rock can be quantified in terms of reflection coefficient (R). Reflection coefficient can be both positive and negative and depends upon whether softer rock overlies harder rock or vice versa. Mathematically it can be described as:

$$\text{Reflection coefficient (R)} = (Z_2 - Z_1) / (Z_2 + Z_1) \quad (\text{Andreassen, 2009})$$

Seismic reflections are usually described in terms of polarity (fig 2.6). Seismic polarity can be Normal or reversed based on acoustic impedance of the layer.

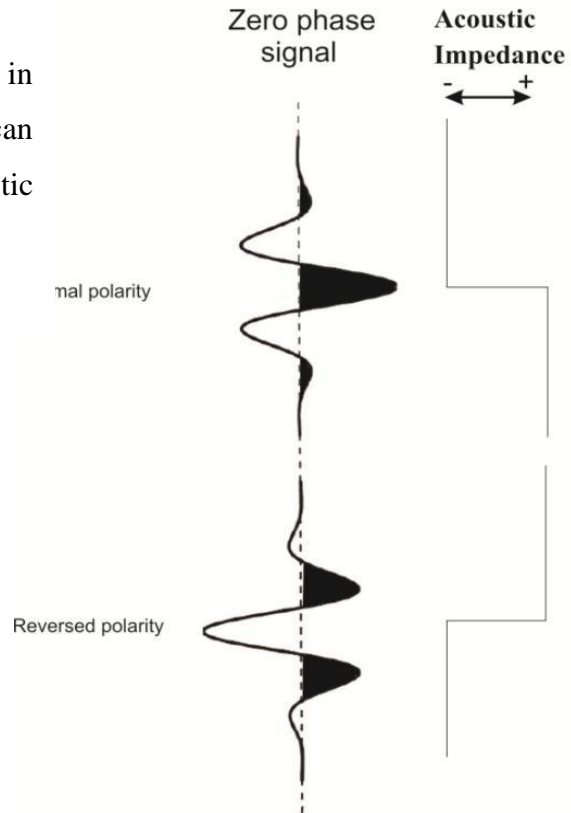


Fig2-6: Schematic diagram of Polarity convention of seismic signal (Sheriff and Robert, 1995)

2.4.2 Artefacts

Artefacts are the noisy features that degrade the quality of seismic data and have to be considered during interpretation. Artefacts commonly take the appearance of amplitude variance which are not related to the geology and creates distortion for interpreters or it can leads to some loss of detectability of structure and stratigraphy. Or they may also demonstrate as small scale structures features (fig 2.7). Some artefacts may be of equivalent or greater magnitude than the geological attribute being sought. (Galbraith & Hall, 1996).Artefacts are generated during the acquisition process of seismic data that generally arises from a faulty acquisition geometry of the streamers and gun (Marfurt et al., 1998) or it could be generated as a result of towing depth difference of streamers or gun that causes difference in two way travel time. The seismic data has to undergo processing so as to eliminate noise and other errors before being interpreted by Geophysicist.

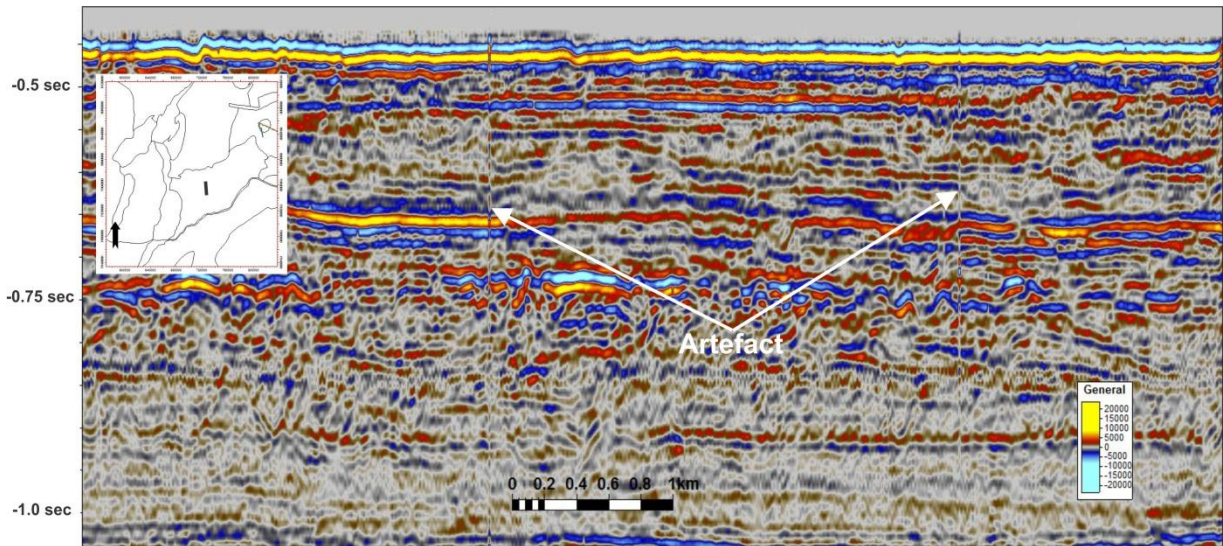


Fig 2-7: NW and SE aligned artifacts with static correction error can be observed in Snøhvit part of SW Barents Sea.

2.4.3 Resolution

Resolution is measured in wavelength and it is defined as its ability to distinguish separate features; the minimum distance between two features so that the two can be defined separately rather than as one (Brown, 1999). Resolution varies greatly with the velocity and the frequency of the waves as shown in fig (2.8). The frequency of the waves decreases with the depth as it attenuates and absorbed with the depth according to Hughes principle so there will be higher frequency at the shallow depth and it dies out at the great depth but contradicted to frequency, the velocity of waves increases with the depth due to compaction of sediment so resolution decreases with the depth. (Brown, 1999)

$$\text{Wavelength } (\lambda) = \text{Velocity (V)} / \text{Frequency (Hz)} \quad (\text{Brown, 1999})$$

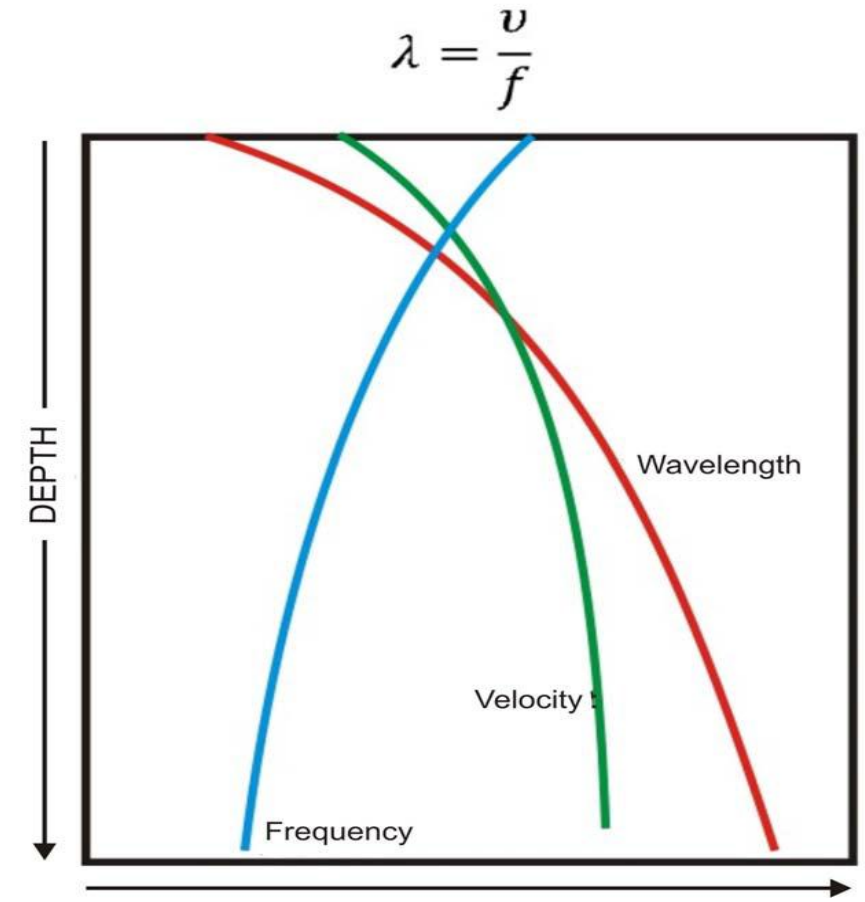


Fig2-8: shows how the relationship between frequency, velocity and wavelength changes with depth. With increasing depth, wavelength and velocity increases whereas frequency decreases with increasing depth (modified from Brown, (1999)

All seismic survey is designed to image a specific target depth which in turn influences the choice of source, sampling rate, survey geometry. Vertical and horizontal resolution is very important factor as they impact on interpretation of resultant seabed imaging. (Bulat, 2005)

2.4.5 Vertical Resolution

The vertical resolution of the seismic data can be defined as its ability to distinguish the top and base of thinning sedimentary beds. (Bulat , 2005)and is a limiting factor in seismic stratigraphy. A seismic trace have a resolution of $\frac{1}{4}$ the wavelength, in a noise-free environments, hence, the shorter the wavelength and the higher the frequency the greater vertical resolution. (Bulat , 2005)

The approximately 3000 seismic lines used during this study were acquired within several tens of surveys. Hence, the frequency bandwidth of these surveys varies depending on the

source system that was used. On average, the peak frequency varies between 40 to 60 Hz. That gives wavelength of 33 to 50 m assuming a velocity of 2000 m/s. In such case, optimum vertical resolution varies between 8 to 12.5 m.

2.4.6 Horizontal Resolution

Horizontal resolution refers to how close two reflecting points can be situated horizontally, and yet be recognized as two separate points rather than one. Fresnel zone concept is an important factor in determining Horizontal resolution (Bulat, 2005). Fresnel zone is an area on the reflector from which the energy returned to the receiver within a half-cycle ($\lambda/4$) after the onset of the reflection (Bulat, 2005) (fig 2.9)

Horizontal resolution depends upon the frequency and velocity of the waves. (Bulat, 2005)

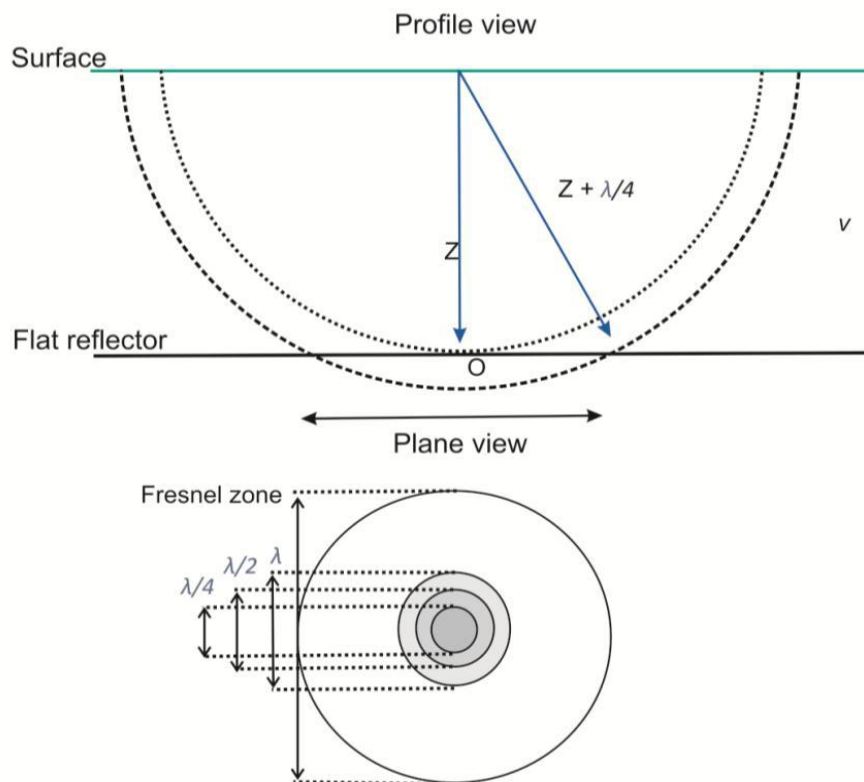


Fig 2-9: explaining the principle of Fresnel zone that can determine the horizontal resolution of seismic data (Fig modified from Bulat, 2005)

$$\text{Fresnel zone radius: } r_F = \frac{v}{2} \sqrt{\frac{t}{f}} \quad (\text{Sheriff \& Robert, 1995})$$

The horizontal resolution for seafloor and deeper horizons are calculated as;

For Seafloor,

The seafloor lies at the average of depth of 400 ms in study area,

$$r_F = \frac{v}{2} \sqrt{\frac{t}{f}} \quad (\text{Sheriff \& Robert, 1995})$$

$$\text{For frequency range of 40 Hz, } r_F = \frac{2000\text{m/s}}{2} \sqrt{\frac{0.4\text{s}}{40\text{ Hz}}} = 100 \text{ m}$$

$$\text{For frequency range of 60 Hz, } r_F = \frac{2000\text{m/s}}{2} \sqrt{\frac{0.4\text{s}}{60\text{ Hz}}} = 81.6 \text{ m}$$

For deeper horizons,

The deeper horizon like Jurassic and Triassic sedimentary packages lies at the average depth of around 2000 ms.

$$r_F = \frac{v}{2} \sqrt{\frac{t}{f}} \quad (\text{Sheriff \& Robert, 1995})$$

$$\text{For frequency range of 40 Hz, } r_F = \frac{2000\text{m/s}}{2} \sqrt{\frac{2.0\text{s}}{40\text{ Hz}}} = 223 \text{ m}$$

$$\text{For frequency range of 60 Hz, } r_F = \frac{2000\text{ m/s}}{2} \sqrt{\frac{2.0\text{s}}{60\text{ Hz}}} = 182.5 \text{ m}$$

2.5 Seismic Interpretation

Seismic Interpretation has been carried out using Petrel 2011 PC Schlumberger software. Horizons are interpreted manually or automatically using Petrel tool based on Well logs and composite lines. In this master thesis I interpreted 2D seismic line together with few 3D seismic cubes so as to cover the regional gap in between the 2D seismic lines.

The data is processed with a zero-phase pulse containing a central peak or trough with two side lobes of opposite signs. Peaks or troughs are selected based on the continuity and larger extent of reflector layer. Sea floor is represented by peak upper zero crossing whereas presence of gas or fluid in the sediments is represented by trough upper zero

crossing

(fig2.10).

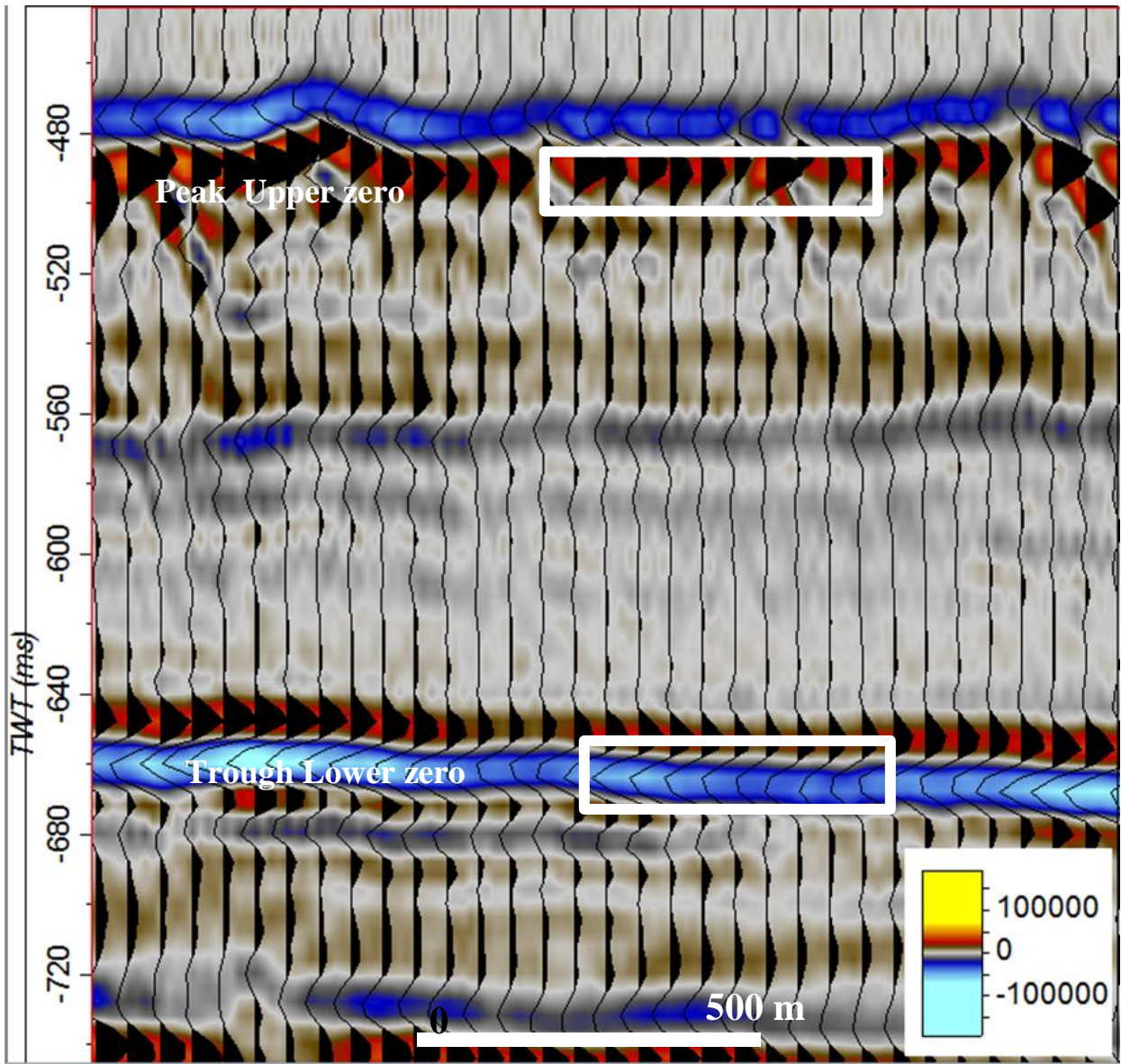


Fig 2-10: Seismic line showing sea floor as peak upper zero crossing and high amplitude anomalies as trough lower zero crossing.

2.5.1 Seismic Interpretation of 2D seismic dataset

In 2D seismic dataset, horizons are interpreted automatically or manually using a Petrel Horizon tool depending upon the reflection strength, continuity of a reflection, presence or absence of faults or unconformities. In most cases horizons are interpreted manually in

more complex area especially in chaotic reflection zone or in low amplitude reflection pattern.

In Petrel, horizons interpretation was performed by using two techniques: (1) Manual interpretation, where interpretation can manually picked key points and interpolates between the key points; (2) Seeded 2D autotracking, where interpretation will track along a reflection events based on the parameter .

In order to create surface from this horizons, I went through the make/ edit process which is effective way of creating surface by performing grid computations. In my Interpretation, I used automatic grid size and position geometry with grid increments of 200 x 200 depending upon line spacing between the survey lines in my study area.

In my thesis, I interpreted eight horizons on the basis of presence of 60 bore holes that were drilled in SW Barents Sea and on the basis of composite line, joining different survey lines together but sometimes composite line doesn't give you authentic prove of the presence of particular formation in specific survey area so I used the combination of well logs and composite line so as to extends the regional stratigraphy of an area. The eight horizons interpreted in my thesis are:

2.5.1.1 Sea floor.

2.5.1.2 Torsk Formation.

2.5.1.3 Kolmule Formation.

2.5.1.4 Hekkingen Formation.

2.5.1.5 Snadd Formation.

2.5.1.6 Ørn Formation.

2.5.1.7 Bottom Tertiary Unit.

2.5.1.8 Bottom Cretaceous Unit.

2.5.2 Seismic Interpretation of 3D seismic cubes

In 3D seismic dataset, horizons are picked automatically or manually on subset of the data and then propagated throughout the rest of volume using Petrel 3D Horizons tracking tools. On 3D seismic cubes, I interpreted Torsk, Kolmule, Hekkingen, Snadd and Ørn formation as shown in fig (2.11, 2.12, and 2.13)

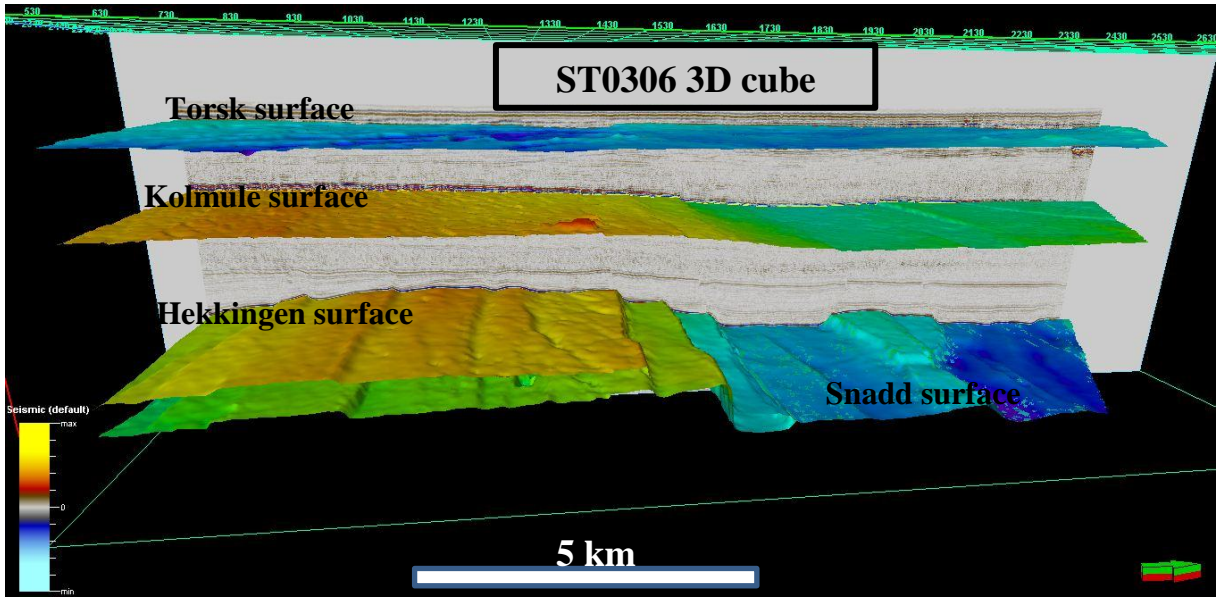


Fig2-11: Interpreted surface of ST0306 3D cube with vertical exaggeration of x10.

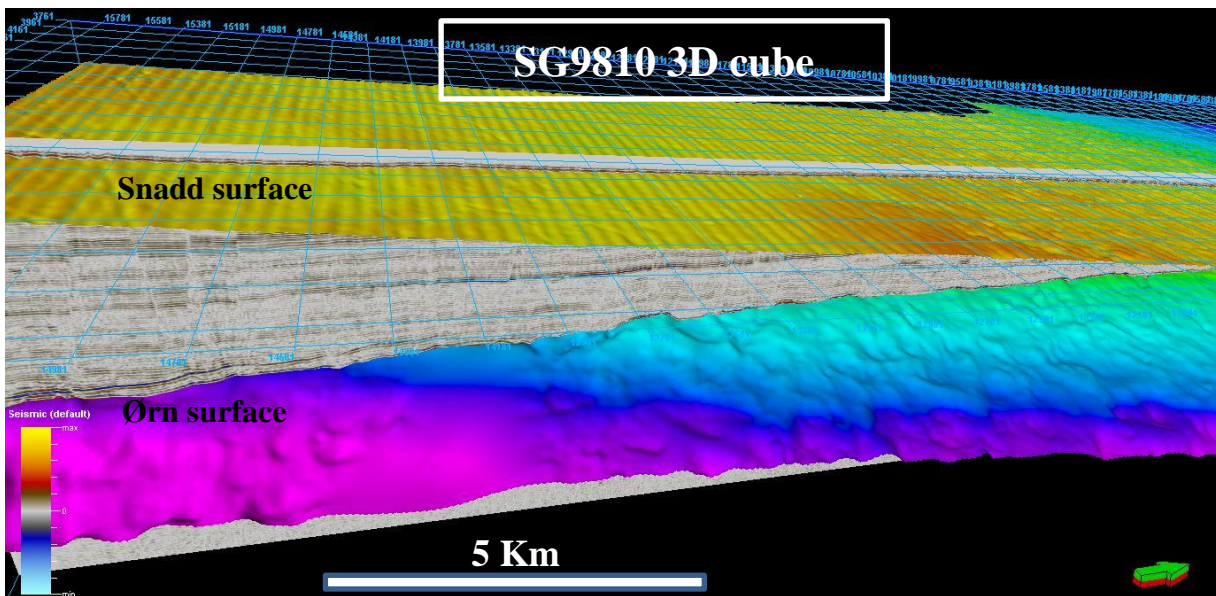


Fig2-12: Interpreted surface of SG9810 3D cube with vertical exaggeration of x10.

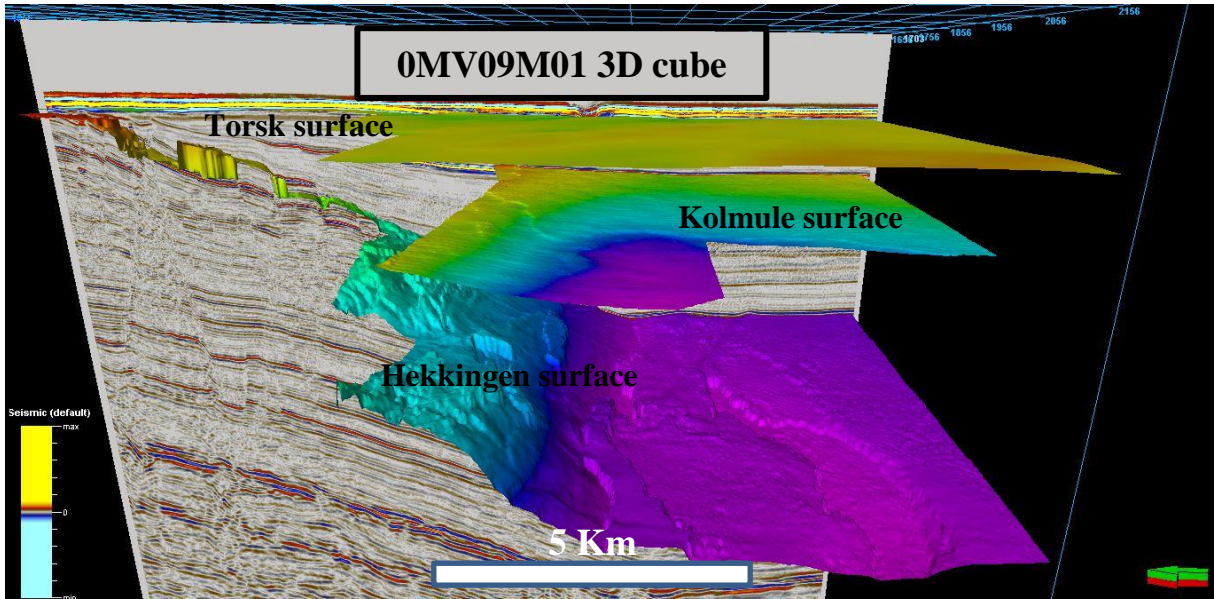


Fig2-13: Interpreted surface of OMV09M01 3D cube with vertical exaggeration of x10.

3 Results

The result chapter is divided into two main parts: the first part shows the interpretation of seismic horizons whereas the second part is mainly concerned with interpreting fluid flow features.

3.1 Interpretating Seismic Horizons

The main task of my thesis is to map out the late Paleozoic , Mesozoic and Cenozoic sedimentary succession. For this purpose I interpreted six horizons that are extended regionally but in western part of SW Barents Sea, which is tectonically more complex than eastern side, it became difficult for me to follow all six horizons especially in Sørvestsnaget Basin, Vestbakken Volcanic province, Tromsø Basin and Loppa High. The interpretation of seismic horizons are purely based on different well logs that are penetrated in my study area that are correlated to seismic reflector continuity, strength and amplitude pattern together with composite section, through joining various 2D line of different seismic survey (fig 3.1) During my interpretation of horizons, Torsk, and Kolmule formation are more regionally exposed than other horizons especially Hekkingen formation are mostly exposed east of Hammerfest Basin. Hekkingen, Snadd and Ørn formation are either present too deep or data is too bad in the eastern side to be interpretable. Seismic stratigraphy indicates shallowing from all direction towards the Loppa High at all stratigraphic level. The other two horizons including Bottom Tertiary unit (BTU) and Bottom Cretaceous unit (BCU) are locally extended along the western margin of Loppa High and in Sørvestsnaget Basin as shown in Fig (3-2) and they are very important in relationship with the fluid flow.

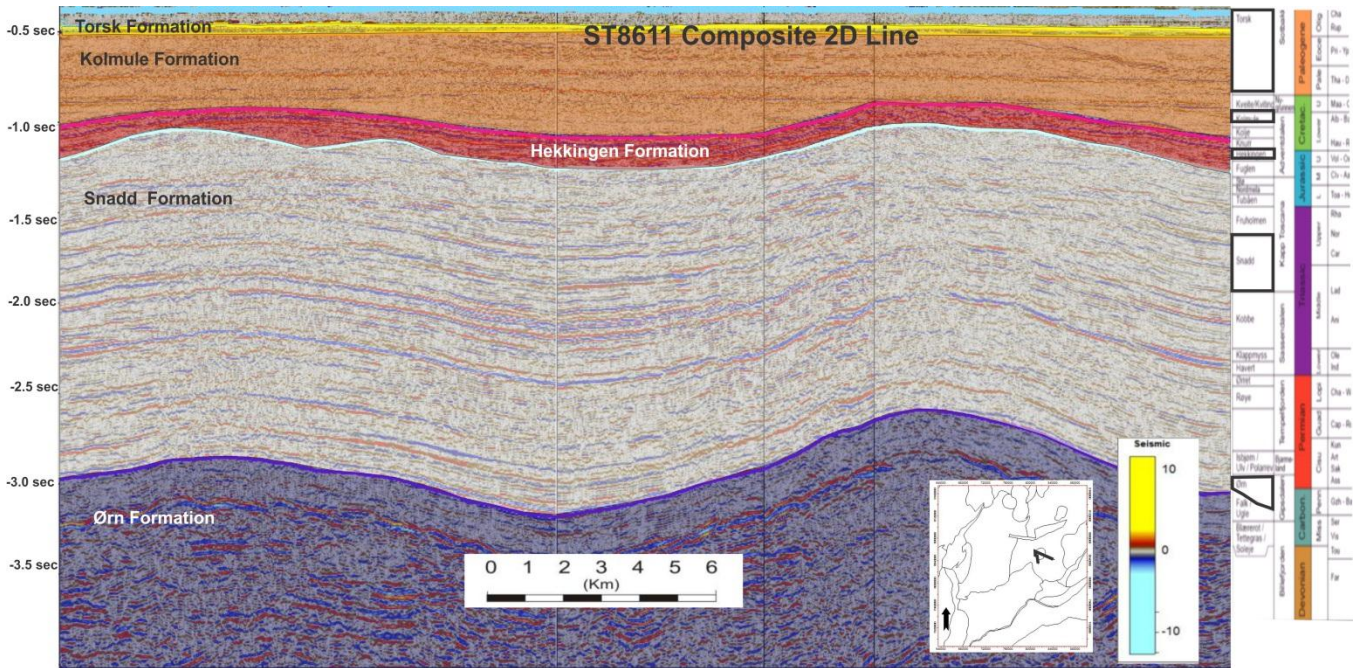


Fig 3-1: Composite line showing interpreted horizons of ST8611 seismic dataset across the SW Barents Sea whereas small box shows the location of seismic line.

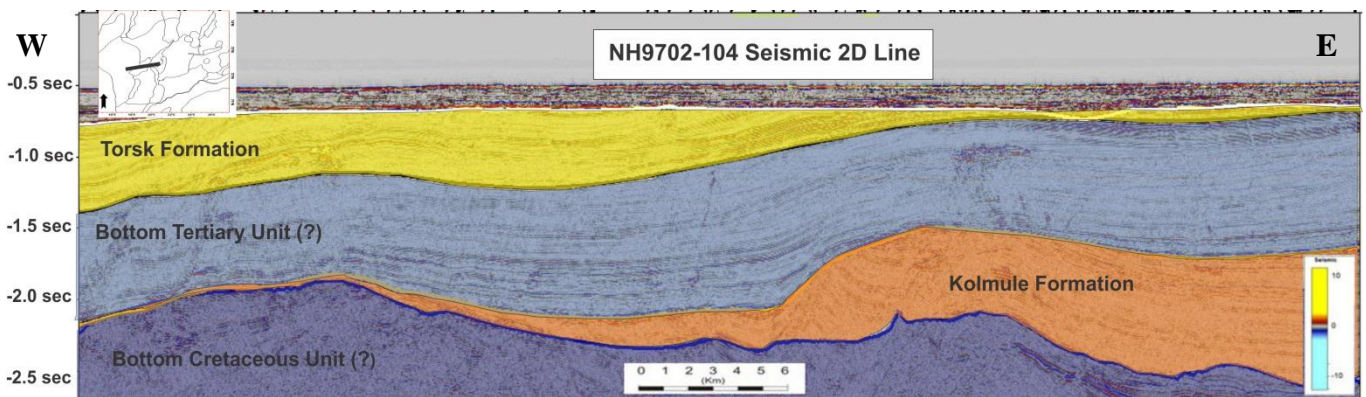


Fig3-2: Seismic line showing the depositional pattern of BTU and BCU beneath the Torsk and Kolmule formation. Small box showing the location of seismic line.

3.1.1 Sea floor

The present day topography of the Barents Sea was mainly affected by major glacial event during late Weichselian deglaciations event. Seafloor is easy to interpret and it exhibits excellent continuity pattern throughout my study area (fig 3.3).In my study area, the seafloor is marked by curved furrows with U-shape or V-shaped profile (fig 3.4) that are

interpreted to be iceberg pockmark indicative of glaciomarine environment or it could be caused by leakage of fluid underneath the seafloor horizons. Due to 2D seismic data, there is limited ability to recognize depressions like furrows on seafloor. Calved iceberg covered large distances and where the keel of Iceberg and ice-rafted sediments got contact with the seafloor they scour the seafloor. Sets of scours have generally random orientation on the seafloor indicating wandering drift track of individual icebergs. Individual scours can be of several kilometers in length, tens of meters wide and deep. (Dowdeswell et al., 1993; 2007) Pockmarks-like depression can be observed on seafloor especially in the area of Snøhvit, Loppa High, Bjørnøya Basin and Tromsø Basin part of Barents Sea and are interpreted to be derived from gas chimneys and leakage along faults deep beneath the seafloor or by drifting of Iceberg along the seabed (Andreassen et al., 2007b).

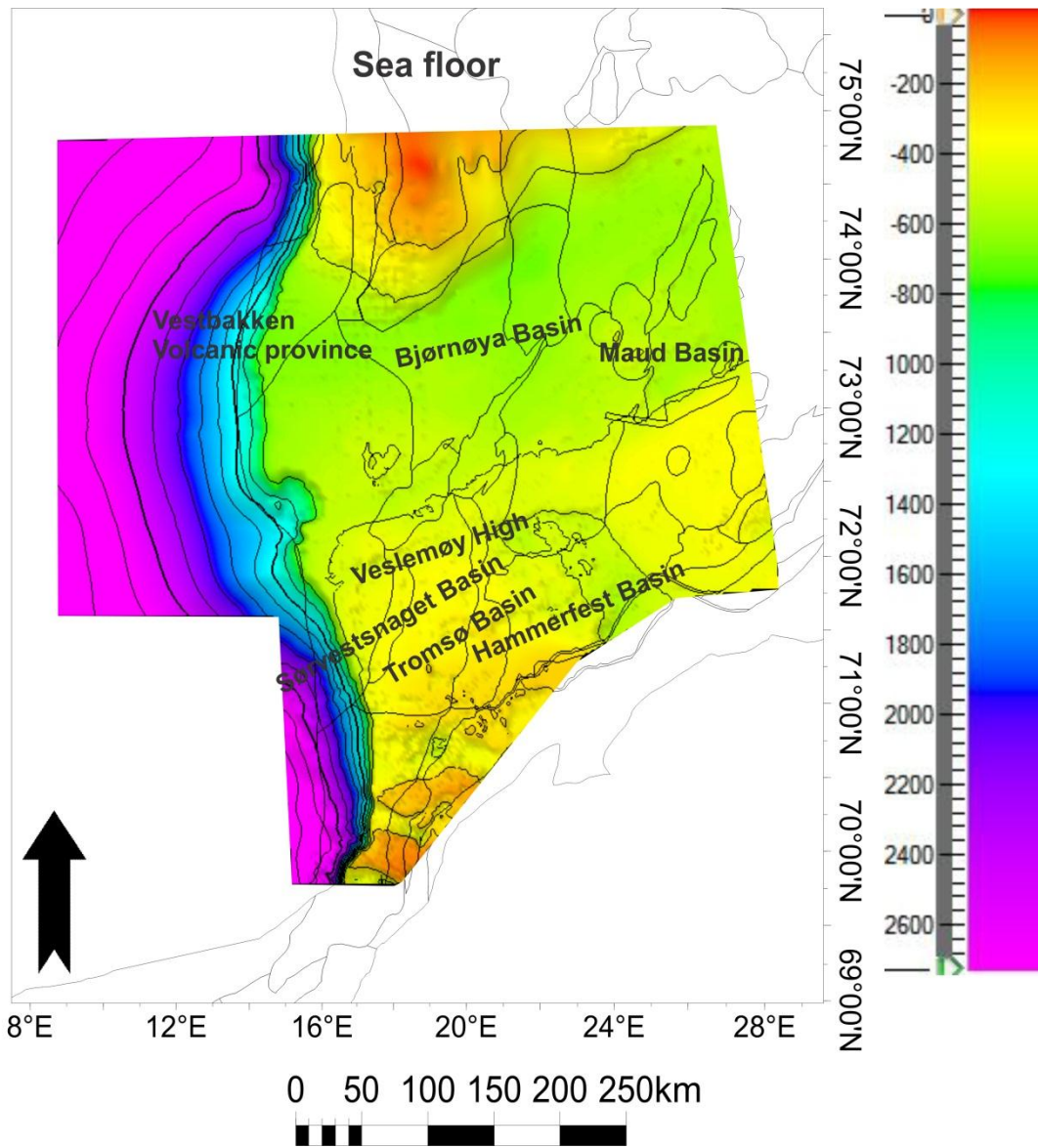


Fig3-3: showing overall seafloor bathymetric map of the study area with structural elements defines the overall pattern of seafloor.

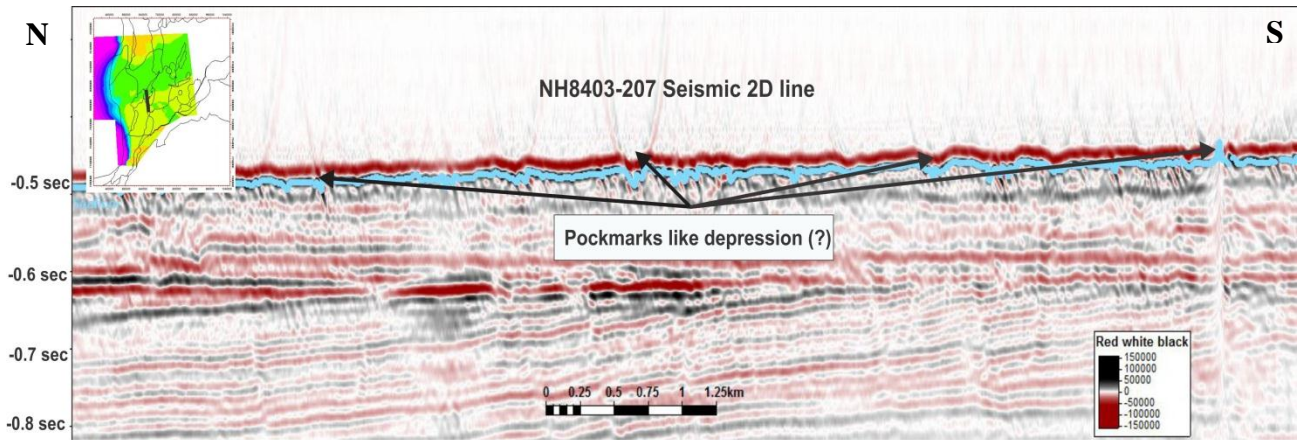


Fig3-4: showing the distribution of Pockmarks like depression on seafloor while map window shows the location of seismic line

3.1.2 Torsk Formation

The Torsk formation is present almost everywhere in my study area of SW Barents Sea except in Loppa High (fig 3.5 and 3.6). The Torsk Formation reveals a medium to good continuity and exhibit a medium to high amplitude reflection pattern. URU (Upper regional unconformity) is significant regional erosive surface truncates the underlying older sequences and is characterized by overdeepened, glacially eroded trough (Vorren et al., 1989). The top of the Torsk formation varies in depth but mostly lies at shallow depth ranges from 300 ms to 600 ms (TWT) except in Sørvestsnaget Basin, where top of the Torsk formation penetrated at the depth of 1900-2000 ms (TWT).

The thickest part of Torsk unit occurs at shelf break and showing stepwise progradational depositional pattern toward Paleo slope and parallel layering to the basin floor. The upper part of the unit is characterized by low angle, shingled clinoforms that are dipping towards the south-west (fig 3.5) and are interpreted to be probably formed in response to the uplift of Loppa High which acts as a sediment source during Eocene to mid-Miocene (Vorren et al., 1991). The overlying sequence of Torsk formation could be glacial in origin showing chaotic reflection pattern representing slumped material or mud flow deposits in areas of Tromsø Basin, Vaslemøy High, southern Bjørnøya area, Loppa High.(fig 3.5)

Towards the Loppa High the base of Torsk formation is defined by marked angular unconformity of BTU representing hiatus on the Loppa High area (fig 3.7)

The Torsk Formation is getting thinner on eastern side of the study area including areas of Veslemøy High, , Hammerfest Basin, Stappen High and southern Bjørnøya area. (fig 3.6)

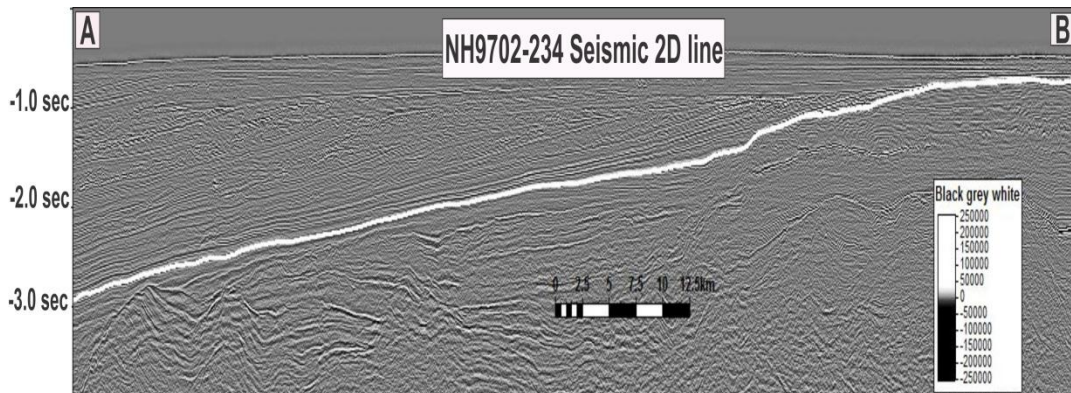
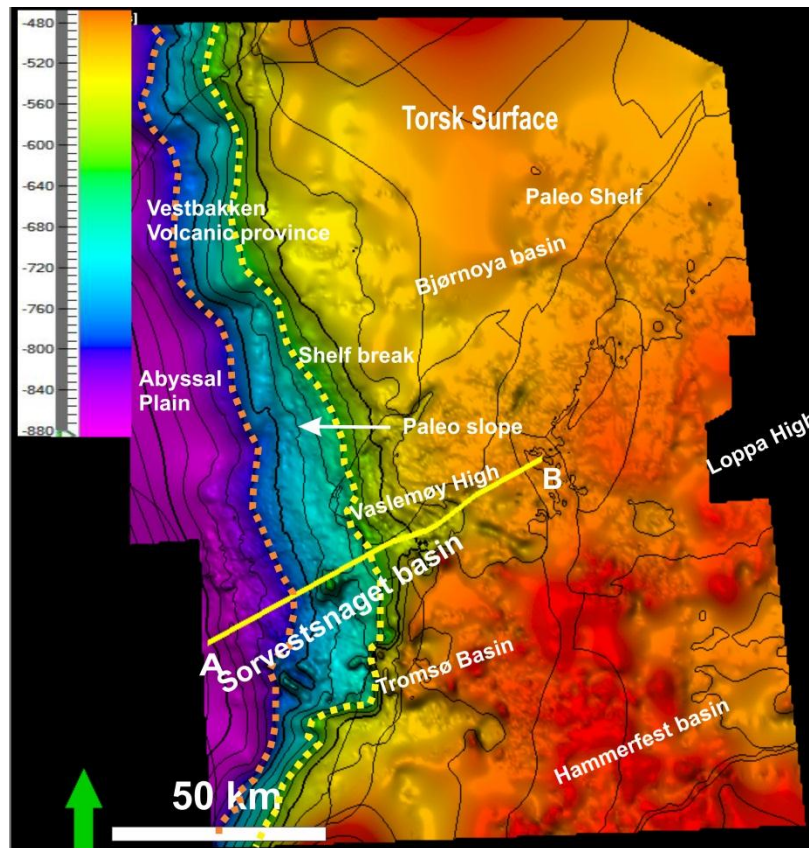


Fig 3-5: showing progradational depositional pattern of Torsk formation around the eastern side of Loppa High and Sorvestsnaget Basin.

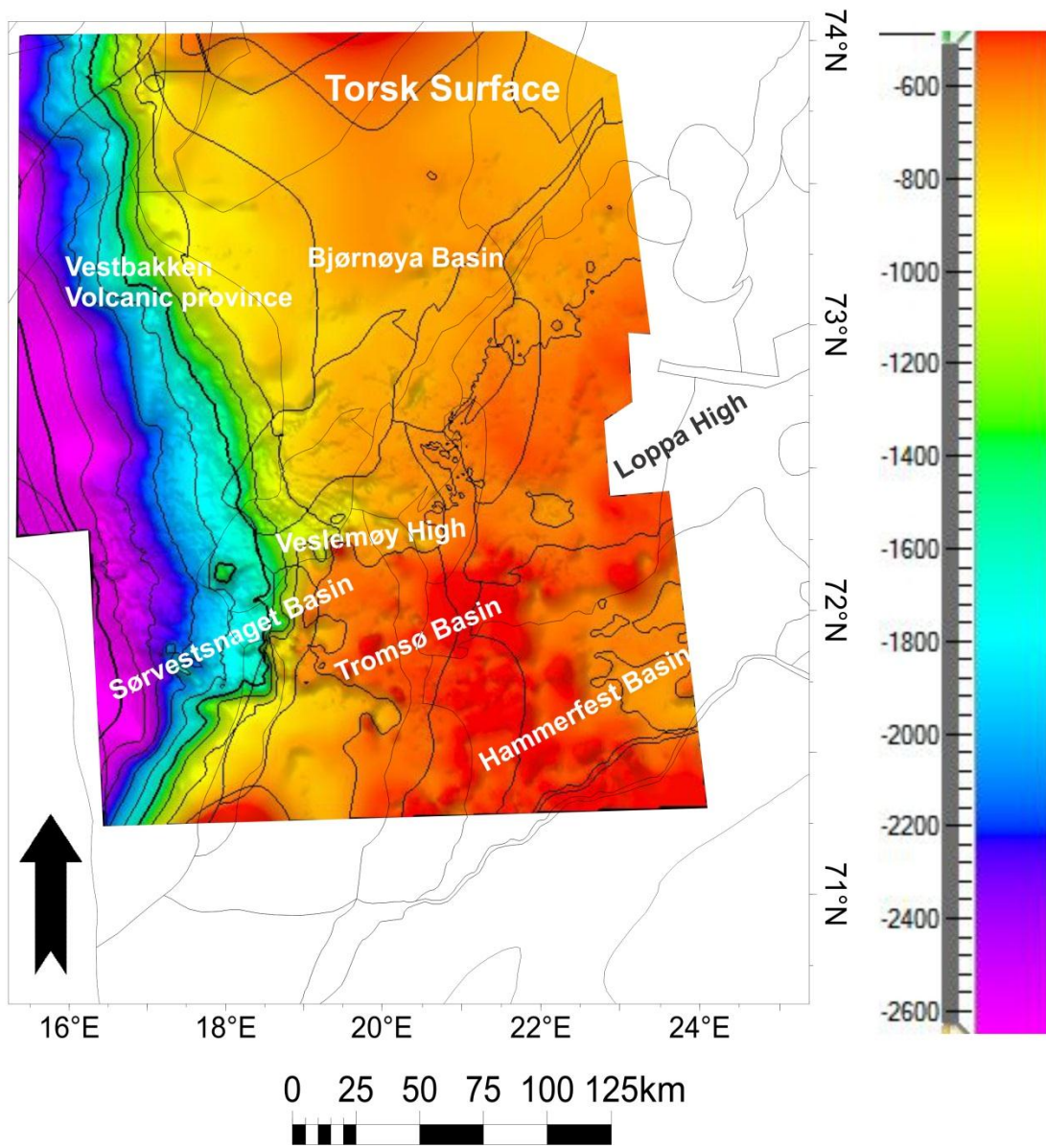


Fig3-6: showing the distributional pattern of Torsk Formation on western side of the study area.

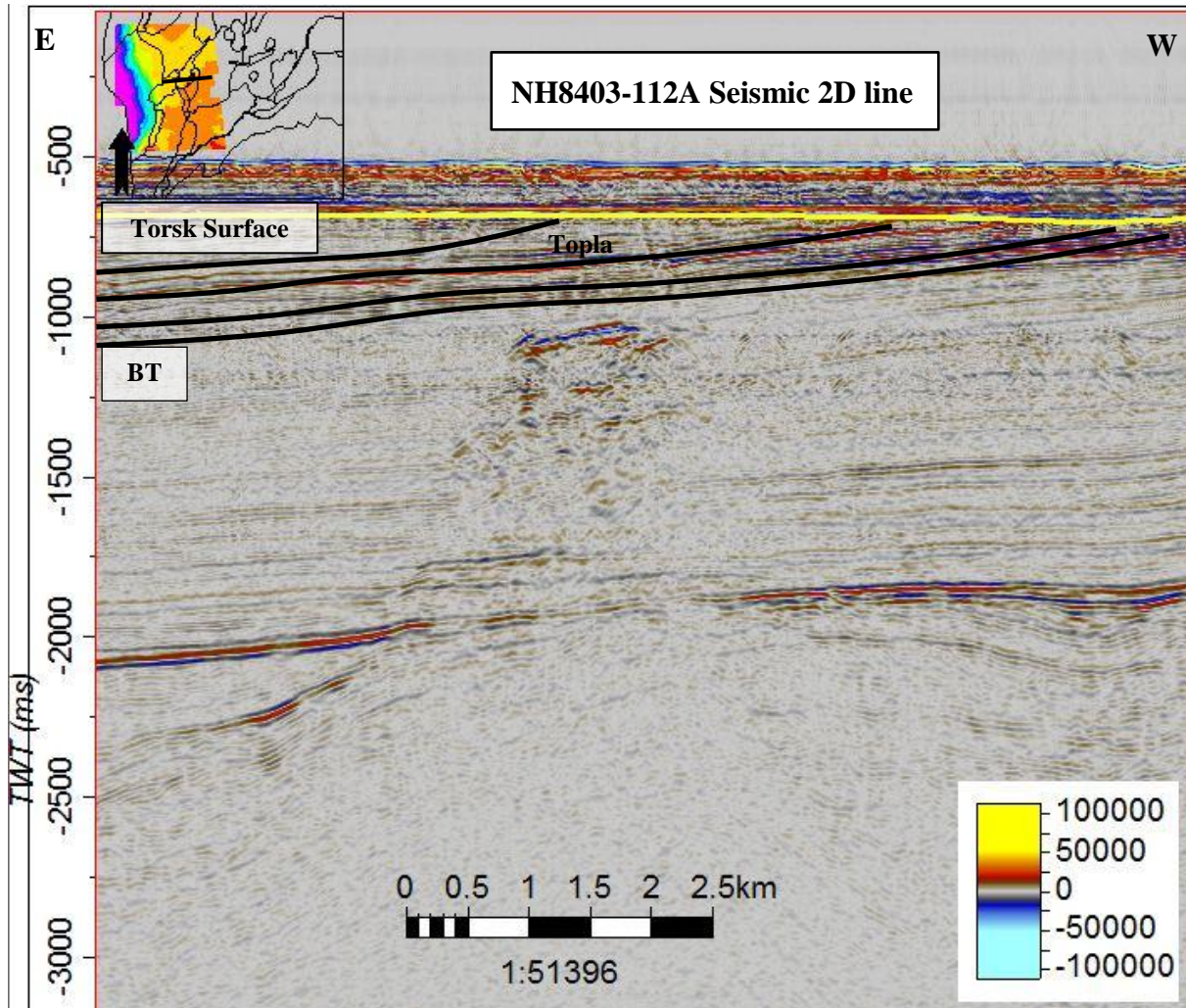


Fig3-7: showing the underlying dipping layer of Bottom Tertiary unit (BTU) cross cutting the Torsk formation in western flank of Loppa High.

3.1.3 Kolmule Formation

The Kolmule formation is a lower Cretaceous unit in SW Barents Sea and is well exposed in my study area except in Loppa High where it is interpreted to be eroded from uplift of the Loppa High (fig 3.8). The Kolmule formation reveals a medium to good continuity and exhibit a medium to high amplitude reflection pattern. It represents a part of paleo shelf sediments with prograding dipping reflections in the Veslemøy High area and in Sørvestsnaget Basin .Internal configuration of Kolmule formation is marked by random

distribution of high amplitude anomalies. Kolmule formation varies in depth from 1200 ms (TWT) to around 4000 ms (TWT) in Sørvestsnaget Basin.

The Kolmule surface shows the gentle, low relief surface in area of Veslemøy High and like Torsk surface, it shows progradation and a clinoformal depositional pattern in Sørvestsnaget Basin (fig3.10). In the Tromsø Basin, Kolmule surface are bulged into dome like structures caused by salt diapirism structure (fig 3.9; fig 3.11).

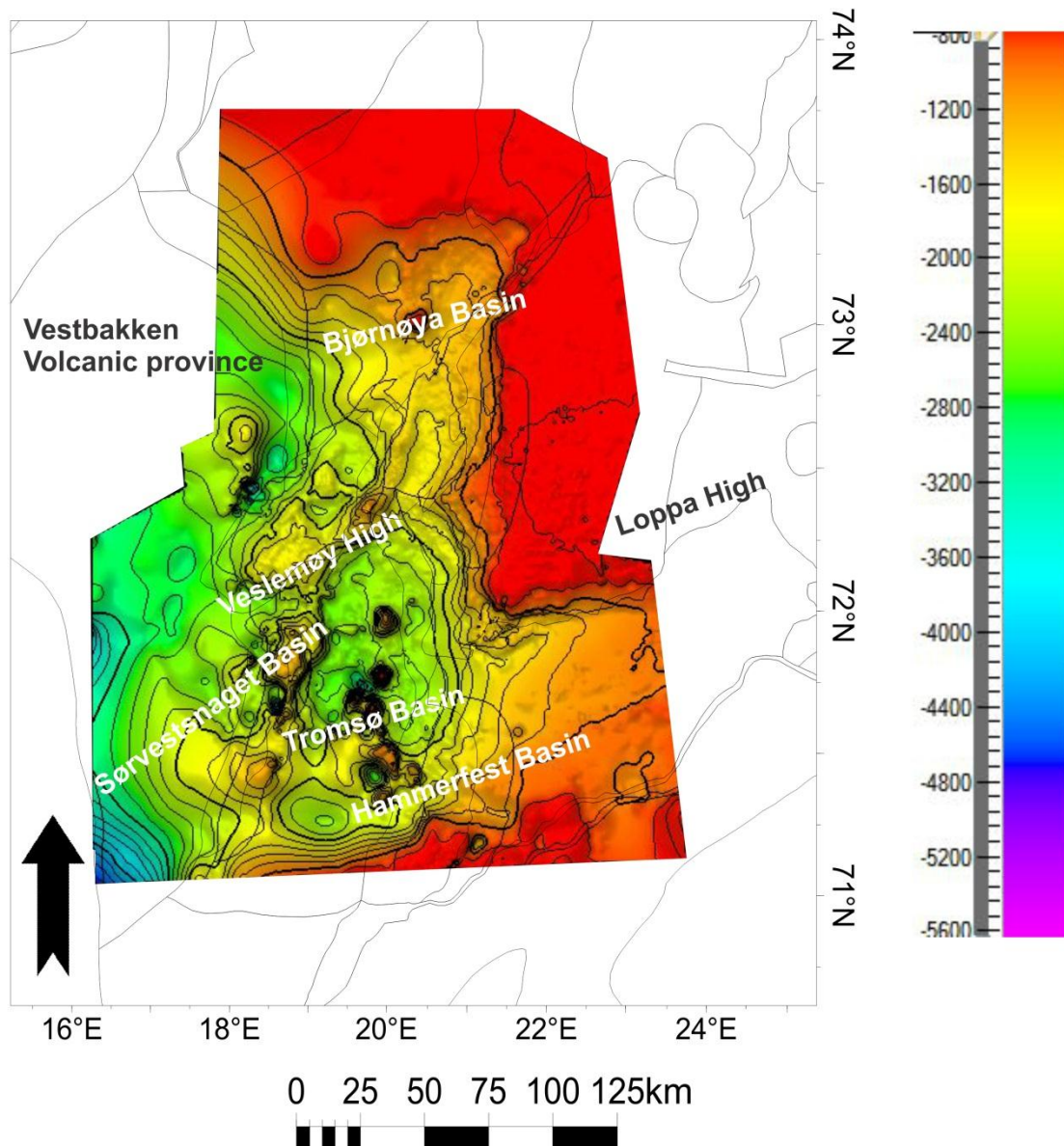


Fig 3-8: Map window showing the distribution of Kolmule formation towards the western side of the study area while on eastern side it is truncated by Loppa High.

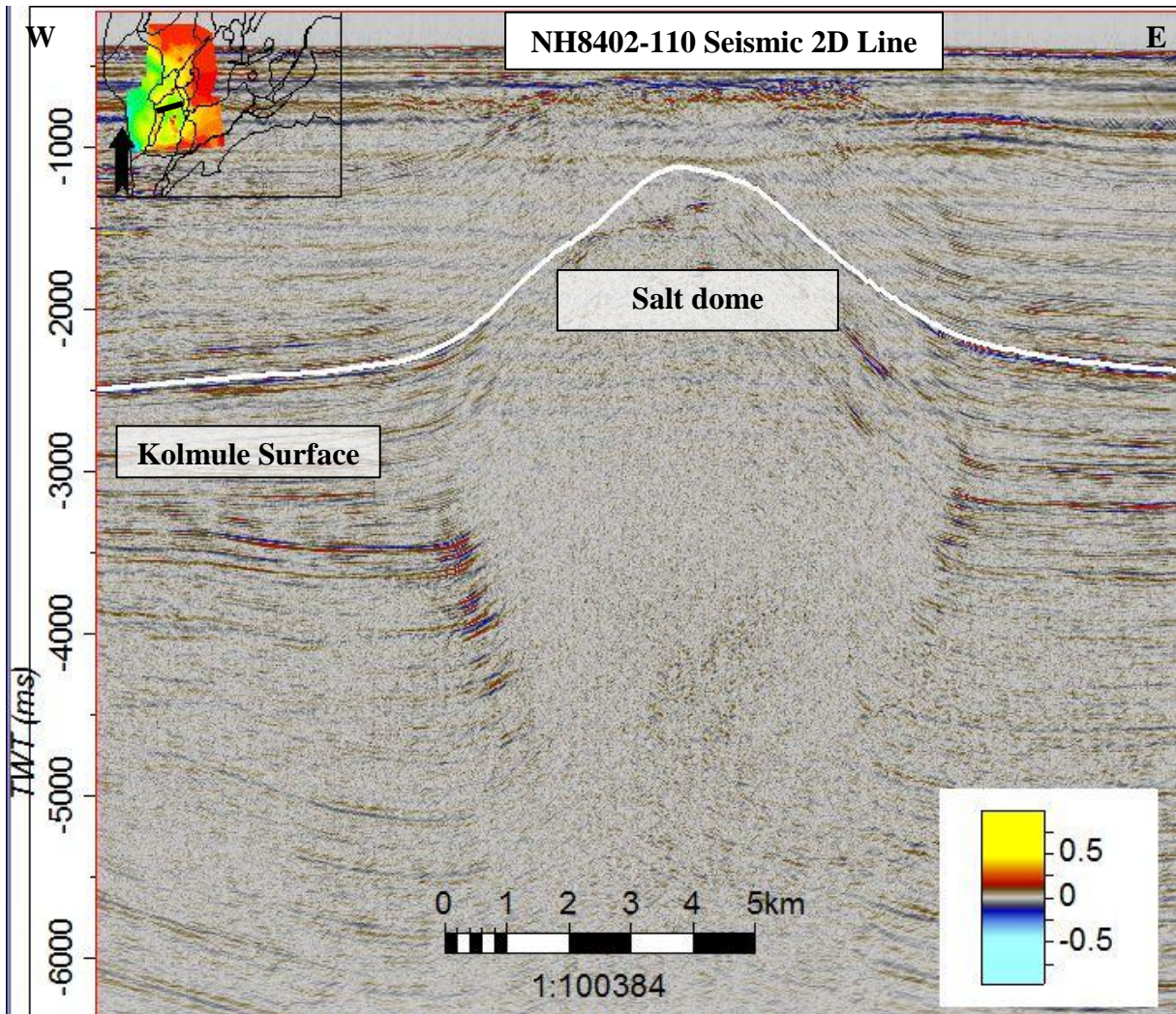


Fig 3-9: showing the bulging out of Kolmule formation caused by salt diapirism in Tromsø basin of SW Barents Sea. While Map window in the small box showing the location of seismic line

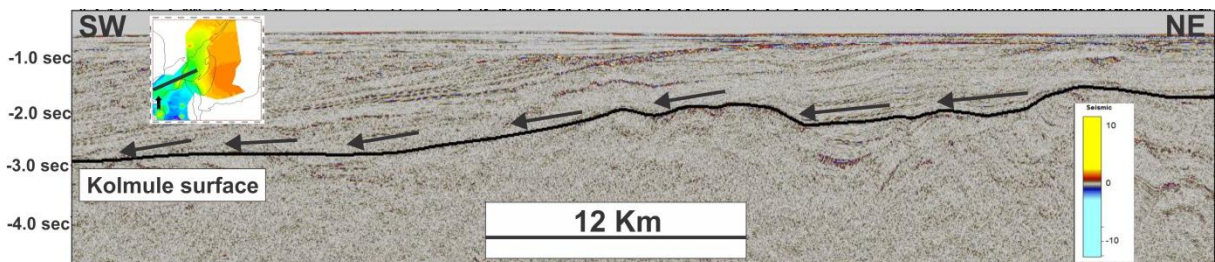


Fig 3-10: showing progradational depositional pattern of Kolmule surface in western margin of the study area (Sørvestsnaget Basin).

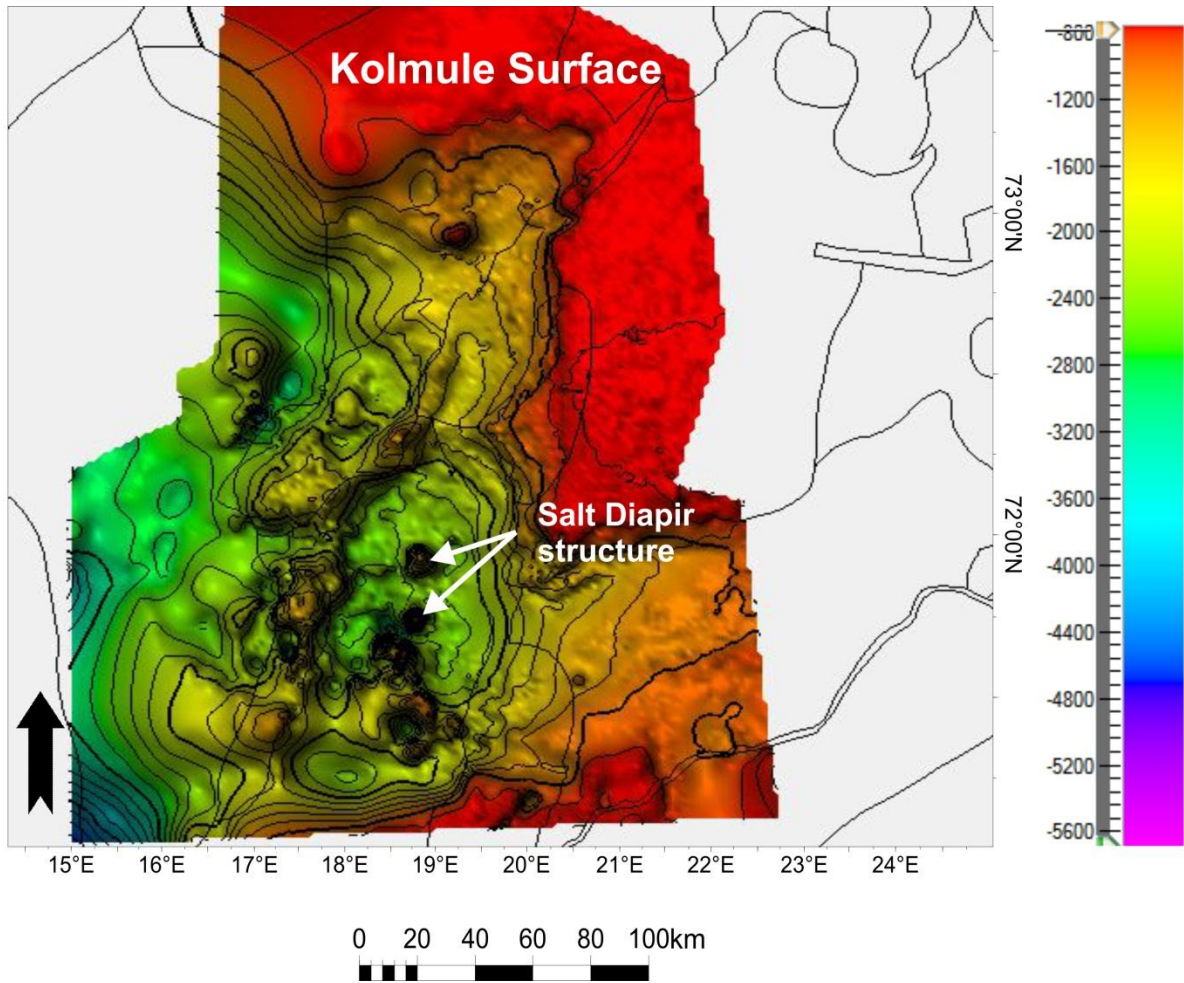


Fig3-11 showing salt diapirs structure on Kolmule surface

3.1.5 Hekkingen Formation

The Hekkingen formation of the upper Jurassic units occurs mostly in the eastern half of the Barents Sea. It is characterized by cross cutting semi graben faulted structure that have high amplitude reflection pattern and can easily be recognized on seismic data (fig 3.13). In the western half of the study area, Hekkingen formation cannot be recognized by two reasons; either it is too deep to be mapped or data is very bad or chaotic. It is prominent in the area of Hammerfest Basin, Finnmark west, Maud Basin, Svalis Dome. It varies in depth from 2000 ms (TWT) in Hammerfest Basin and getting shallower in the Finnmark West area and Maud Basin where it lies at depths of around 1000 ms (TWT) and 800 ms (TWT) respectively. Hekkingen formation pinches out in the area of the Tromsø Basin , Bjørnøya

Basin and Loppa High (fig 3.12). In areas of Hammerfest Basin, internal configuration of Hekkingen formation is severely disturbed by gas chimneys (3.28; 3.30 and 3.36). Hekkingen formation tends to be shallower in NW part of Hammerfest Basin (fig 3.14)

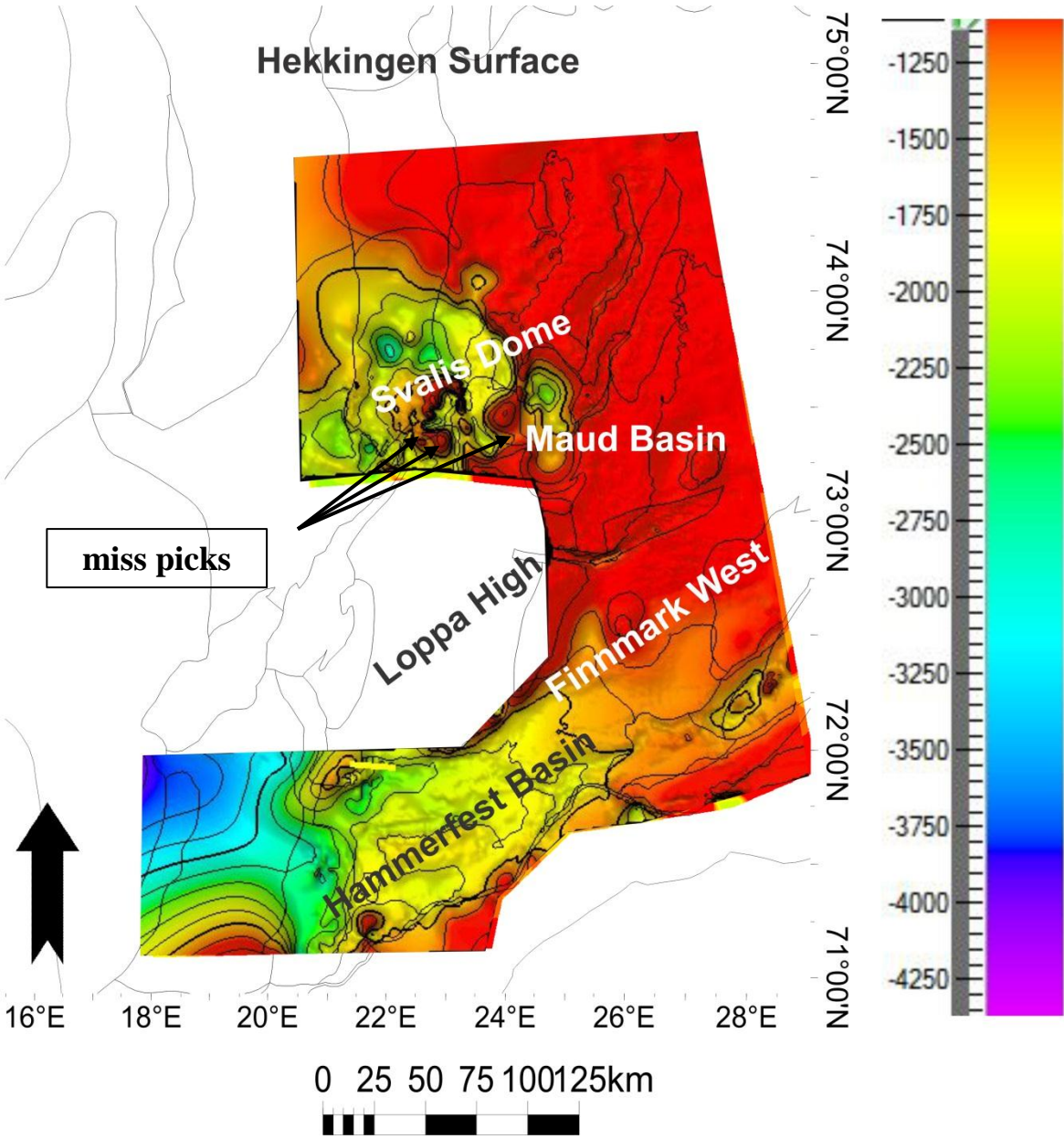


Fig3-12: showing the distributional extent of Hekkingen formation together with NPD structural elements in my study area which are mostly exposed in the eastern side and are truncated by Loppa High in western side.

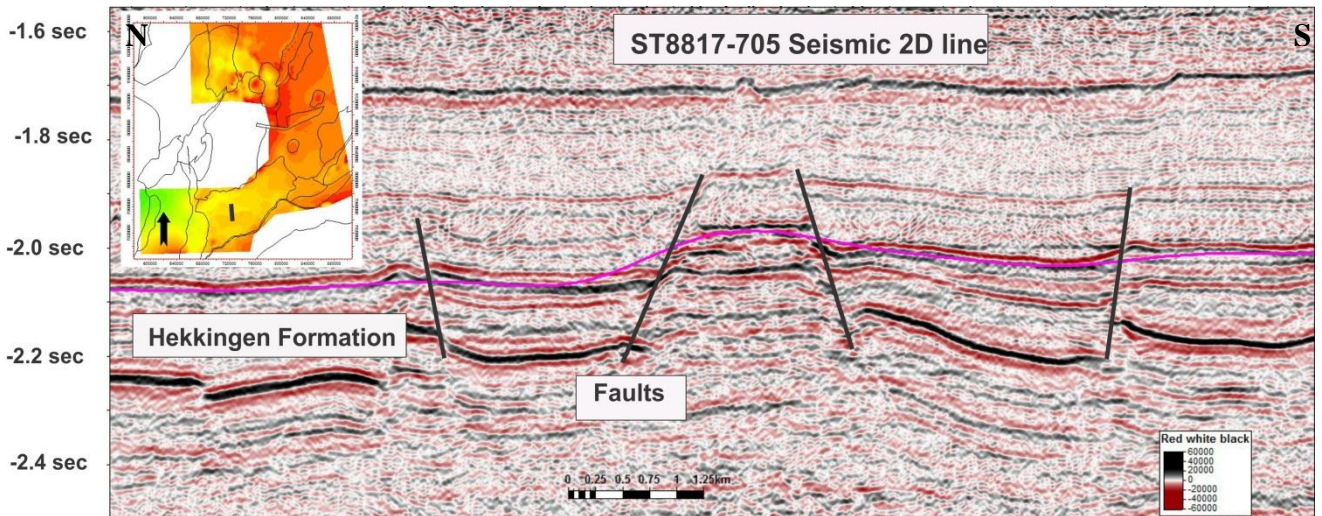


Fig3-13: showing the semi graben structures that are characteristic of Hekkingen formation in most part of my study area. Whereas map window in the small box showing the location of seismic line.

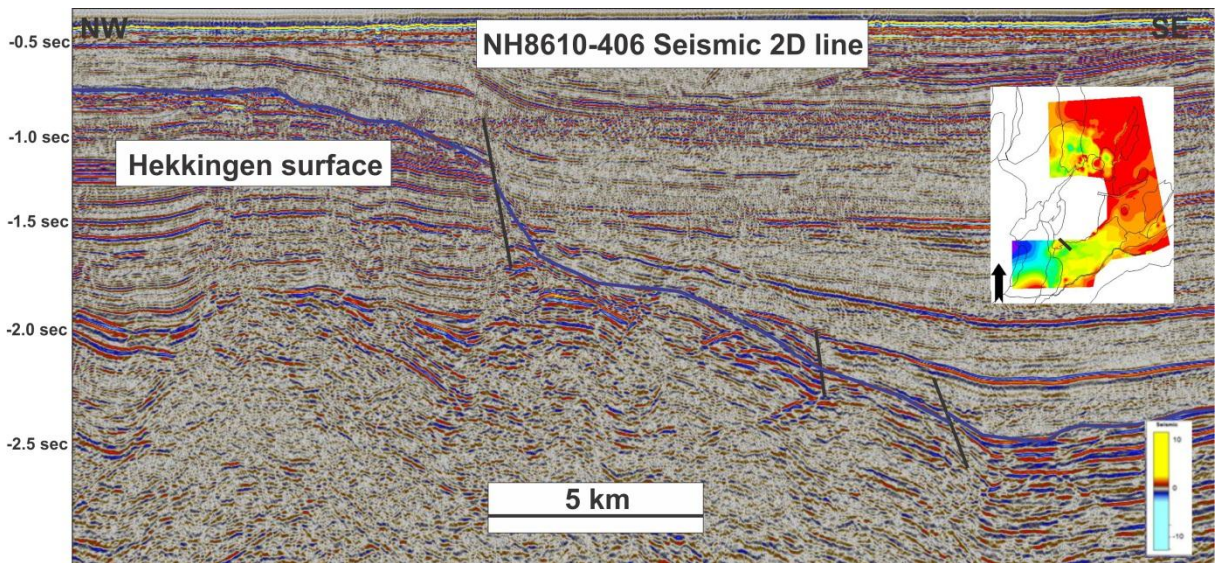


Fig3-14: showing the shallowing of Hekkingen formation that has been crosscutted by several faulting on northwestern side of Hemmerfest Basin whereas map window showing the location of seismic line.

3.1.6 Snadd Formation

The Snadd formation is a lower Triassic unit that mostly occurs in parts of southern Bjørnøya Basin, around the Veslemøy High and further east in the area of Finnmark West

and Maud Basin. The surface shows westward thickening over the Loppa high area and northward thickening in the study area as shown in fig 3.15. Snadd formation is correlated with S4 unit of Glørstad-Clark et al., (2010). It is characterized by continuous, high amplitude and parallel seismic reflection pattern. In some areas, internal configuration of Snadd formation is marked by randomly distribution of medium to high amplitude reflection pattern. The clinoforms have limited to no topset and bottomset development. Towards the Loppa High the sequence is eroded by base cretaceous unconformity or the Upper Regional Unconformity (URU) so it is hard to determine any thickness variation. (fig 3.16)

Towards the east of Loppa High, it is characterized by discontinuous, high amplitude and parallel seismic reflector. On western flank of Loppa High, Snadd formation slipped westward due to Ringvassøy-Loppa Fault Complex contributing to the formation of tilted fault block as shown in fig 3.17.

Snadd formation varies in depth from -2200 ms (TWT) to -1200 ms (TWT) in Hammerfest Basin and southern Bjørnøya Basin.

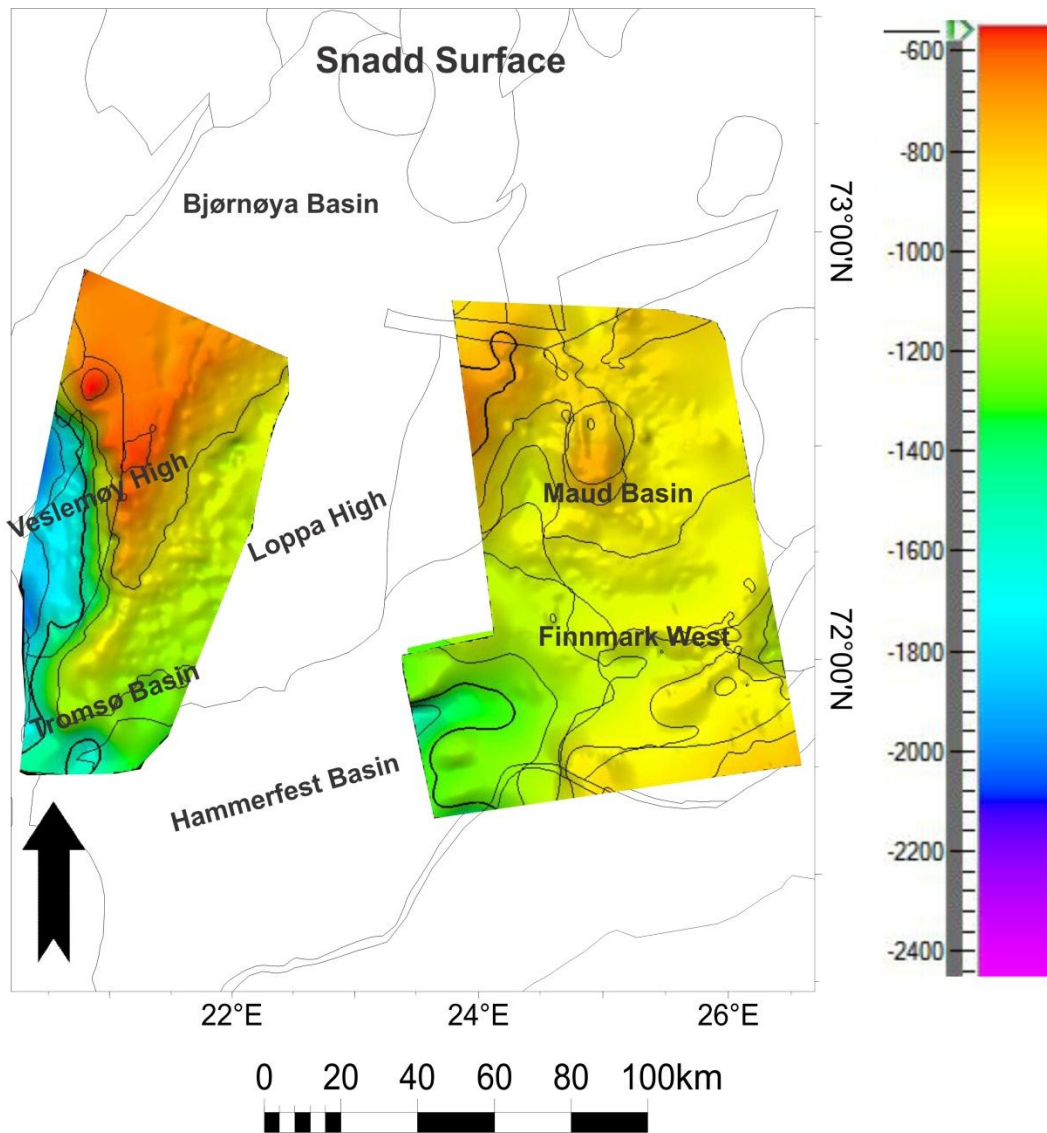


Fig3-15: showing overall distribution extent of Snadd formation in study area.

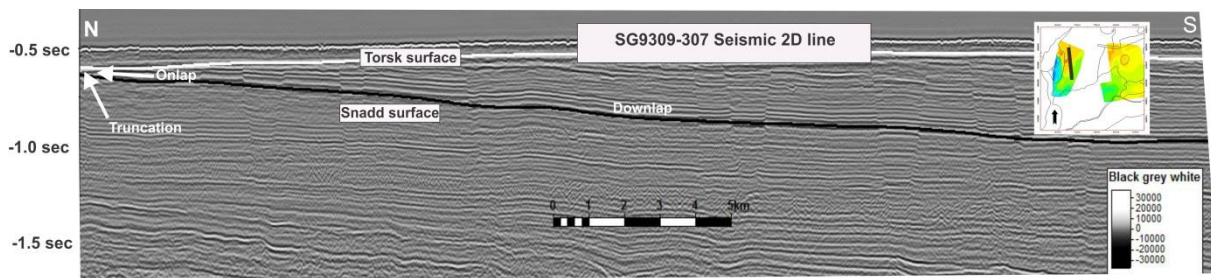


Fig3-16: showing the onlapping of Snadd surface towards the Torsk surface where they are truncated towards the western direction at the depth of around -0.7 ms (TWT) in southern Bjørnøya area of SW Barents Sea.

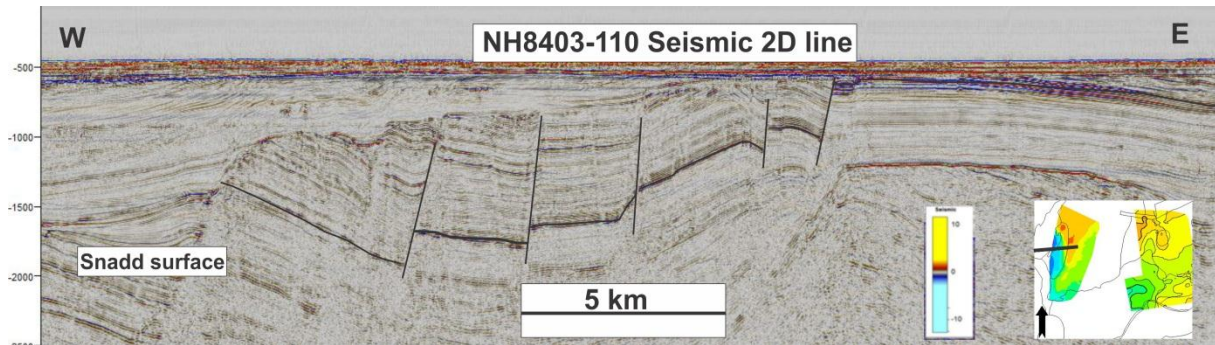


Fig 3-17: showing the westward slippage of Snadd surface caused by Ringvassøy-Loppa Fault Complex in the western flank of Loppa High. Map window showing the location of seismic line.

3.1.7 Ørn Formation

The Ørn formation is a lower Carboniferous unit in Western Barents Sea and occurs in southern part of Bjørnøya Basin and east of Loppa High (fig 3.18). The top of the formation reflection reveals a very bad continuity due to disrupted ,partly chaotic of the seismic data and exhibit a low to medium amplitude reflection pattern The internal seismic reflector vary from high reflectivity band representing carbonate facies. The low frequency part of the group has a more chaotic to subparallel appearance. This unit varies in depth from -1200 ms (TWT) to -2500ms (TWT)..Some downlapping clinofolds are observed at the eastern flank of Loppa High (fig 3.19). It is correlated over to the western side of paleo-Loppa High.

The weak seismic amplitude at depth of the Ørn Formation limits the possibilities of a good interpretation and due to this reason it cannot be interpreted towards the western side of the study area.

The Ørn formation is generally thinning from the Finnmark West towards paleo-Loppa High, , and further continues to thin along the eastern flank of paleo-Loppa High (fig 3.20). Ørn formation is not identified west of the Ringvassøy-Loppa Fault Complex which could be caused by changes in depositional environment, topography or the poor seismic resolution due to deeper burial in the western basin may change the seismic signature of Ørn formation.

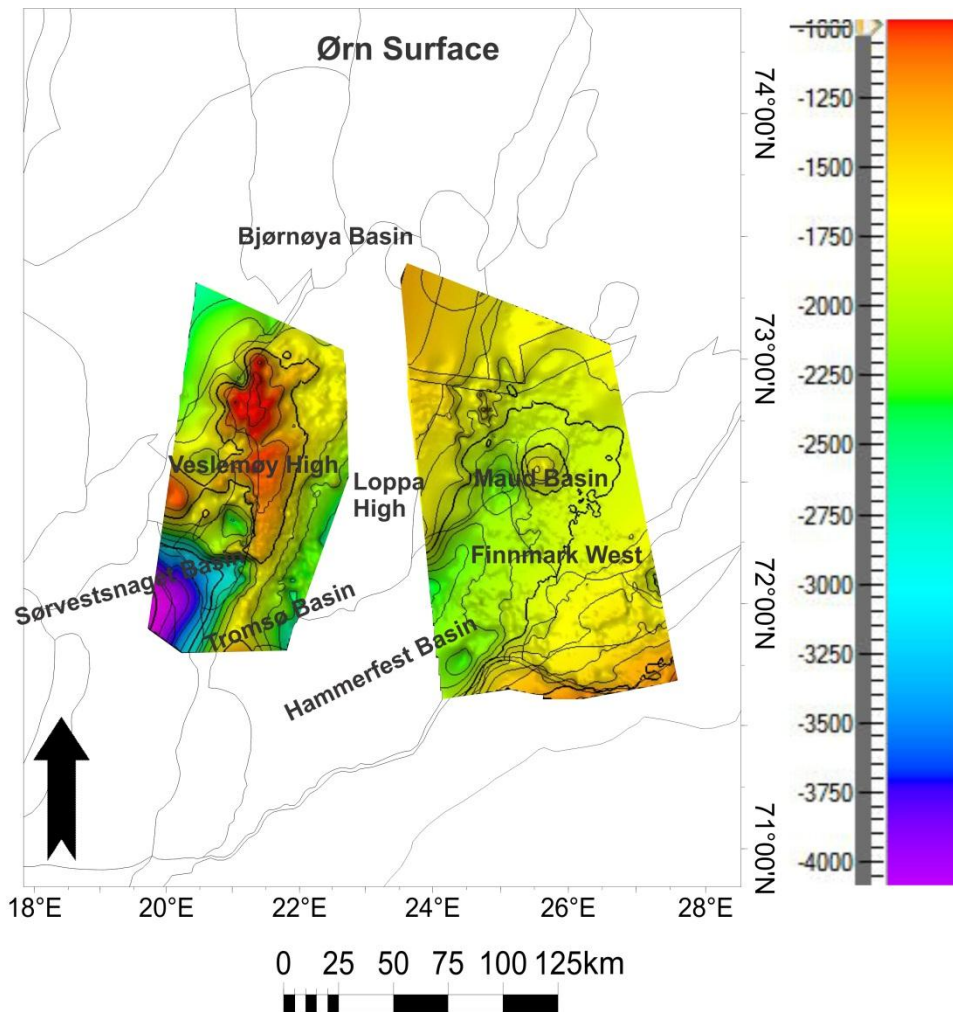


Fig 3-18: Map window showing overall distribution of Ørn surface across the study area.

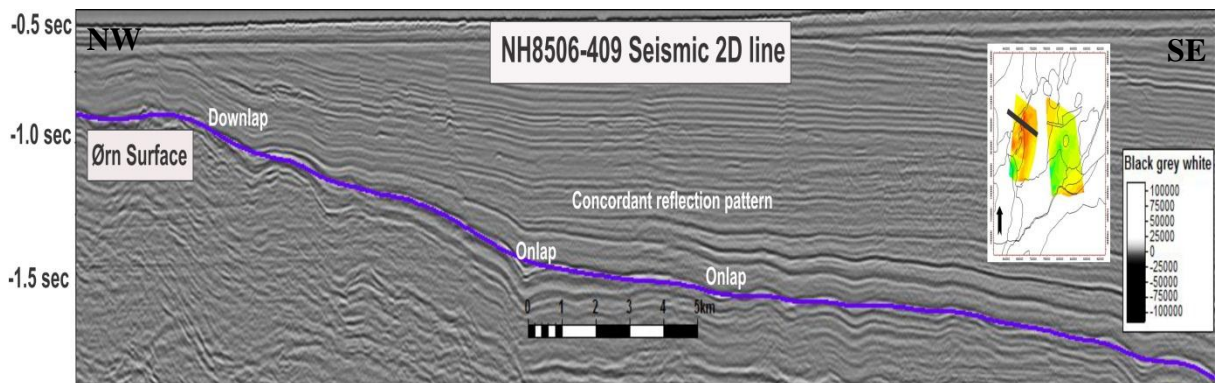


Fig3-19: showing interpreted onlap and downlap of Ørn surface west of Loppa High area. The layer above the Ørn surface shows the Concordance reflection pattern in accordance with Ørn surface. Map window in the small box shows the location of seismic line.

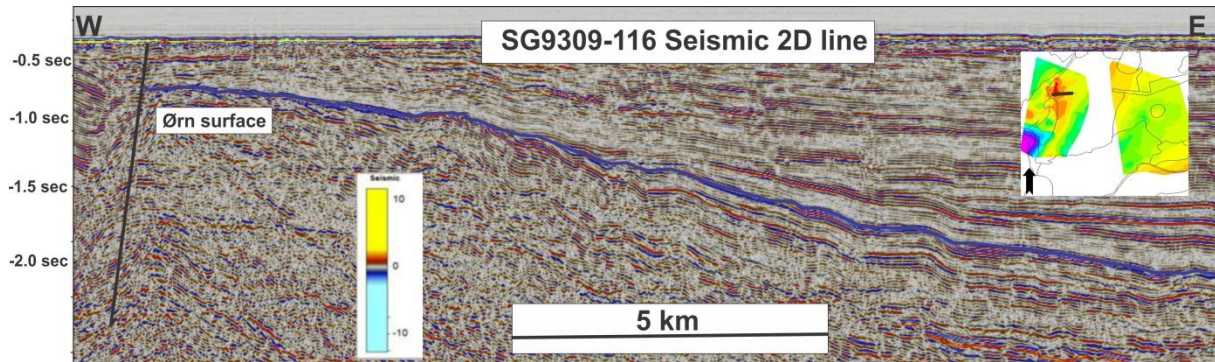


Fig3-20: showing the thinning of Ørn formation towards the western side and are truncated by Ringvassøy-Loppa Fault Complex whereas map window in the small box shows the location of seismic line.

3.1.8 Bottom Tertiary Unit (?)

Bottom Tertiary Unit (BTU) lies between Torsk and Kolmule formation and is characterized by medium to very high reflection pattern. Just like Torsk formation, it also shows progradational depositional pattern that are dipping towards south west in Sørvestsnaget Basin (3.22). It is also characterized by random distribution of high amplitude anomalies. On western side of Loppa High It is truncated by Upper Regional Unconformity where westerly dipping strata truncated against URU. It varies in depth from -800 ms (TWT) to over -3000 ms (TWT).

BTU is locally distributed in study area along the western flank of Loppa High, Sørvestsnaget Basin, Veslemøy High and in some part of Tromsø Basin. (fig 3.21)

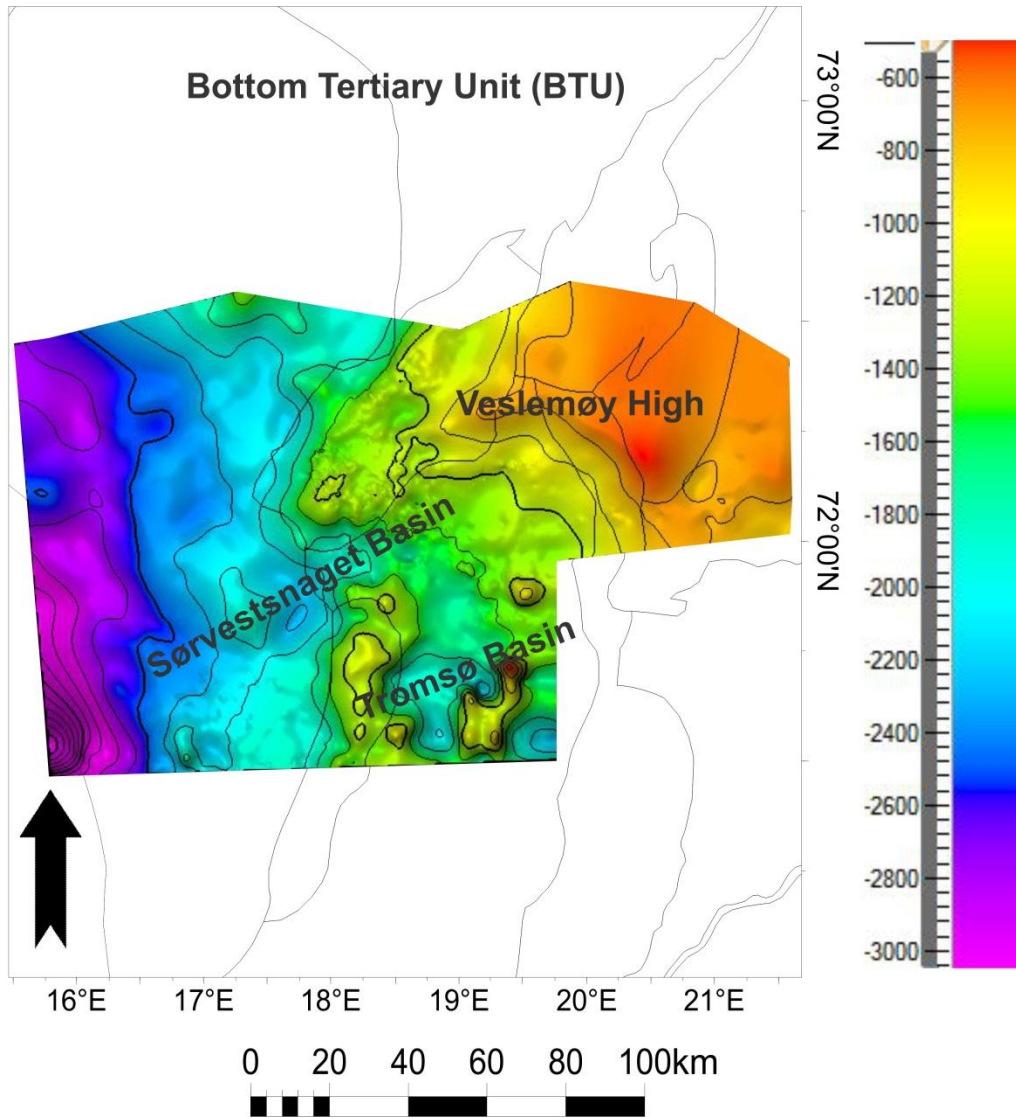


Fig 3-21: Map window showing the overall distribution pattern of Bottom Tertiary Unit.

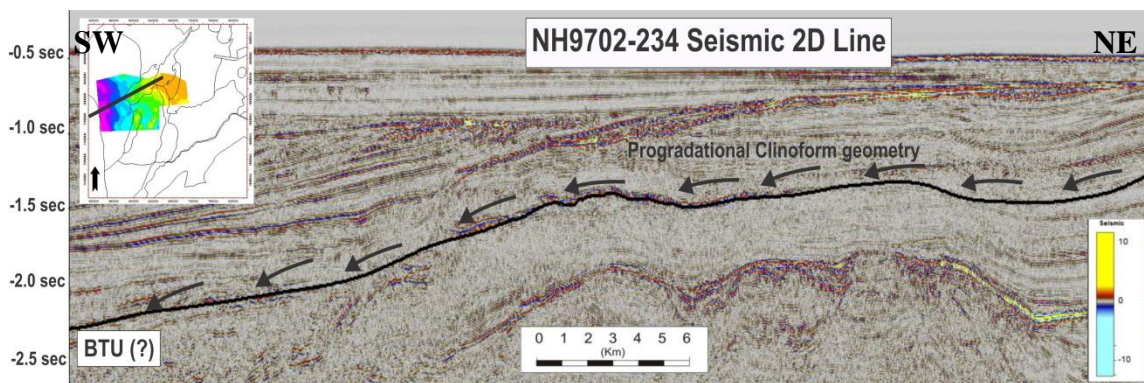


Fig3-22: showing progradation clinoform geometry of Bottom Tertiary Unit whereas small box indicating the location of seismic line.

3.1.9 Bottom Cretaceous Unit (?)

It represent the erosive horizons at the top of the listric asymmetrical fault block where horizons prograding westwards that are cut down into deeper strata(fig 3.24). BCU unit is controlled and limited by the main faults (Bjørnøyrenna Fault Complexes) due to this continuity of BCU is difficult to interpret (fig 3.24). These Faults are asymmetrical normal fault that are characterized by less lateral extent, N-S trending and dipping towards west .They are mostly penetrated in western side of Loppa High, some parts of Tromsø Basin so they are locally extent (Fig 3.23).It varies in depth from -1000 ms (TWT) to -2000 ms (TWT).BCU reveals low to medium seismic reflection pattern and in some area randomly distribution of high seismic anomalies can also be observed.

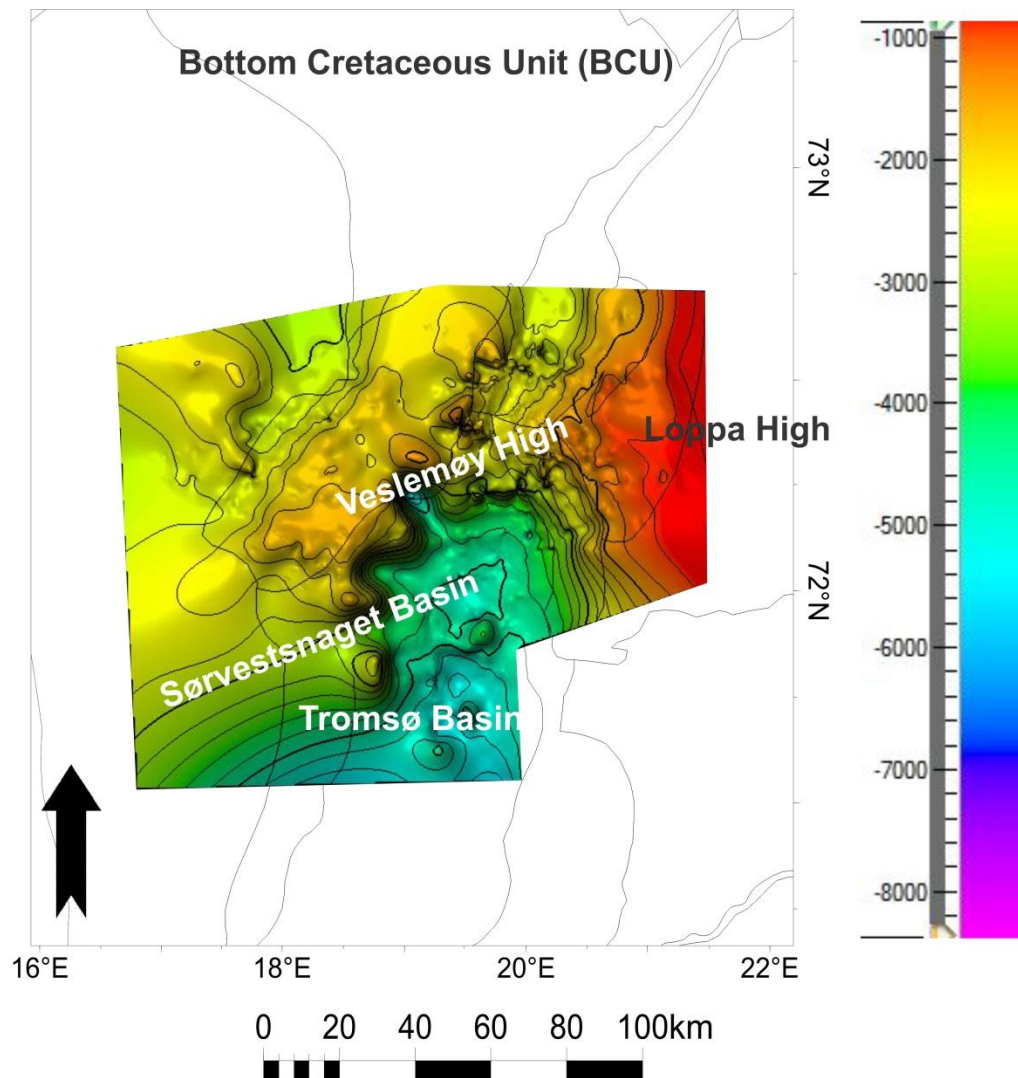


Fig3-23: Map window showing the overall distribution pattern of Bottom Cretaceous Unit.

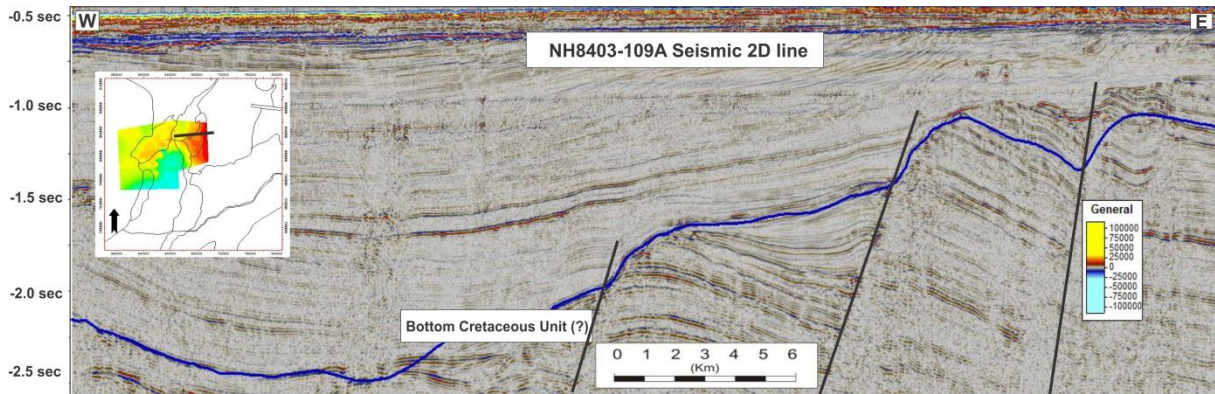


Fig3-24: showing depositional pattern of BCU over east of Loppa High appeared as erosive surface crosscutted by faults. Small box showing the location of seismic line.

3.2 Fluid Leakage Features

Seismic reflection methods have been important tools in shallow-gas investigations as they provide a rapid means of identifying and mapping fluid leakage features (Judd and Hovland, 1992). Hydrocarbon leakage can often be recognized on seismic data as it causes an acoustic, mechanical or diagenetic changes in the geological sequences. Direct indication for fluid migration and seepage can be identified in specific features both at seabed and in the subsurface including gas chimneys, mud diapirs, bright spots, acoustic turbidity zones and paleo-surface expression such as buried mud volcanoes and pockmarks (Hovland & Judd, 1988; Cartwright et al., 2007; Løseth et al., 2009).

Areas with vertical seismic masking occur in several places in the study area. These zones vary in horizontal and vertical extent and, shape. The zones of acoustic masking in vertical columns terminate in amplitude anomalies mostly in the shallow subsurface. The amplitude anomalies are chaotic, discontinuous, and in some places show slightly lower frequency and push-down effects. Such seismic indicators are related to focus fluid migration from deeper to shallower levels. The upper termination is defined where the acoustically masked zone goes over to an amplitude anomaly. Lower termination is defined where the acoustic masked seismic stops. The presence of gas is inferred from high amplitude anomalies and reverse polarity of seismic reflection compared with seafloor polarity showing positive polarity

In this part of the result chapter, I will present observations and interpretations of fluid leakage structures and fluid accumulations from the different basins and basement highs of the SW Barents Sea. The last sub-section will then show the overall distribution of fluid leakage structures in the SW Barents Sea that has been earlier mapped by Vadakkepuliambatta et al., (2012) and integrated into this study.

Based on the distribution of fluid flow features, I have sub-divided fluid leakage chapter into five parts which are;

3.2.1 Gas Chimneys.

3.2.2 Fault related fluid leakage.

3.3.3 Small pipe like structures.

3.3.4 Salt diapirs structure.

3.3.5 Distribution of fluid flow features.

3.2.1 Gas Chimneys:

Gas chimneys (Gas clouds) result from migration of hydrocarbon through faults between source rocks and seabed. Due to capillary resistance, the fluid moves up towards the surface, thereby dropping the pressure and solution gas is released and as a result some gas still present in pore spaces of sediment causing the change in acoustic property of the rock. (Heggland 2003; Heggland et al., 2001; De Groot, 2001).

Gas chimneys are found to be very common in the study area. All of the chimneys terminate with a high amplitude anomaly at the top where Torsk formation lies. Gas chimneys in my study area are characterized by intense acoustic masking. At some places acoustic masking is too intense to identify the lower termination of gas chimneys.

Generally gas chimneys could be originated from deep seated faulted or from Hekkingen or older formation. Chimneys break through the different stratigraphic packages including Snadd formation, Hekkingen formation, Bottom Cretaceous unit (BCU), Bottom Tertiary unit (BTU) and Kolmule formation but its upper termination by bright spots in sediments of Cenozoic age (Torsk formation). Most of the chimneys structure seems to be related with faults. Some of the examples are described below showing appearance of gas chimneys in my study area including:

In the following figure 3.25, the chimney zone disturbed wide vertical zone of around 5 km in width. The base of chimney zone cannot be recognized due to the limitation of seismic data whereas top of the chimney is recognized by high amplitude reflection and shallow gas accumulation just beneath the Torsk formation. The chimney structure resemble like a domal structure. The internal seismic reflection is better seen as compared to the lower part where seismic reflection appears to be chaotic and disturbed. The vertical extent of chimney zone is around -1000 ms where high amplitude anomalies and shallow gas accumulation can be observed at the depth of around -1000 ms (TWT) and -800 ms (TWT) respectively. On eastern part of seismic section fluid tends to migrate upward through Kolmule formation from chimneys zone thereby given the impression of narrow zone of chaotic reflection pattern across the westerly dipping strata.

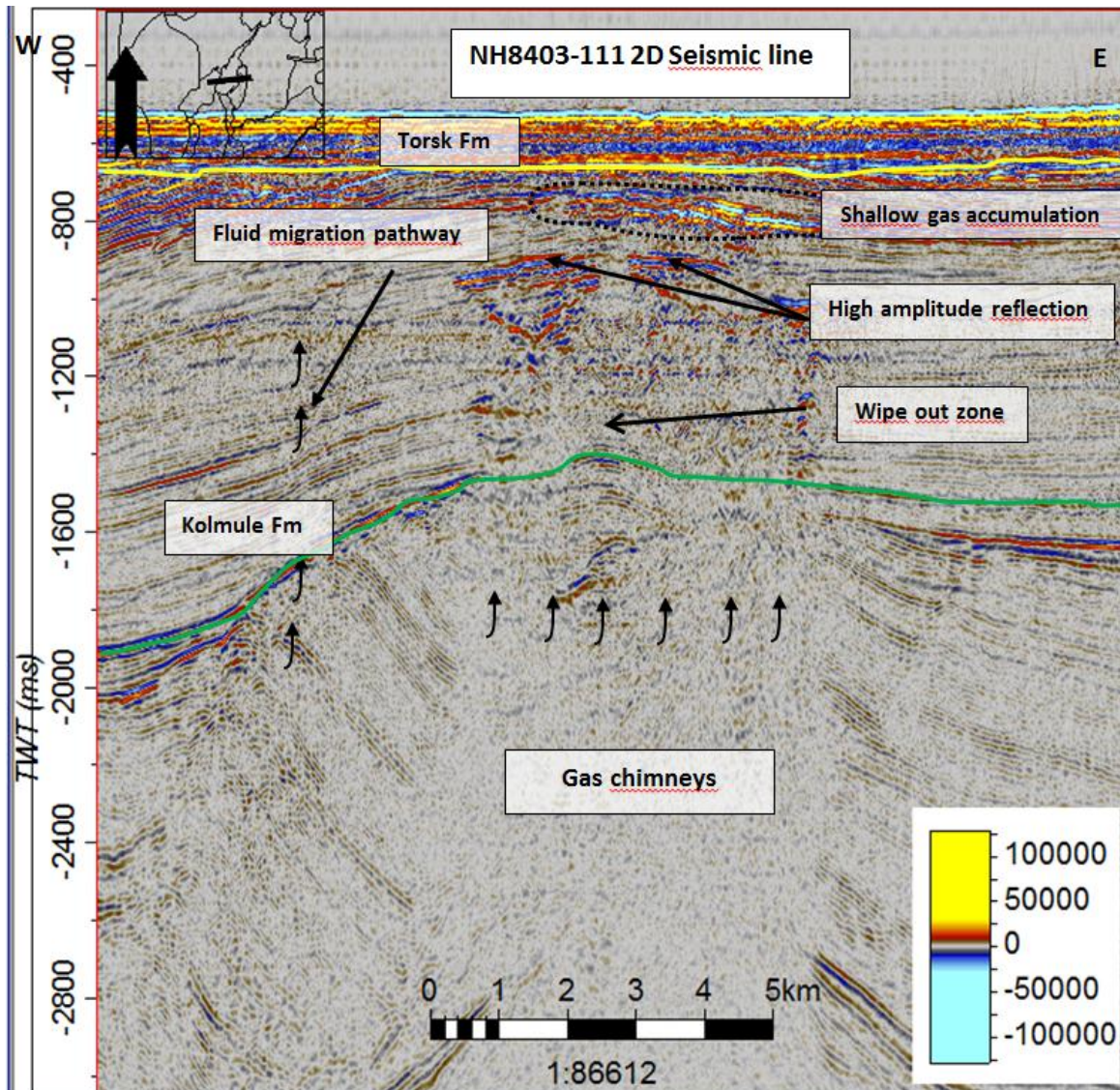


Fig3-25: The fluid migrating vertically from gas chimney zone that have distorted the seismic reflection.

Chimney is wider and longer, having no basal termination but on seismic section it seemed to be originated from -2800 ms TWT and reaching the top at -600 ms TWT just beneath the Torsk formation (Figure 3.26). It shows a lateral extent of 8.5 km². An interesting feature can be seen at around -700 ms (TWT) where high amplitude anomalies are cross cutting lithological boundaries suggested to represent the formation of gas hydrates. At around 1100 ms (TWT) Bright spots features can be observed. In addition to this, acoustic masking related features can be observed beneath the cross cutting high amplitude anomalies. Acoustic masking disturbed the sequence of Kolmule and BCU. They start as distorted

reflections and evolve to a full zone of acoustic masking as the high amplitudes develop to a maximum. The seismic character of the stratigraphic interval beneath high amplitude reflector showing chaotic reflection and discontinuous reflection suggested to be resulted by presence of fluid in the sediment. On the eastern side of the seismic section at the depth of around -2000 ms (TWT), deep seated fault can be observed providing conduit pathways for fluids to be migrate from deeper hydrocarbon reservoir into shallower part of seismic section but it is not possible to follow the fault deep beneath the seismic section due to the presence of giant zone of acoustic masking

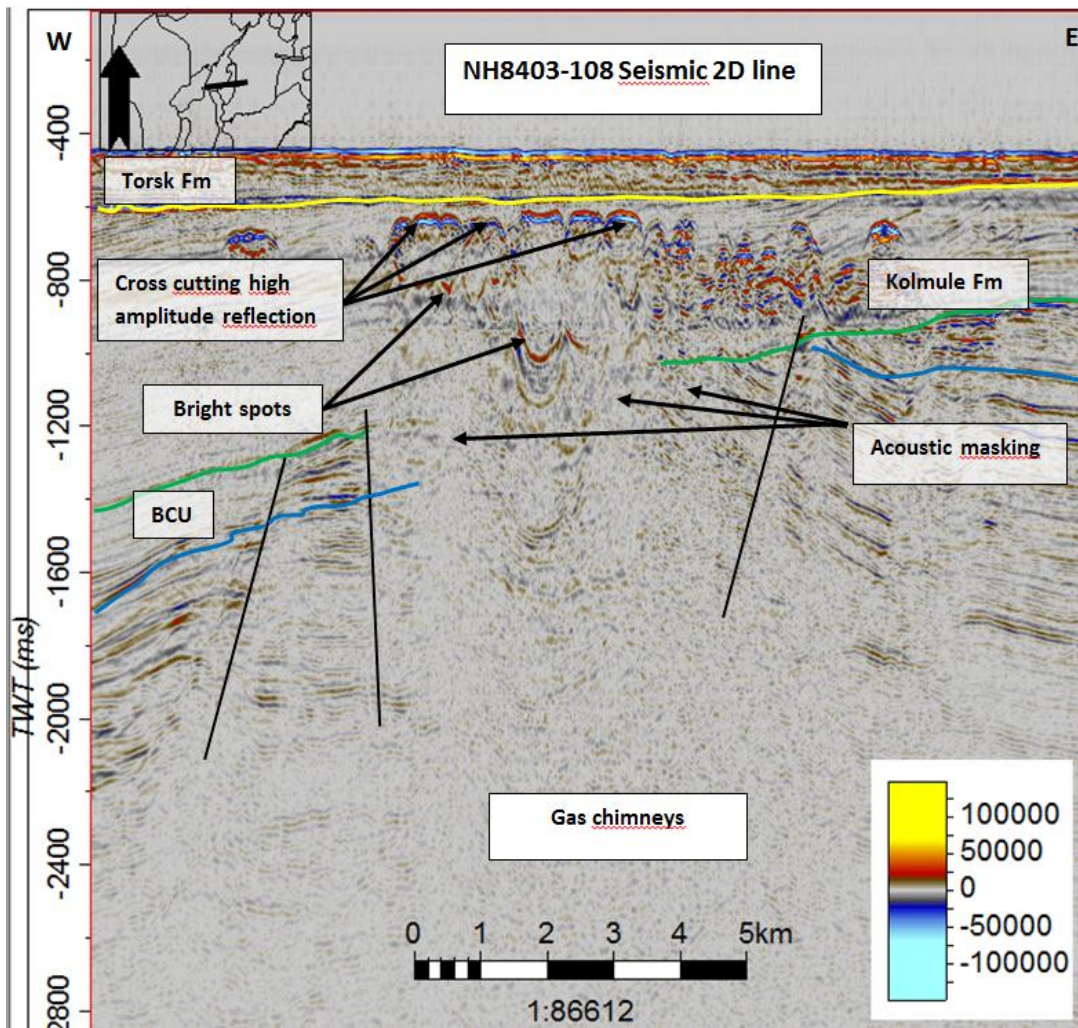


Fig 3-26: showing the t gas chimneys distorted the vertical section of the seismic section thereby creating seismic acoustic masking

On the western flank of the Loppa High along Ringvassøy-Loppa Fault complex, a large zone of acoustic masking is observed with an average width of ~10 km². The acoustic

masking is terminated by a high amplitude anomaly of Bottom Tertiary unit (BTU) that could be possibly (BSR??) that extends for ~11600 m in N-S direction, before it reaches the limit of the dataset (fig 3.27). The high amplitude anomaly occurs around -1100 ms (TWT) showing reversed polarity and dipping towards west. Another interested feature related to the possible BSR is the presence of high amplitude reflection on the eastern side as compared to the western side. The stratigraphic interval between the -600 ms (TWT) and -1000 ms (TWT) showing dipping reflector towards the west and terminated at almost horizontal reflector at -600ms (TWT) representing Torsk Formation.

The reason why this high amplitude reflector resembles like BSR?? , it runs almost parallel to seafloor although it is dipping in east-west direction, cut through major stratigraphic layer at around -600 ms (TWT) and showing reversed polarity.

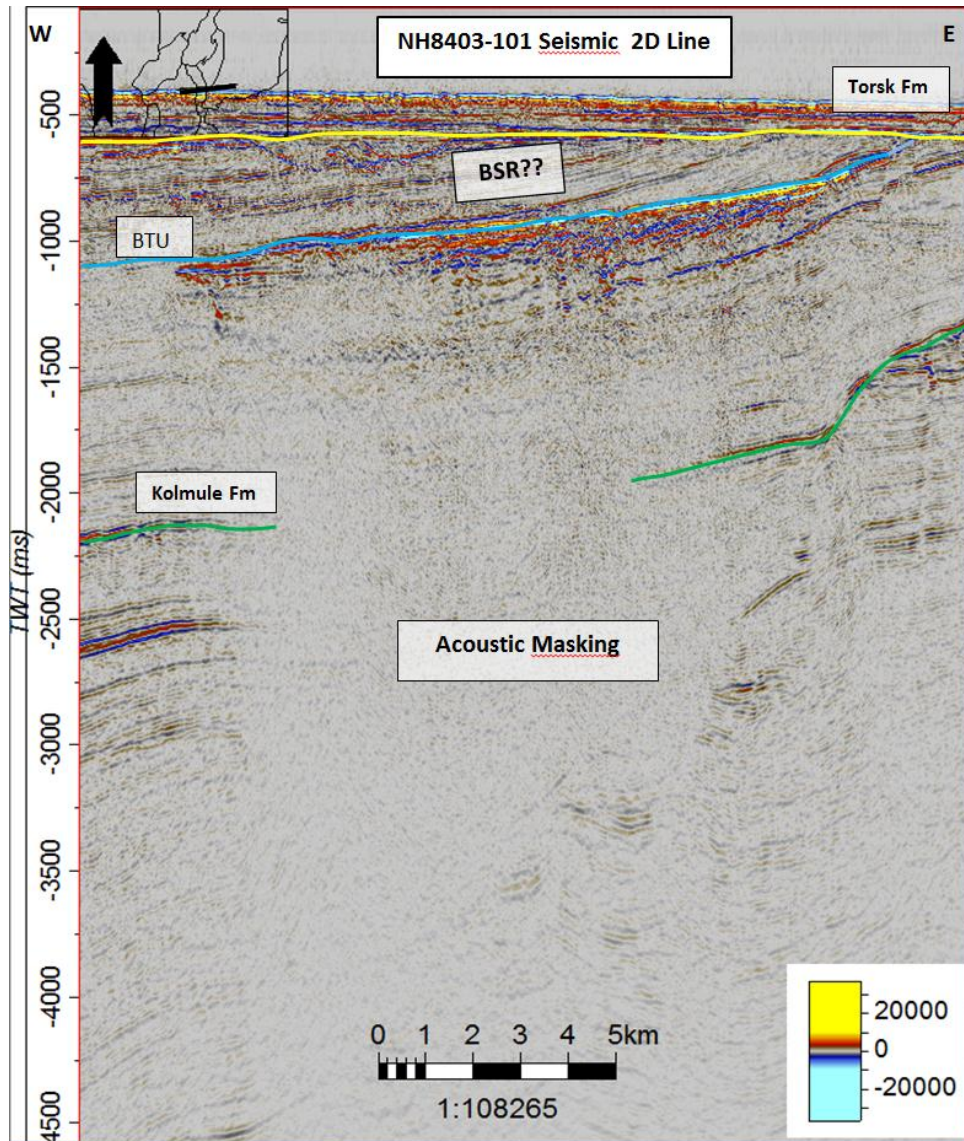


Fig 3-27: Possible gas hydrate accumulation zone west of Loppa High showing westerly dipping reflector. Heavy acoustic masking below the BSR (?) indicates vertical fluid flow.

On the Snøhvit part of Hammerfest Basin, shallow gas accumulation can be observed at the interval of around -800 ms (TWT) just beneath the Torsk formation (fig 3.28). This shallow gas accumulation shows reversed polarity as compared to the seafloor. On southwestern side, at the depth of -800 ms (TWT), the seismic character shows chaotic reflection which continue to penetrate till the end of seismic section suggesting the presence of chimney zone. The chimney zone has a width of around 5 km².

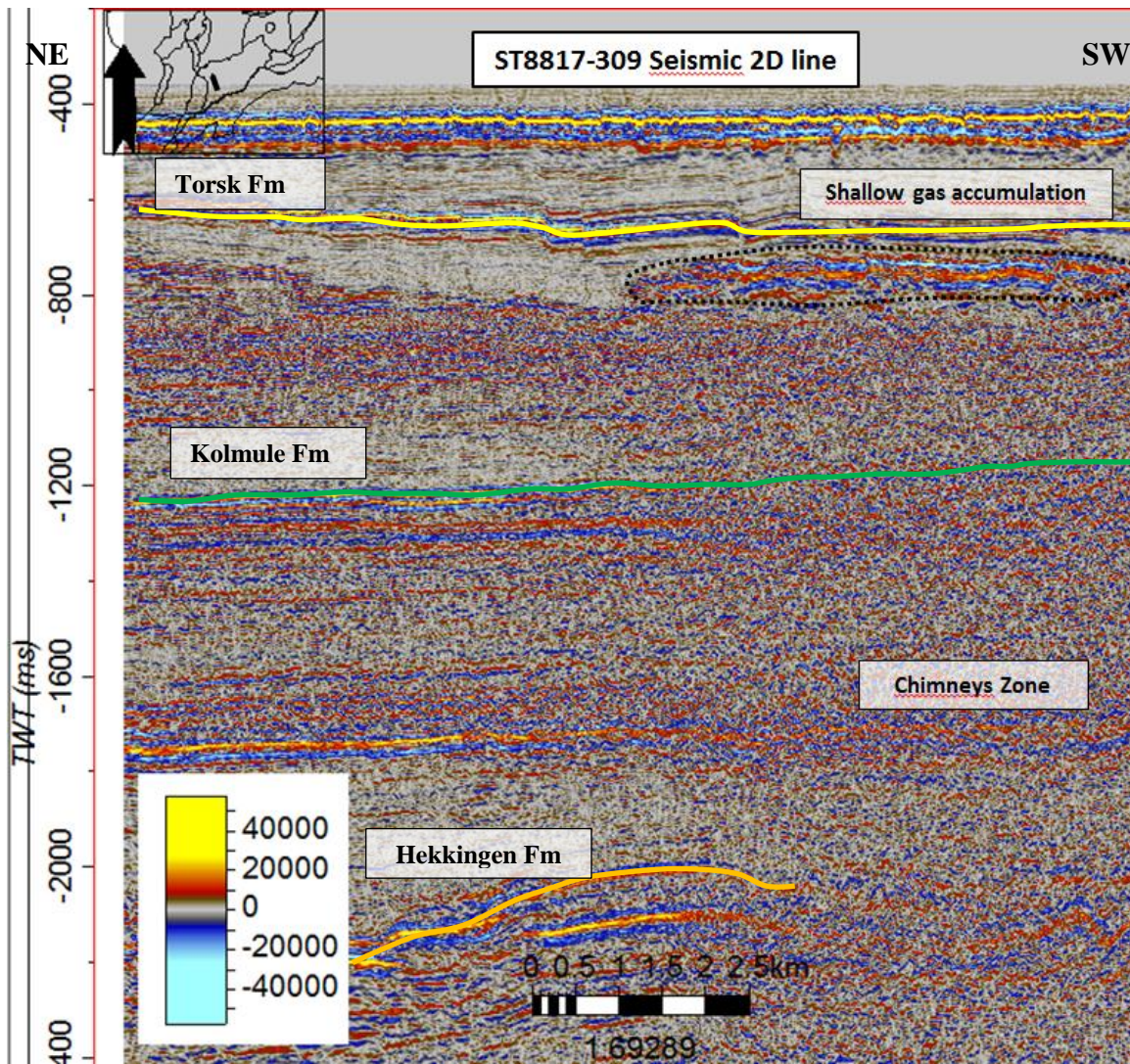


Fig3-28: showing the chimney zone feeding the gas into the shallower part of seismic section results in the shallow gas accumulation.

The zones show different sizes, both in width, shape and vertical extent. The top of the structure shows high amplitudes with reversed polarity compared to the seafloor reflection. Gas chimney distorted the entire sequence of seismic section extends down to more than ~2400 ms TWT as its basal termination is not sure yet but it can be penetrated deep, whereas its upper termination in a high amplitude reflection anomaly (bright spot) at ~-700 ms TWT (Fig 3.29). Below its upper termination acoustic masking effects can be observed that can be caused by the vertical migration of fluid to the overlying sediments. Phase reversal seismic character can be observed at the depth of around 1000-1100 ms (TWT) indicated presence of hydrocarbon in the sediments.

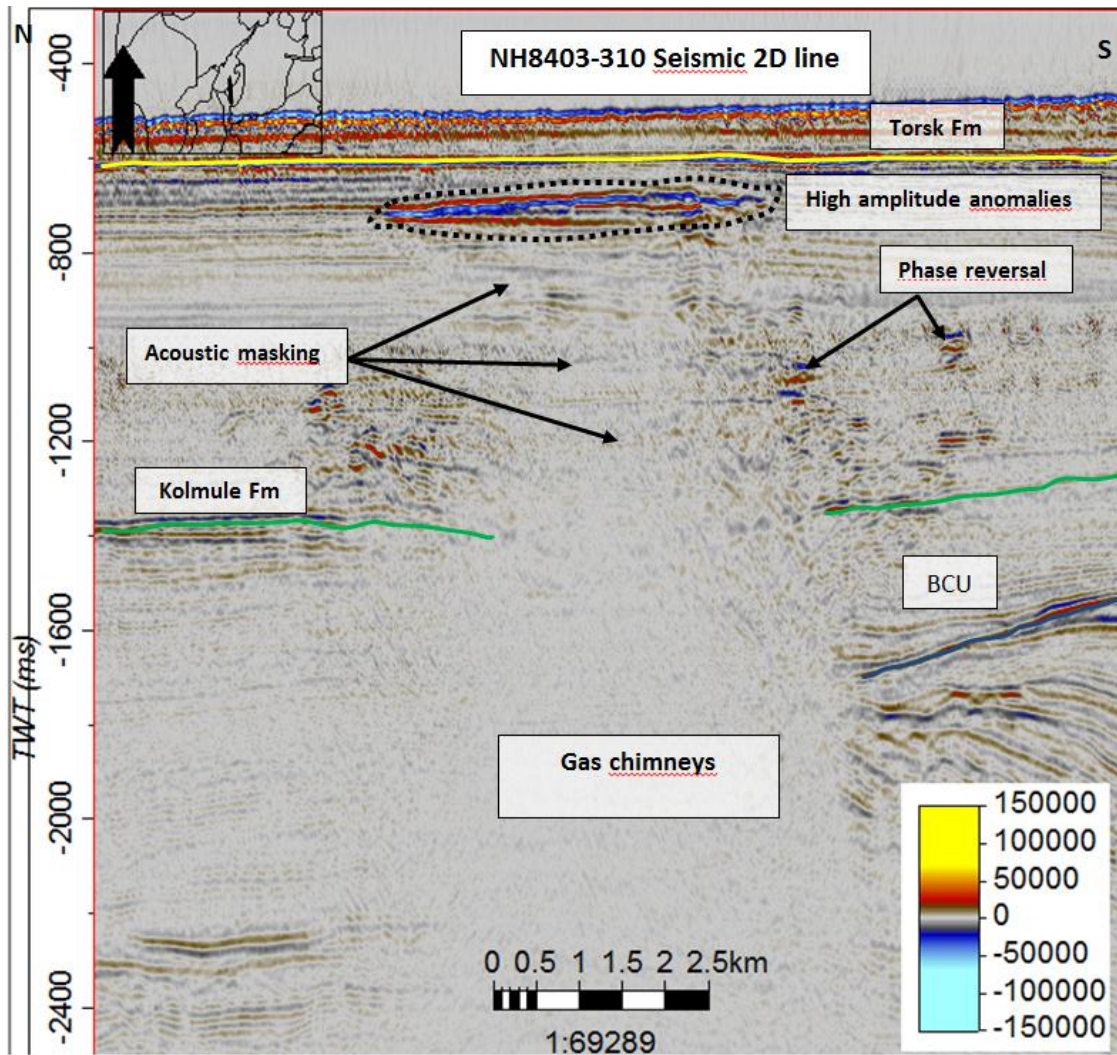


Fig 3-29: showing the gas chimneys distorted the vertical section of the seismic section thereby creating seismic acoustic masking

3.2.2 Fault related fluid leakage

Leakage through faults and fractures are also prominent in my study area suggested that source of hydrocarbon escaping through deep seated fault.

On the Snøhvit area of SW Barents Sea, fluid tends to migrate along the deep seated fault creating pathway for fluids that migrated to the shallower part of seismic section. It seemed that fluid originated deep beneath the faulted zone but due to the limitation of seismic section best possible origination of hydrocarbon cannot be detected. At the depth of around -2200 ms (TWT) vertical migration of fluids distorted the reflectors including Bottom

Cretaceous unit (BCU and Kolmule formation), thereby creating pathway for fluid migration to the shallower depth (fig 3.30). At around -1300 ms (TWT) chaotic reflection zone can be seen caused by presence of pore fluid in the sediment. It has been evident from seismic section, zone of highly fractured sediments provides conduits pathway for migration of fluids into the shallower subsea bed sequences. At the depth of around -900 ms (TWT), just above the chaotic zone, shallow gas accumulation can be observed.

The possible shallow gas accumulation is at a horizon which is up-dip from the area of vertical gas migration. Shallow gas accumulation results from migration of gas from a deeper structure area or they formed as a result of migration of gas from chimney area or perhaps accumulated against fault. The presence of fluid at a deeper prospect assumed to be the source of the migrating gas inferring that presence of gas chimneys and other associated features may be indicative of deeper prospective reservoirs.

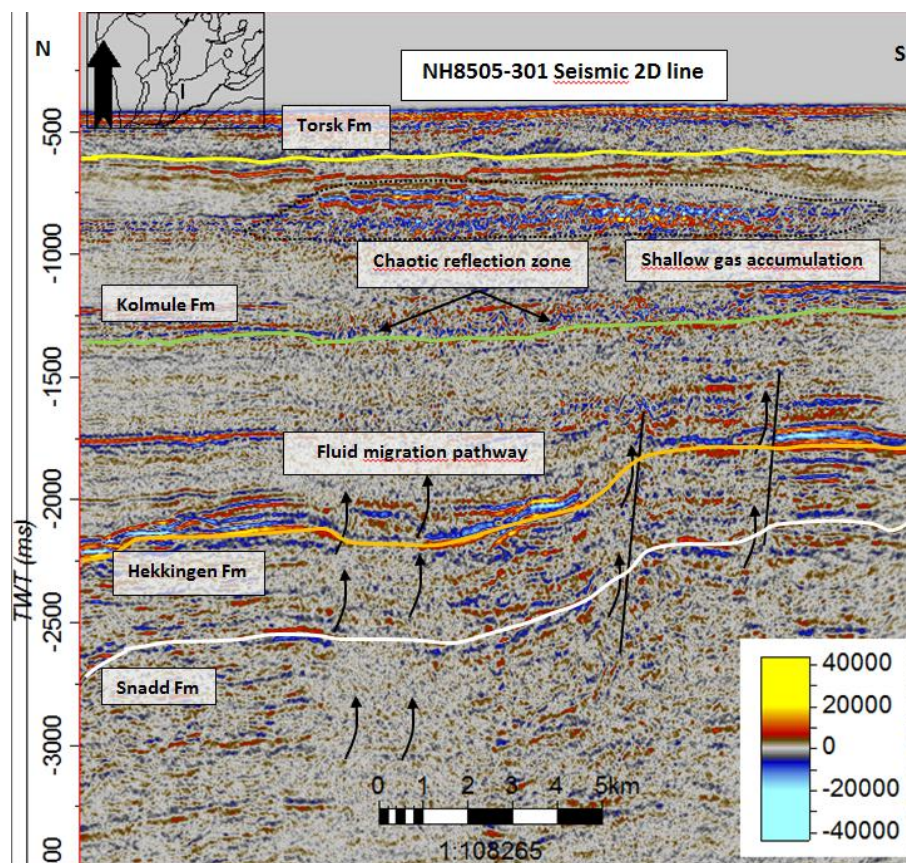


Fig3-30: showing fluid migration pathway along the faults accompanies with shallow gas accumulation in Snøhvit part of SW Barents Sea.

In south Bjørnøya region of SW Barents Sea, fluids appear to migrate along the parallel to sub parallel near vertical fault planes penetrated at the depth interval of around -1500 ms (TWT) to -600 ms (TWT). Faults are mostly oriented in N-S direction providing the conduits pathways if interconnected open fractures network are present within the rock (fig 3.31). Alternatively it can also act as fluid barrier where impermeable fault gouge forms during the shearing process (cataclasis) or post deformational cementation (Gartrell et al., 2004). These kind of features is similar to Ligtenberg (2005) who interpreted fluid flow along faults tend to follow columnar pattern. It might be possible that fluid migrated laterally along the surface until it encountered fault which then act as conduits pathway for these fluid to the subsurface. On eastern side of seismic section, Bright spot can be observed at the depth of around -600 ms (TWT) suggesting that hydrocarbon might have been leaked along fault.

In some cases, interesting observation regarding leakage of fluid along faults is related to regular spaced interval of pockmarks like depression (??) on the seabed suggesting that fluid flow might occur in diapiric mechanism (Ligtenberg, 2005).

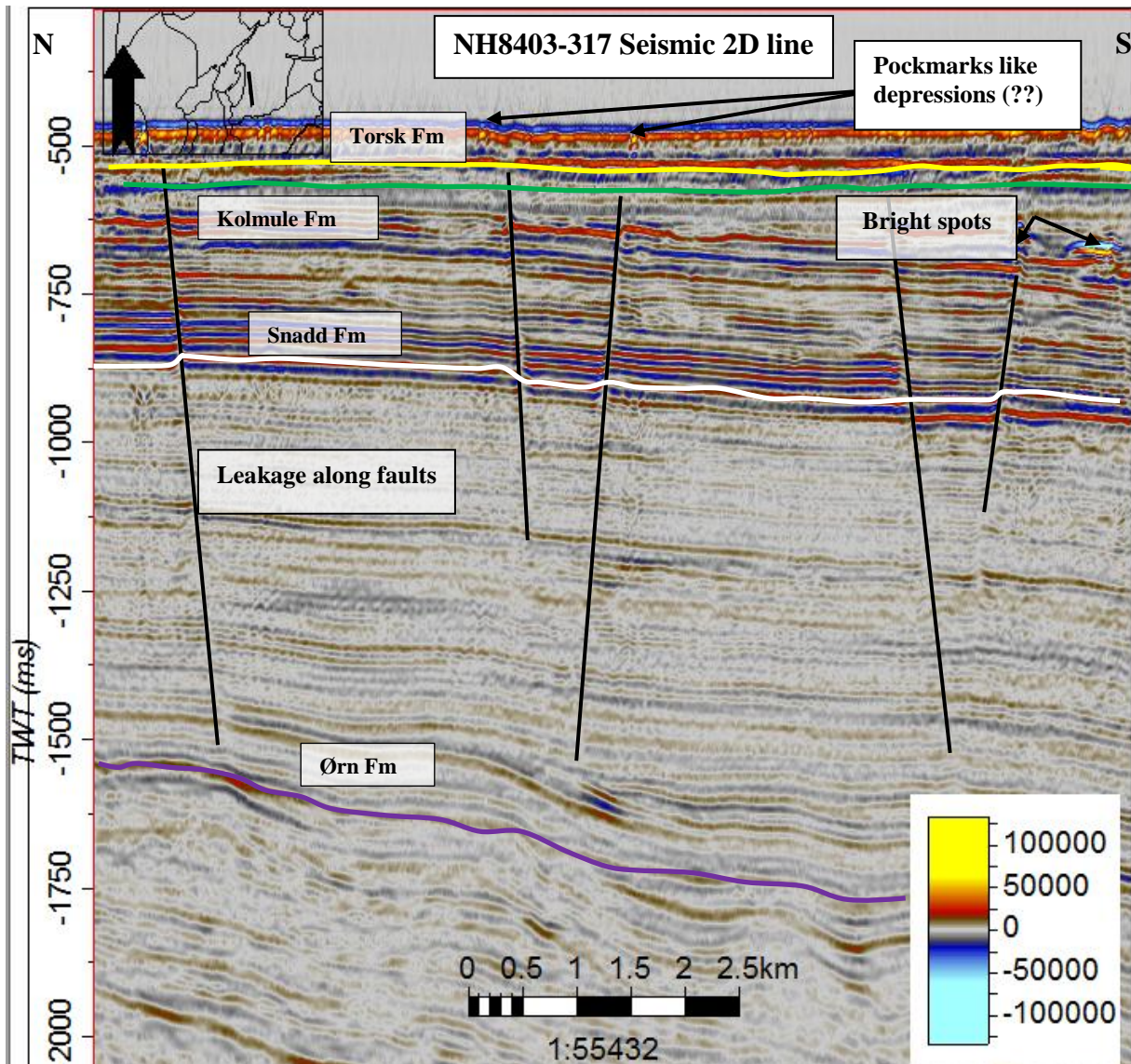


Fig3-31: showing leakage of fluid along faults is related with pockmarks like depression (?) on seabed in south Bjørnøya Basin of SW Barents Sea.

In Bjørnøya region, leakages of fluid along the fault are common. Some of the deep seated fault system appears to have been feeding fluid into the overlying sediments results in shallow gas accumulation. Seismic gas indicator often occurs along vertical to sub vertical fault that extends upward from the fault. There is also indication of migration of gas and fluid laterally along the faults in following fig 3.32, several sub vertical deep seated and faults at shallow depth provides conduits pathway for fluid to be migrated into the shallow part of seismic section. NW-SE orientated sub vertical fault planes are also observed in the

vicinity of the chimney zone on a level from -2500 ms (TWT) to around -700 ms (TWT). At the depth of around -2000 ms (TWT) two small fluid chimneys of around 1.5 km². both in east and western part of seismic section originated from basal gigantic chimney zone suggesting the main source of hydrocarbon reservoir. Due to limitation of seismic section, the base of gigantic chimney zone can't be determined. On western part of seismic section, shallow gas accumulation with the characteristic feature of chaotic internal pattern and phase reversal can be observed at the depth of around -700 ms (TWT) suggesting the presence of pore fluids in the sediments..

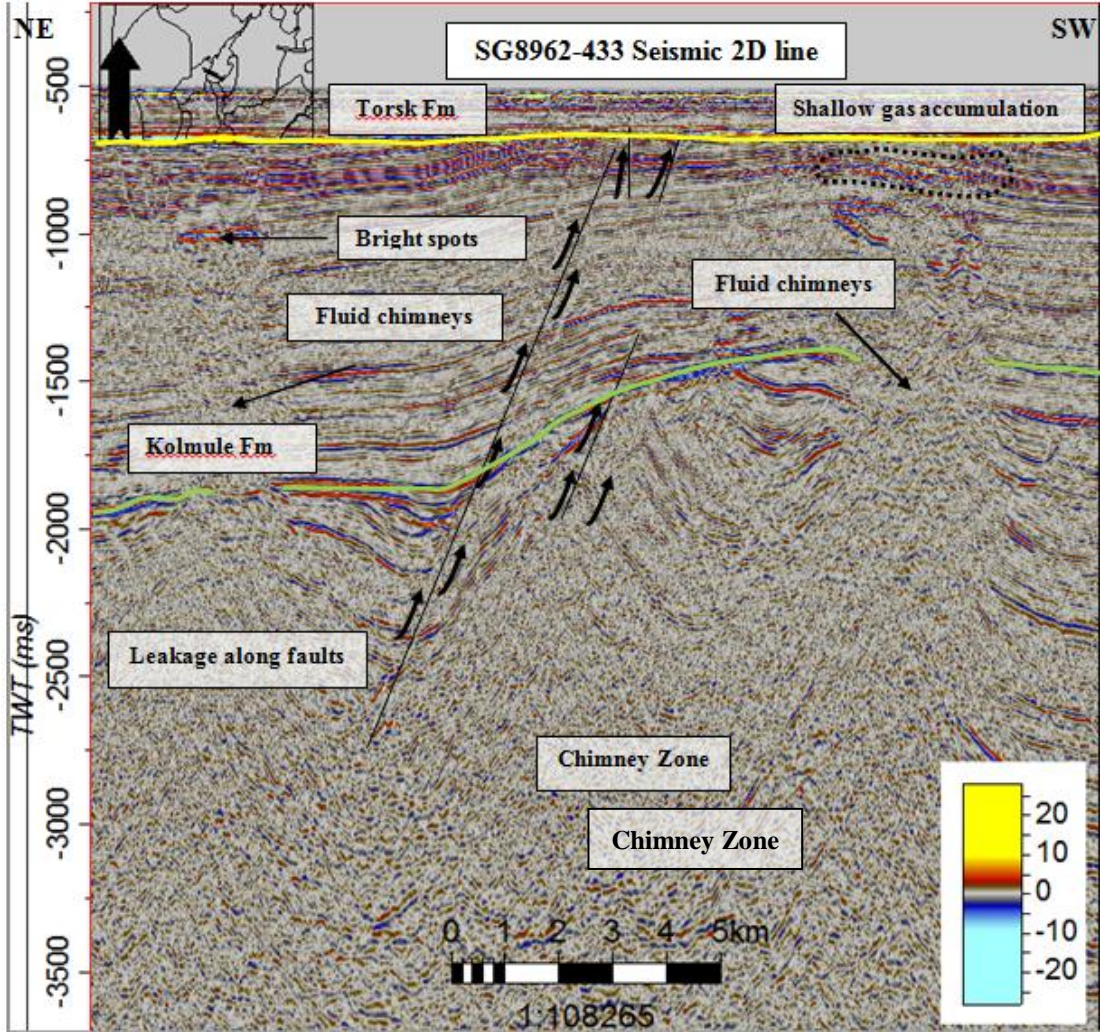


Fig 3-32: showing migration of fluid along faults toward the shallow part of seismic section.

In the following figure 3.33, fluid chimneys acts as a reservoir feeding the overlying strata with fluid at shallower depth results in shallow gas accumulation at the depth of around -600 ms (TWT). There is some small interconnected N-S oriented sub vertical fault plan indicates leakage of fluid on western side of seismic section. A bright spot can be observed at the interval depth of around -1100 ms (TWT) gives evidence of leakage of fluid to the overlying sediments.

There are two zones of leakage of fluids, one is on the western side and other is on the central part of seismic section however there can be possibility that fluid migrated along the reflector.

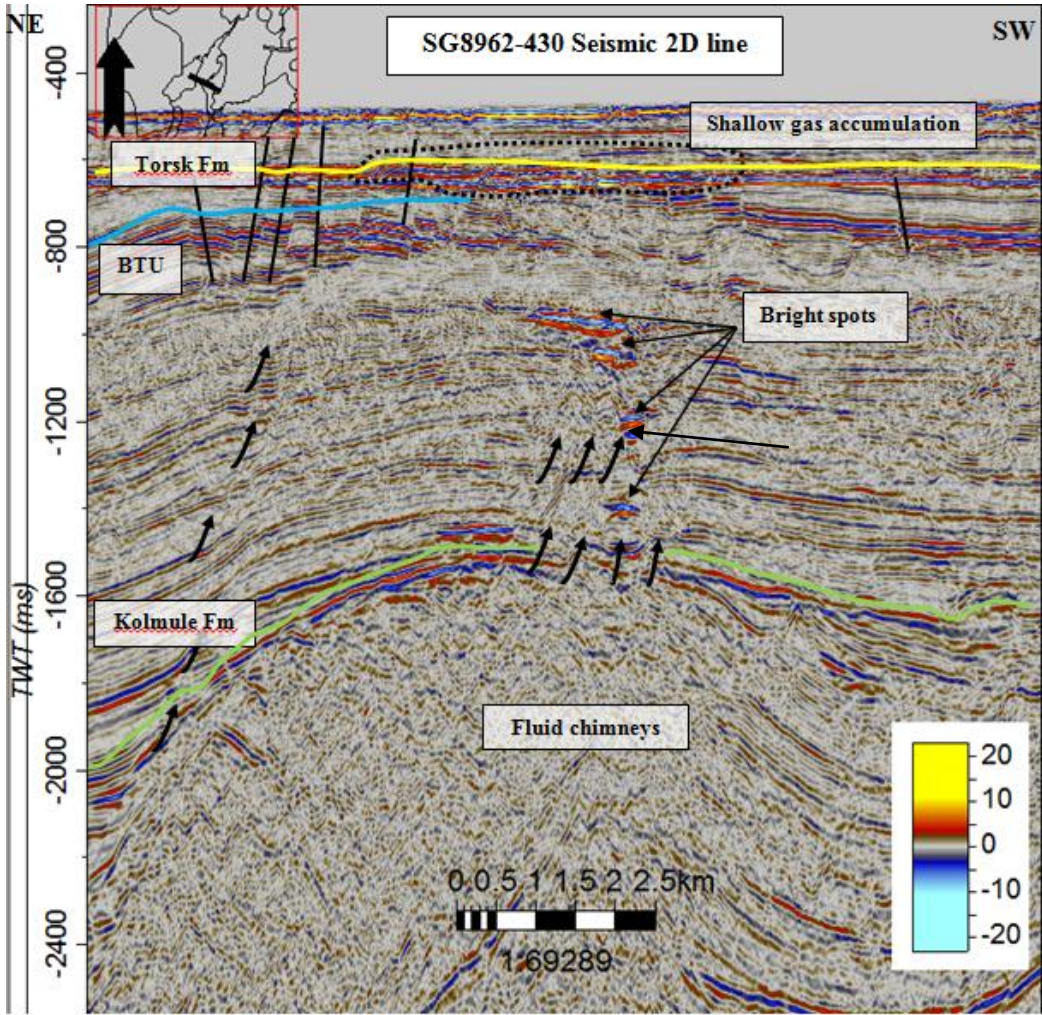


Fig3-33: Leakage of fluid from the fluid chimney zone tends to accumulate in shallow gas accumulation zone.

In the following figure 3.34, several rotated fault blocks with high amplitude are observed. The overlying strata show low frequency and are dipping in western direction. The base of rotated fault blocks shows chaotic reflection pattern which could be the chimney zone but due to the limitation of seismic data, chimneys zone (?) can be recognized. Several N-S orientated sub vertical deep seated fault planes within rotated fault block are responsible for leakage of fluids to the shallower part. An interesting features related to the bright spots can be observed at the depth of around -800 ms (TWT) which resembles like wedge shape showing the reverse polarity as compared to seafloor indicates the presence of hydrocarbon.

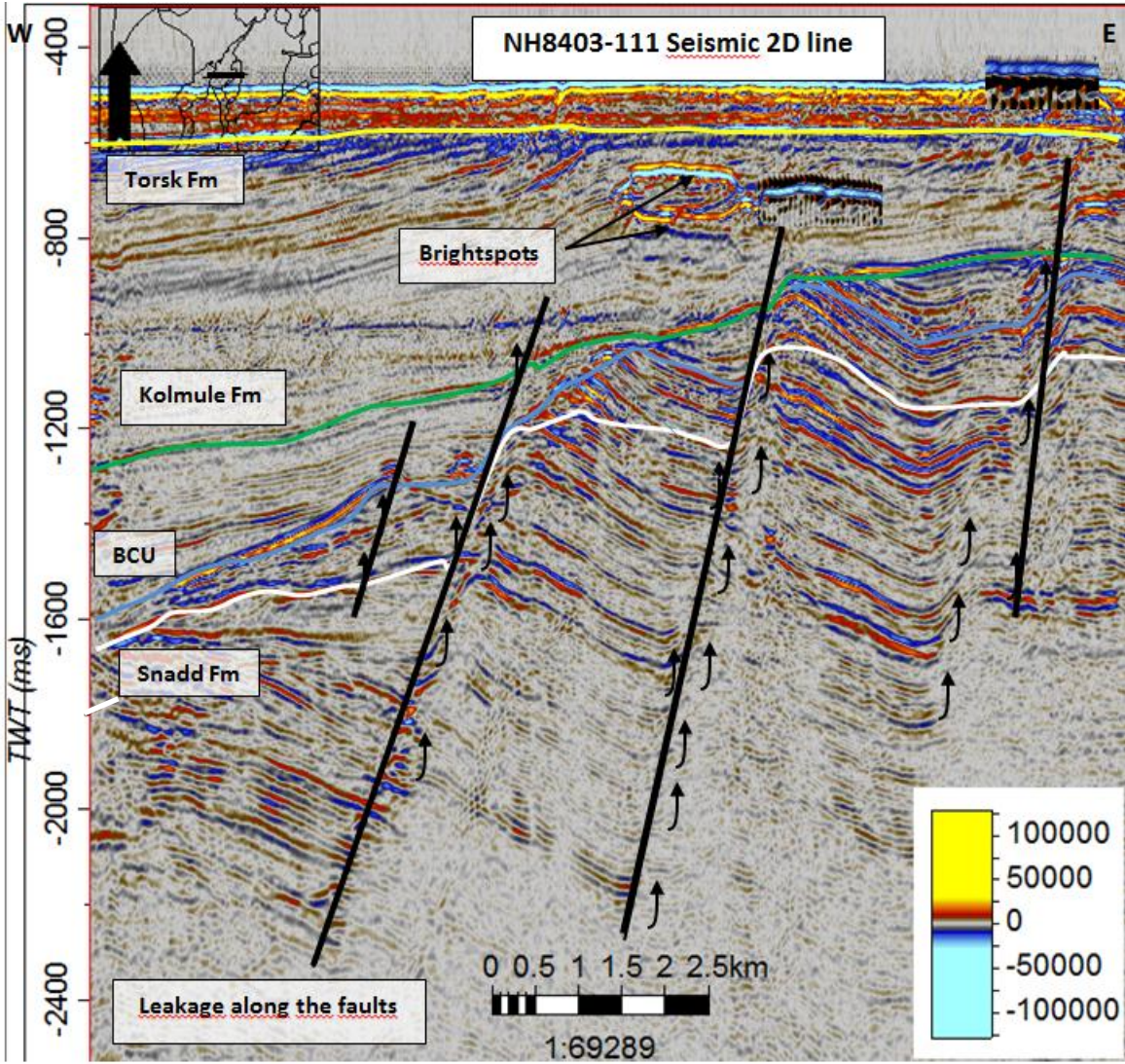


Fig 3-34: Leakage of fluid along fault, the wedge shape high amplitude anomalies above the fault are related to Bright spot by comparing the polarity with seafloor.

In the following figure 3.35, several multiple deep seated N-S oriented fault zones provided conduits pathway for fluids to be migrated into the shallower part. These faults are present in the vicinity of chimney zone which act as reservoir. The strata around faults are rotated in accordance with the orientation of faults. There is somehow low frequency interval in between fault bounded strata suggesting migration of fluids along the reflector as well. On eastern side of seismic section, chimney zone tend to open itself given rise to high amplitude reflection given evidence of presence of hydrocarbon at the shallow depth of around -700 ms (TWT). It is interesting to note that leakage of fluid along fault tend to follow the same pattern where chimney open but there could also be possibility that some of the fluid migrated vertically as well evident from presence of some disturbed or chaotic reflection on western side of the seismic section as well.

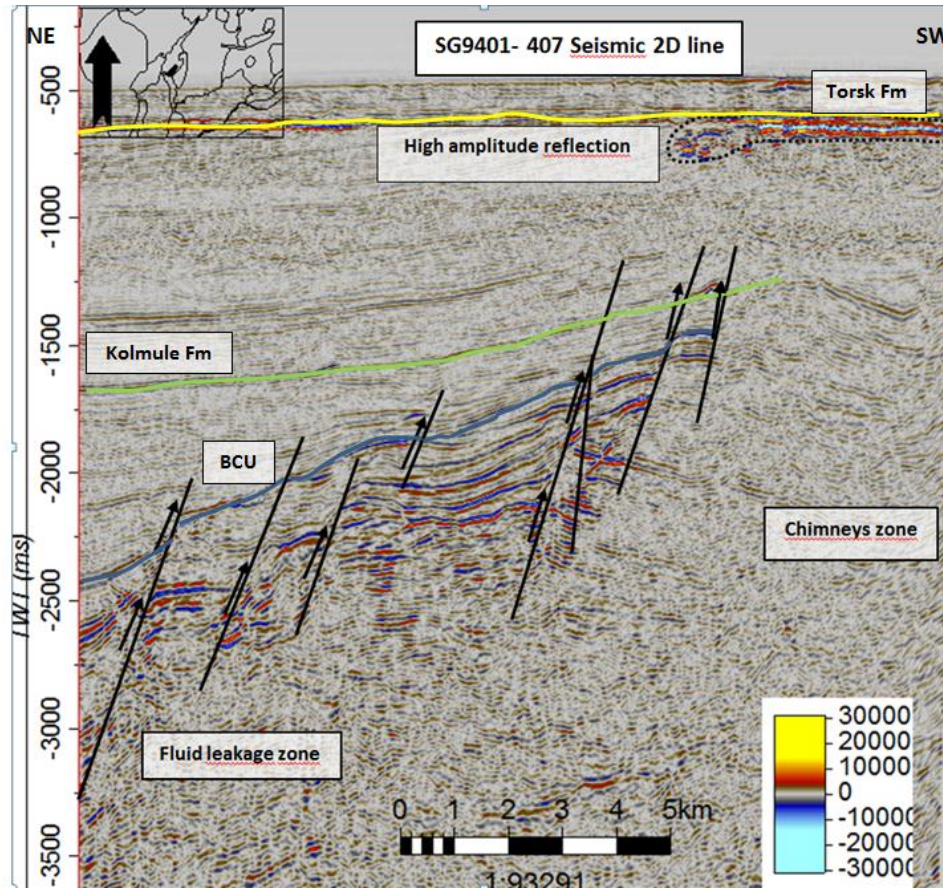


Fig3-35: showing the leakage of fluids along the deep seated parallel to subparallel faults in association with chimneys zone that are main source of fluids feeding the overlying sediments with fluids.

In the following fig3.36, fluids tends to migrated from reservoir rock at -2200 ms (TWT) and then migrated upward at level from -2200 ms (TWT) to around -700 ms (TWT) where it encountered acoustic masking and bright spot at an interval of -750 ms (TWT) and -650 ms (TWT). It is interested to note that there are two zones of chaotic reflection pattern (-1700 ms (TWT) to -900 ms (TWT) with minor interval of normal strata sequence, interpreted to be caused by vertical fluid migration of fluid or by localized migration of hydrocarbon along the strata.

Pockmark like depression are also seen on seafloor having an irregular depression caused by escape of fluid or gas into the water column (Hovland and Judd, 1988)

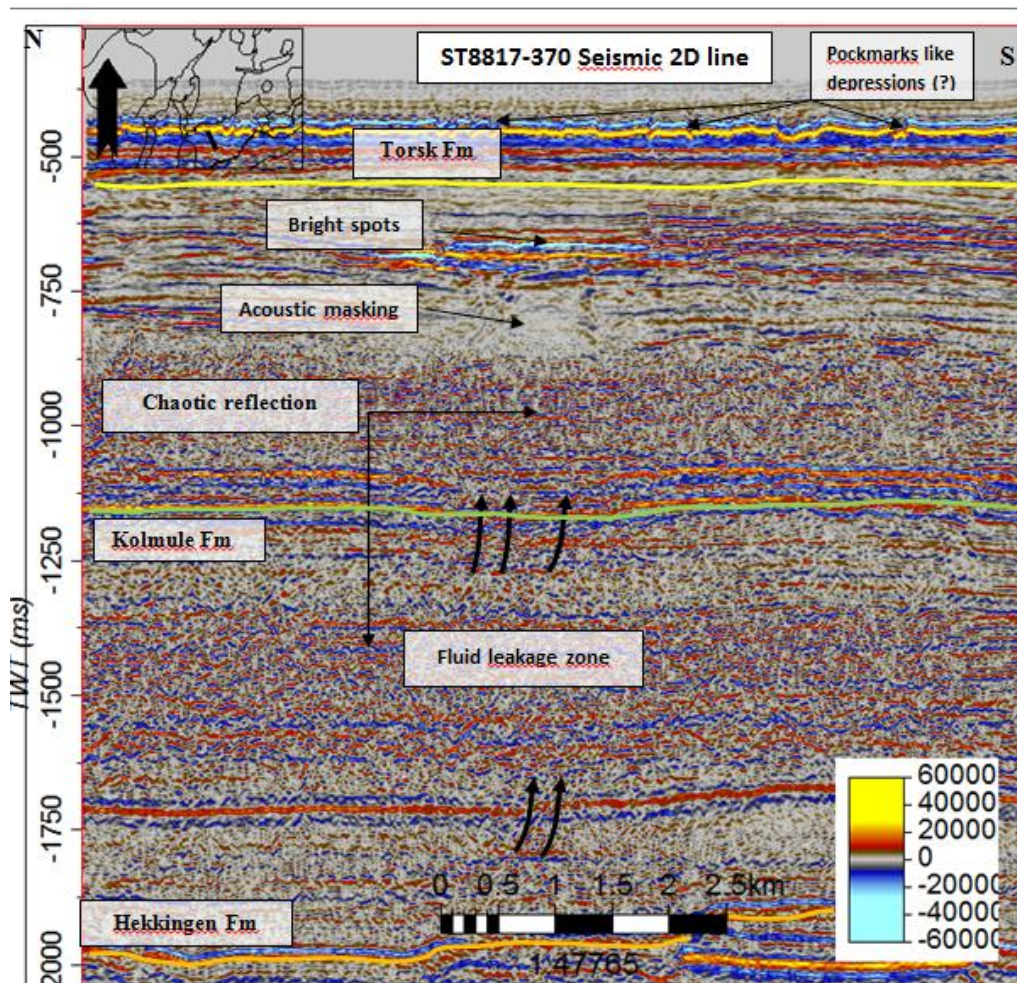


Fig3-36: showing leakage of fluid across the surface thereby creating chaotic reflection on the seismic section due to the presence of fluids in the sediments

3.2.3 Seismic pipe structure

In SW Bjørnøya area, unique seismic pipe like structure can be recognized on the following (fig 3.37). Seismic pipe structures are formed when high fluid overpressure in the reservoir generated hydro-fracture from the reservoir to the seafloor where mixtures of gas and fluid flowed at high speed to form pipe like structures (Løseth et al., 2009). Seismic pipe structures have a width of around 40 m and are oriented in N-S direction. The base of seismic pipe like structure is unknown due to the limitation of seismic data whereas its top part is terminated at seafloor. The flanks of the pipe are dipping approximately toward the center. The reflection of layer sequences along the edges of pipe structure follows a tiny anticline with a vertical central zone comprising of distorted seismic signal

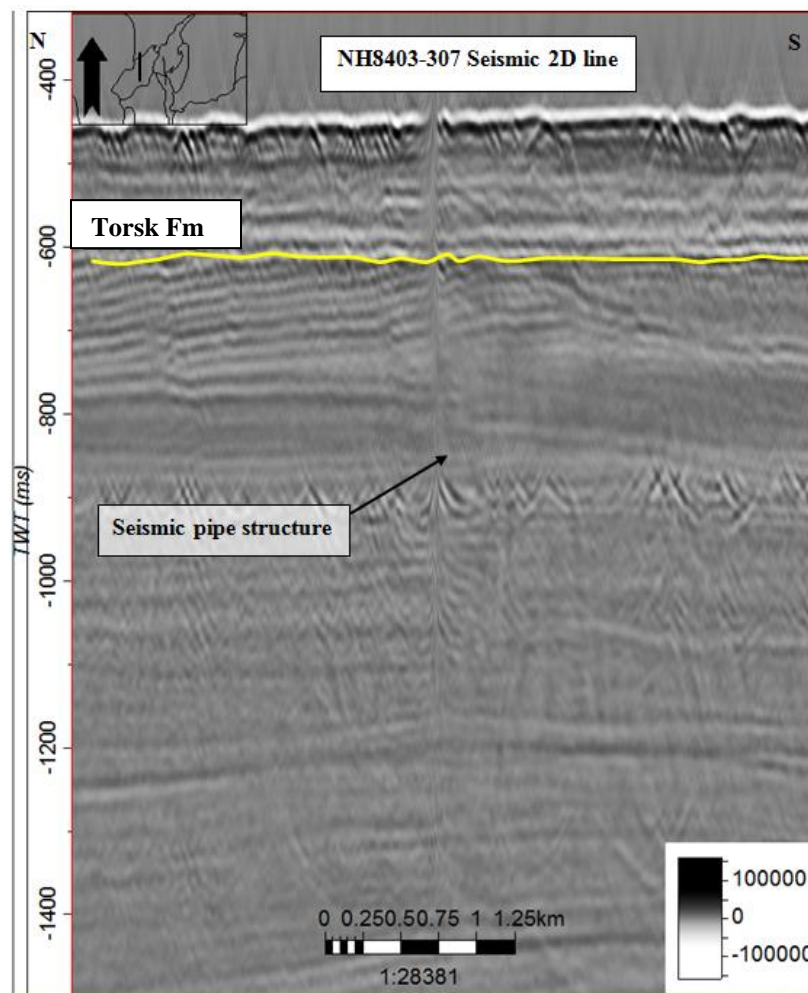


Fig3-37: Seismic pipe like structure that can distorted narrow vertical zone of seismic section are terminated at the seafloor.

3.3.4 Salt Diapirs structure

Salt diapirs structures are commonly observed in Tromsø Basin part of my study area. The diapirs in general, pierce through the overlying layers and are terminating at the level where Torsk formation lies.

In Tromsø Basin, quite a few salt diapirs structure can be observed creates abrupt vertical distortion of seismic data ranging at the depth of around -1000 ms (TWT) while its base is unknown due to limitation of seismic data. Salt diapir has a width of around 8 km².. Salt diapirs take the shape of anticlinal structure. At the apex of structure, Bright spots features can be seen at the depth of -500 ms (TWT). Interested features can be observed where strata around the edges of salt diapir are tilted. (Fig 3.38)

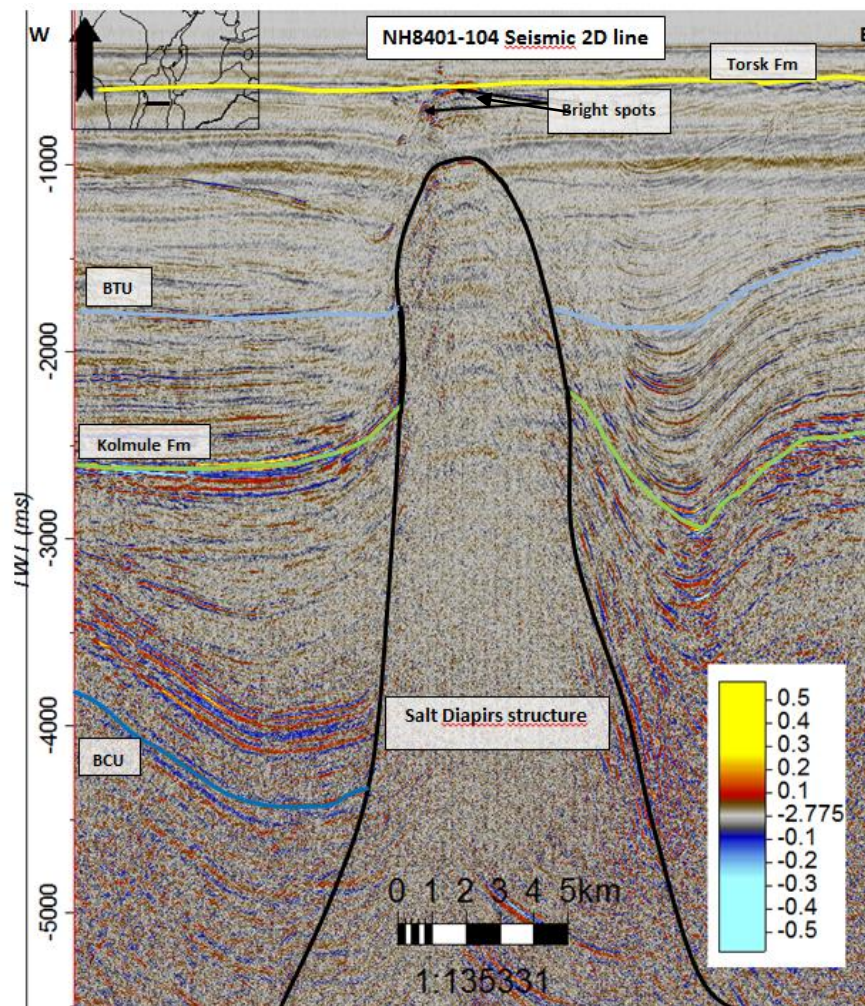


Fig3-38: showing the salt diapirs structure with width of around 8 km. On top of salt diapirs structure, bright spot can be observed in Tromsø Basin of SW Barents Sea.

In the following fig 3.39, two pronounced salt diapirs can be recognized on the same seismic 2D line. These two salt diapirs seemed to be originated from same base. The salt diapir on the eastern side is narrower than from other which is almost present at the centre of the seismic section. The narrow salt diapir has a width of around 3.5 km². whereas salt diapir at the centre of seismic section has a width of around 7 km². The internal seismic character of salt diapirs shows very low frequency and chaotic reflection pattern typical of chimneys zone. At the apex of these two salt diapir there is presence of bright spot at the depth of around -1000 ms (TWT).The strata in between the salt diapir is also tilted in accordance with the dispirs structure.

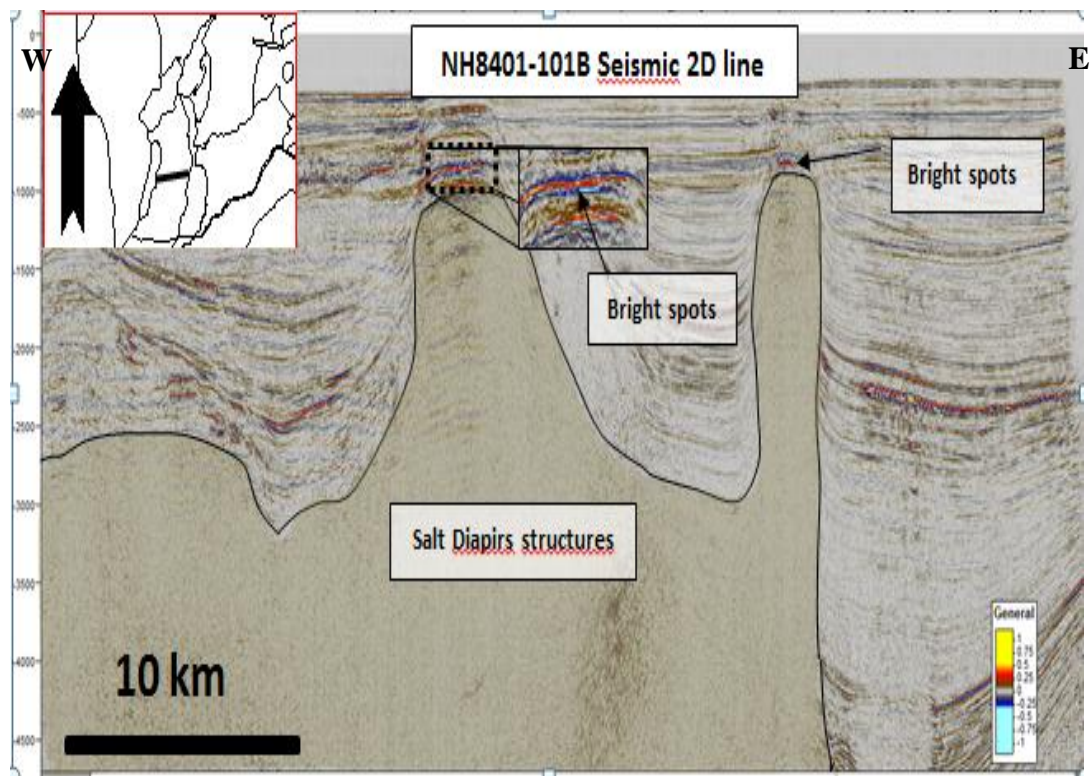


Fig 3-39: Two salt diapir structures that have the same basal structure are common features in Trossø Basin of SW Barents Sea.

3.3.5 Distribution of fluid flow features

The fluid flow features are widely distributed in study area but they are more scattered in the western part than in the eastern part of study area (fig 3.40). Based on NPD structural boundaries, it appears that distribution of fluid flow features can be related with structural

elements of SW Barents Sea. Most of the fluid flow features are location near to the major fault boundaries like Ringvassøy-Loppa Fault complex and Bjørnorena Fault complex suggesting close relationship between fluid flows and fault. Among the variously observed fluid flow features were gas chimneys, fluid leakage along faults, seismic pipe like structure and high amplitude anomalies due to trapped gas with gas chimneys are the most abundant features observed in the study area.

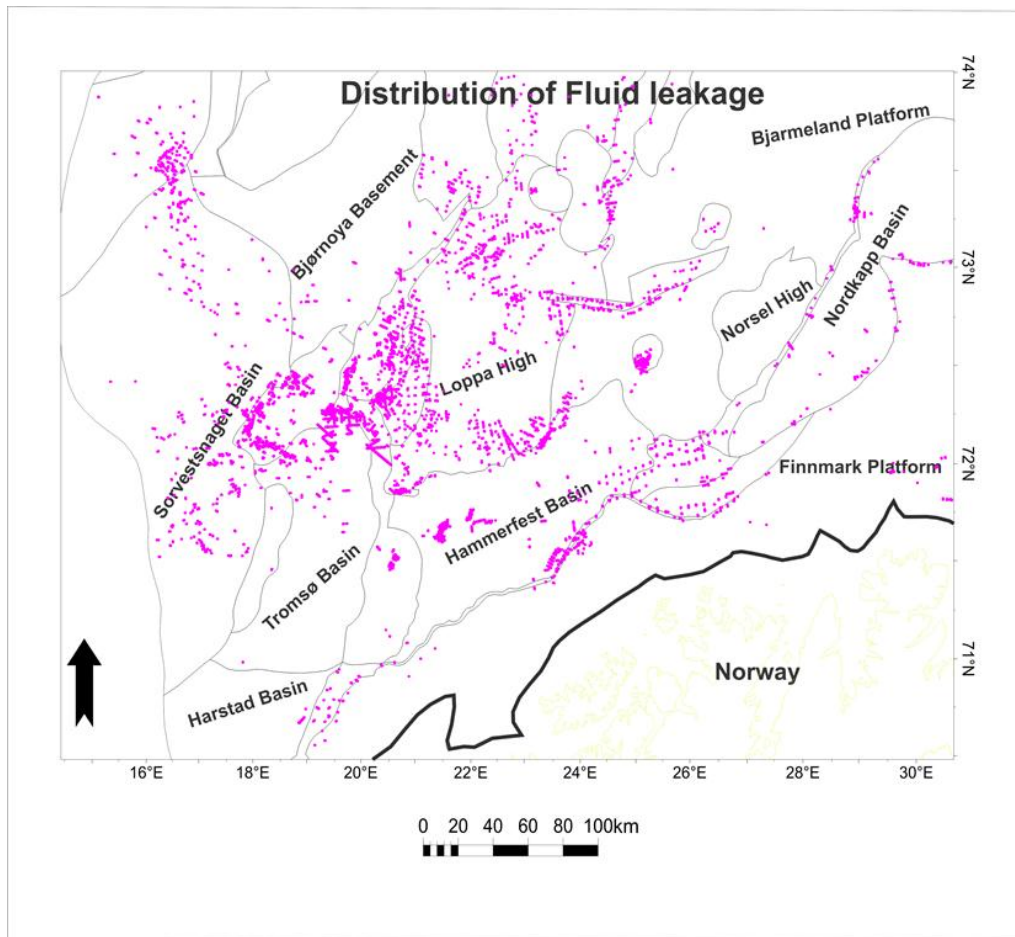


Fig 3-40: Map window showing distribution of fluid leakage feature (Blue dotted) across the SW Barents Sea (Study area), as mapped by Vaddakkepuliyaambatta et al., (2012)

4. Discussion

The discussion aims at identifying general mechanisms, relationship and geological process that control fluid flow in the study area with a major focus on the link to the stratigraphic development of the study area. The discussion aims not at explaining every fluid-flow feature in specific detail. That would go beyond the scope of the thesis and would make it too big. Many of the fluid features have been described and explained in detail in previous theses (Pless, 2009; Kristensen, 2010; Dahl, 2011). This chapter starts with a discussion of the stratigraphic development of seven horizons that have been interpreted in result chapter. This chapter will also focus on geological settings and tectonic and sedimentary processes that might affect fluid flow. Thereafter, the distribution and origin of fluid-flow features are discussed. Finally, the discussion summarizes all observations in a conceptual model.

Based on above mentioned result chapter, discussion part of my thesis will be mainly focused on assessing the relationship of fluid flow features in context with structural development of a study area so for this I have subdivided discussion chapter into five parts:

4.1 Stratigraphic development.

4.2 Distribution of fluid flow features.

4.3 Upper termination of fluid flow features.

4.4 Source of fluid flow.

4.5 Mechanism and geological process leading to the formation of fluid flow features.

4.1 Stratigraphic Development

The stratigraphic developments of study area are closely related with geological evolution as already discussed in 1.2 subchapter. The Barents Sea composed of several basins and highs that have undergone several phases of tectonism and sedimentation since Uralian Orogeny (Smelror et al., 2009). My study area is a part of western Barents Sea which is characterized by Cenozoic tectonic and sedimentation that have affected most part of area of my interest. The depositional evolutions of these units are based primarily on observed seismic character and its lateral and vertical variation within the study area. In my thesis, seven sequences are assigned on the basis of well information and regionally composite

seismic 2D line. The existence of chaotic seismic sequence with few and discontinuous internal reflection above Torsk formation appears to indicate sediment deposition under gravity-driven mass transport mechanism interpreted to be result from rapid deposition of sediment through grounded glacier (Faleide et al., 1996)

In the following section, stratigraphic development of seven horizons with respect to tectonic evolution since the Caledonian orogeny is discussed in further detail.

The extensional geological evolution of the western Barents Sea begins with a rift phase in late Devonian to early Carboniferous form a fan-shaped array of half-graben and high influenced by zone of weakness in the basement (Gudlaugsson et al., 1998)

Late Carboniferous was dominated by regional subsidence with development of a regional sag basin covering the entire Barents shelf (Gudlaugsson et al., 1998).In late Carboniferous time, continental drift has changed the climate from humid tropical to subtropical in western Barents Sea (Henriksen et al., 2011b)

Ørn Formation is part of upper Gipsdalen Group dominated by shallow marine carbonates on the platform areas and interbedded carbonates and evaporites in the more distal ramp to basinal settings (Larssen et al., 2005).There are several uncertainties to the geological history in the upper Gipsdalen Group, but it is very likely that a series of tectonic events have contributed to the depositional patterns, also supported by Larssen et al., (2005). Ørn formation is generally thinning towards the western part of the study area along eastern flank of Loppa High (fig3.19;3.20) which could have been resulted from late Permian and early Triassic uplift and erosion suggesting that Loppa High acting as positive structure in late Paleozoic. (Stemmerik et al., 1999). The changes in depositional pattern of Ørn formation can be related with tectonic development of Paleo- Loppa High that are thought to be formed in early Permian time and had some relief at that time due to activation of Ringvassøy-Loppa fault complex which has uplifted the Loppa High. As a result of this phenomenon, change in deposition pattern of Ørn formation may be caused by the change in topography related to the Loppa High due to this eastwards dipping flank of Ørn formation can be observed (fig 3.19)

Triassic period was characterized by tectonically quiet period in western Barents Sea with passive regional subsidence creating accommodation space for prograding clastic sediments (Smelror et al., 2009; Glørstad-Clark et al., 2010; Henriksen et al., 2011b).Permian Triassic

evolution forms a regional unconformity in the Barents Sea region (Henriksen et al., 2011b). This study supports the observation made by Glørstad-Clark et al., (2010).

Periodic smaller uplift of the paleo-Loppa High created local source area for sediment during early to middle Triassic time. During early Induan times to early Carnian time, paleo-Loppa High shows the infilling of clastic systems, the crest of paleo-Loppa High is a positive feature and an accommodation space was generated on the western side of the Loppa High. On eastern flank, the accommodation space was gradually filled in by prograding sediments system originating from the Fennoscandian Shield in south and the Urals in southeast (Glørstad-Clark et al., 2010; Smelror et al., 2009). A Snadd horizon is early to middle Triassic unit and can be correlated with S4 sequence of Glørstad-Clark et al., (2010). Variation in sea-level and sediment input more likely controlled the depositional sequence of Snadd formation which is gradually filling the accommodation space east of the paleo-Loppa High. Late Induan uplift was followed by a latest Induan transgression lead to a flooding event that allows sediments to be deposited in western basin, accompanied by a retrogradation of the clastic system to the east and south (Glørstad-Clark et al., 2010, Skjold et al., 1998). Interestingly Snadd formation is characterized by clinoformal geometry in the western part of the study area along Loppa High (fig 4.1) and almost parallel seismic reflector in the eastern side along Finnmark West (fig 4.2) appears to be related with regression that form during relative sea level fall as mentioned by (Glørstad-Clark et al., 2010). Snadd formation apparently showing shallowing upward sequence and onlapping towards western flank of Loppa High (fig 3.16) is more likely illustrating the variation in topography of the paleo-Loppa High suggesting that accommodation space on eastern side of the paleo-Loppa High was after short period filled up and start filling up the western basin. During this time, western basin receive large amount of sediment. After the accommodation space in the western basin was filled in middle-Ladnian, Loppa High had become a depocenter for these Triassic sediment (Glørstad-Clark et al., 2010). The time period from middle Ladnianian to middle Carnian show different depositional pattern in the study area where in western flank of Loppa High, Snadd formation showing west-east prograding clinoforms (fig 4.1) representing a new provenance suggesting mixture of local source area to the west and/or Greenland (Glørstad-Clark et al., 2010).

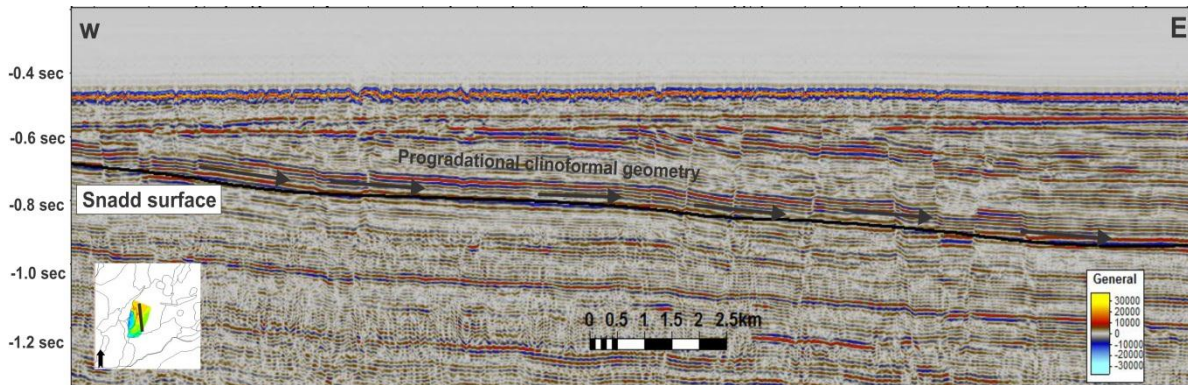


Fig 4.1 showing west-east progradational pattern of Snadd formation

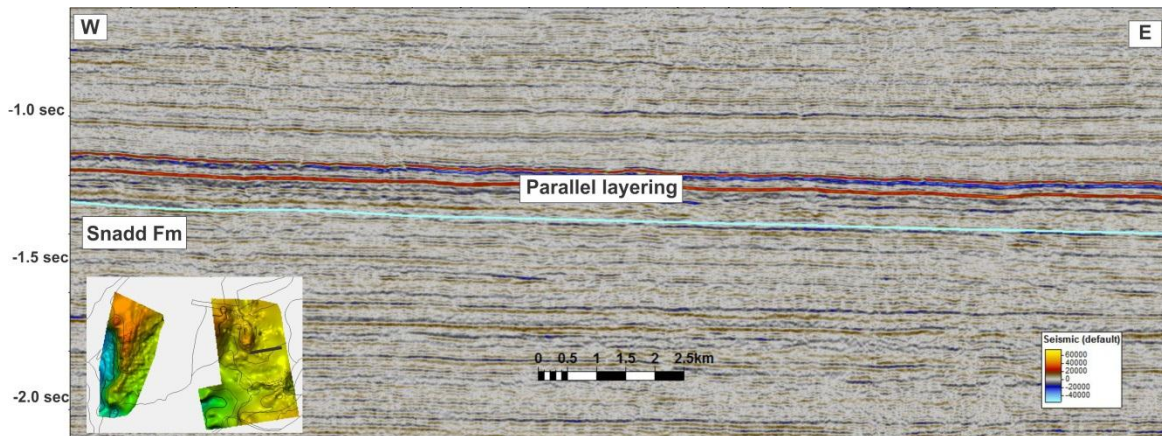


Fig4.2 showing parallel reflector layering of Snadd formation in the eastern side of the study area.

Dore and Gage (1987) suggested that study area was uplifted due to active rifting during middle Jurassic. There are normal faulting in Hekkingen formation interpreted to reflect Mesozoic faulting that have influence the stratigraphic interval of Cretaceous age (Riis et al., 1986)

The Jurassic succession in SW Barents Sea is stratigraphically more complete. Jurassic Hekkingen formation is mostly mapped in eastern side of the study area whereas it is pinching out towards the Loppa High (fig3.12) suggesting erosion of Hekkingen formation due to the Cenozoic uplift of Loppa High. In Sørvestsnaget Basin, since it is too deep which make it difficult to map Hekkingen formation in the western part of the study area.

Early Cretaceous tectonic subsidence in SW Barents Sea results in deposition of thick succession of Cretaceous sediment in Tromsø Basin, Sørvestsnaget Basin, Bjørnøya Basin (fig4.3) (Faleide et al., 1993; Knutsen & Larsen 1996). During Cretaceous, SW Barents Sea

was uplifted and large amount of sediment were shed from the rising continent area in the northeast into deeply subsiding basin in the west (Smelror et al., 2009). Based on time thickness map (seafloor and Kolmule horizons), Kolmule formation are getting thicker on western side of study area and thinner on western flank of Loppa High (fig 4.3) suggesting Loppa High as possible source area for lower Cretaceous unit. Kolmule formation shows prograding clinoformal geometry across the Sørvestsnaget Basin (3.10) suggested sediment source from Loppa High could have been formed during relative sea level fall. Thinning of Kolmule formation interval on Senja Ridge (fig 4.3) indicates that Senja Ridge was a positive structure dominated by uplifting and erosion (Knutsen & Larsen 1996)

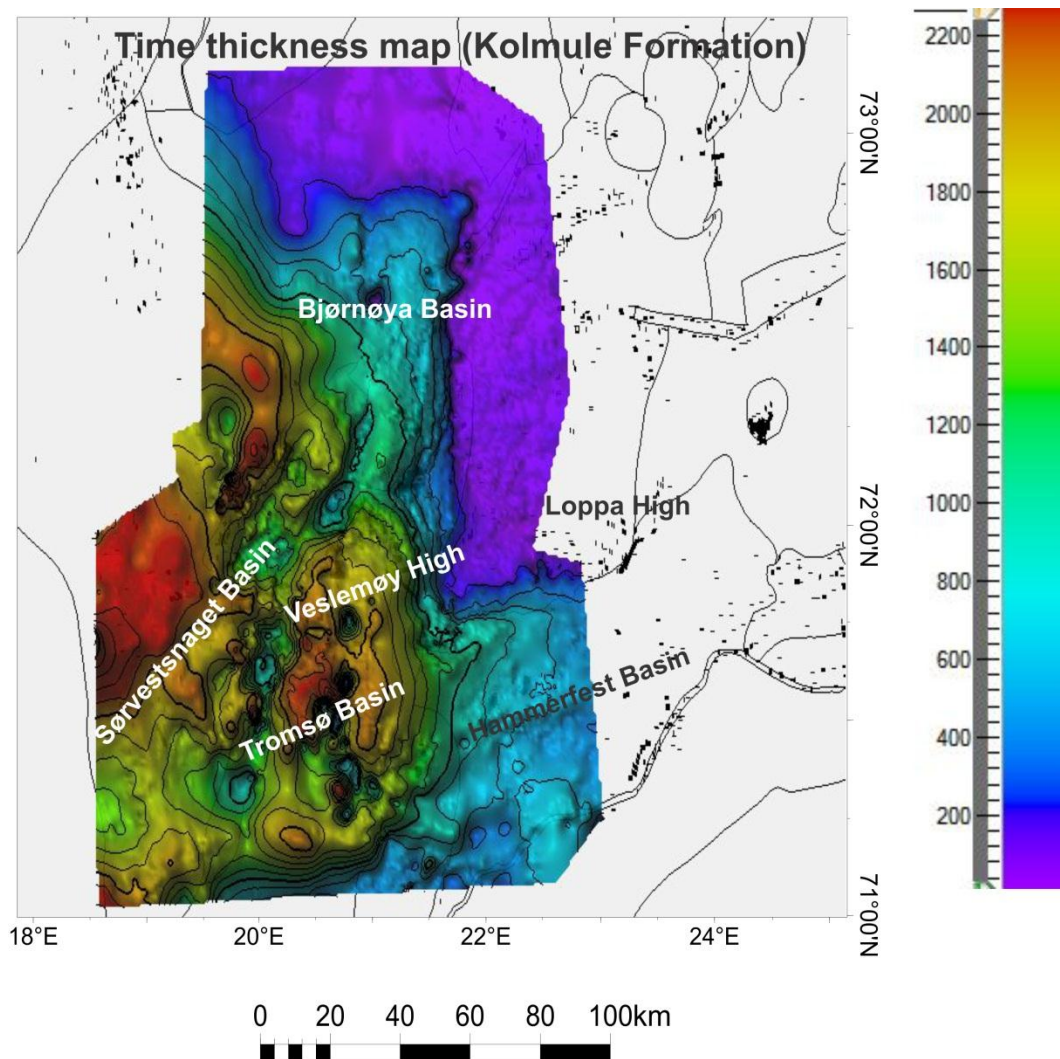


Fig4.3: Time thickness map of Kolmule formation showing overall depositional pattern in study area and black dots indicates the distribution of fluid flow features.

Bottom Tertiary unit (BTU) interpreted in between the Torsk and Kolmule formation. The base of Paleogene sequence is represented by BTU. Based on time thickness map (seafloor and BTU), BTU is thickness on western part of Vaslemøy High where it is found at the depth of around 4.5 s (TWT) and BTU sequence thin towards the Vaslemøy High (fig 4.4) and on western part of Loppa High it truncates with URU forming angular unconformity (fig3.7). Just like Kolmule formation, Bottom Tertiary unit (BTU) interpreted to be derived from Loppa High.

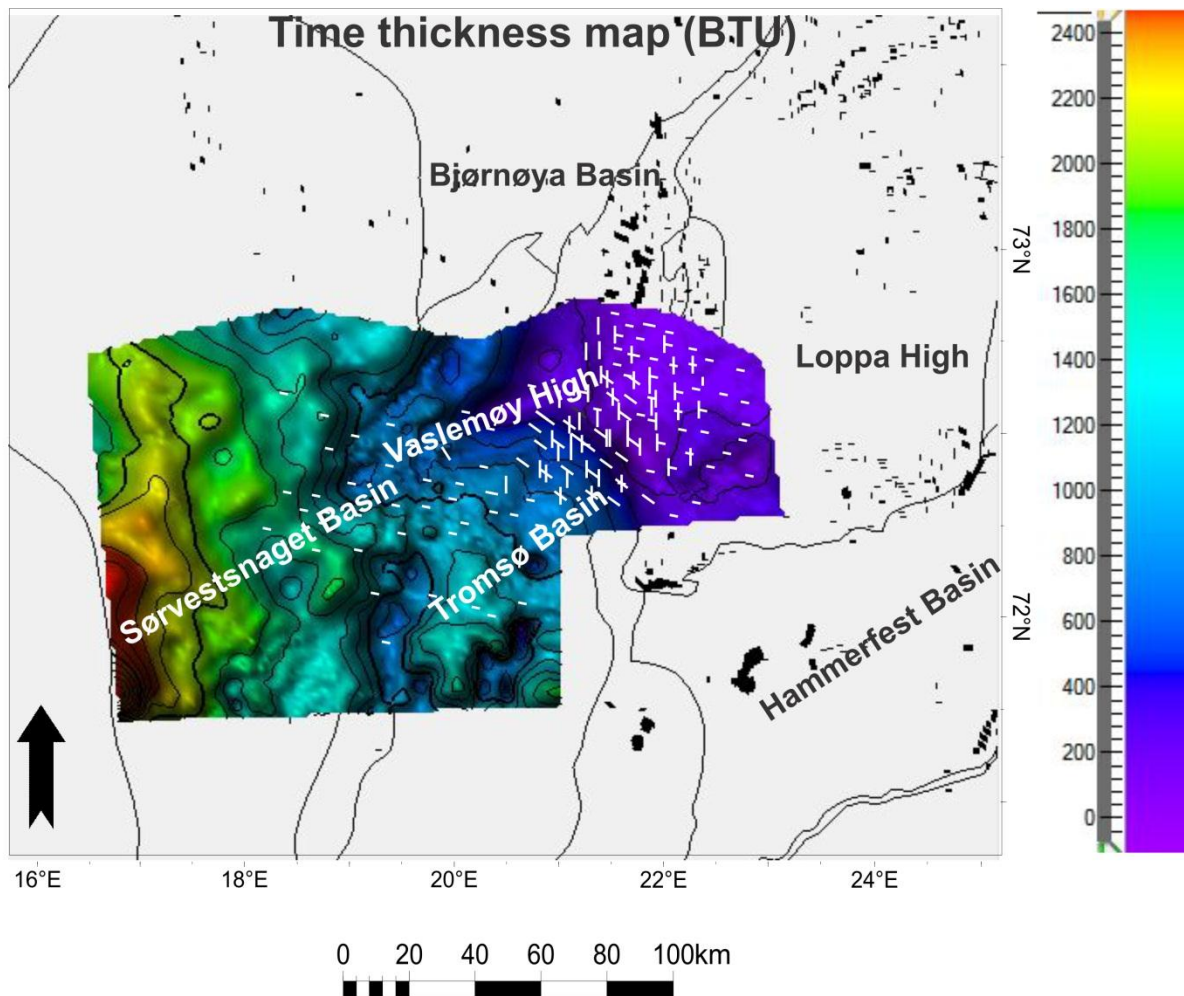


Fig4.4: showing time thickness map of BTU showing overall depositional pattern in study area whereas small dots indicates fluid leakage features across the study area.

Bottom Cretaceous unit (BCU) interpreted beneath the Kolmule formation. Based on time thickness map (seafloor and BCU), BCU unit shallow towards the structural high like Loppa High (fig 4.5) where it is found at the 1-3 s (TWT) whereas it thickens immediately western

part of Vaslemøy High and in Tromsø Basin at the depth of around 4-5.5 s (TWT) suggesting Loppa High as a possible source area for BCU.

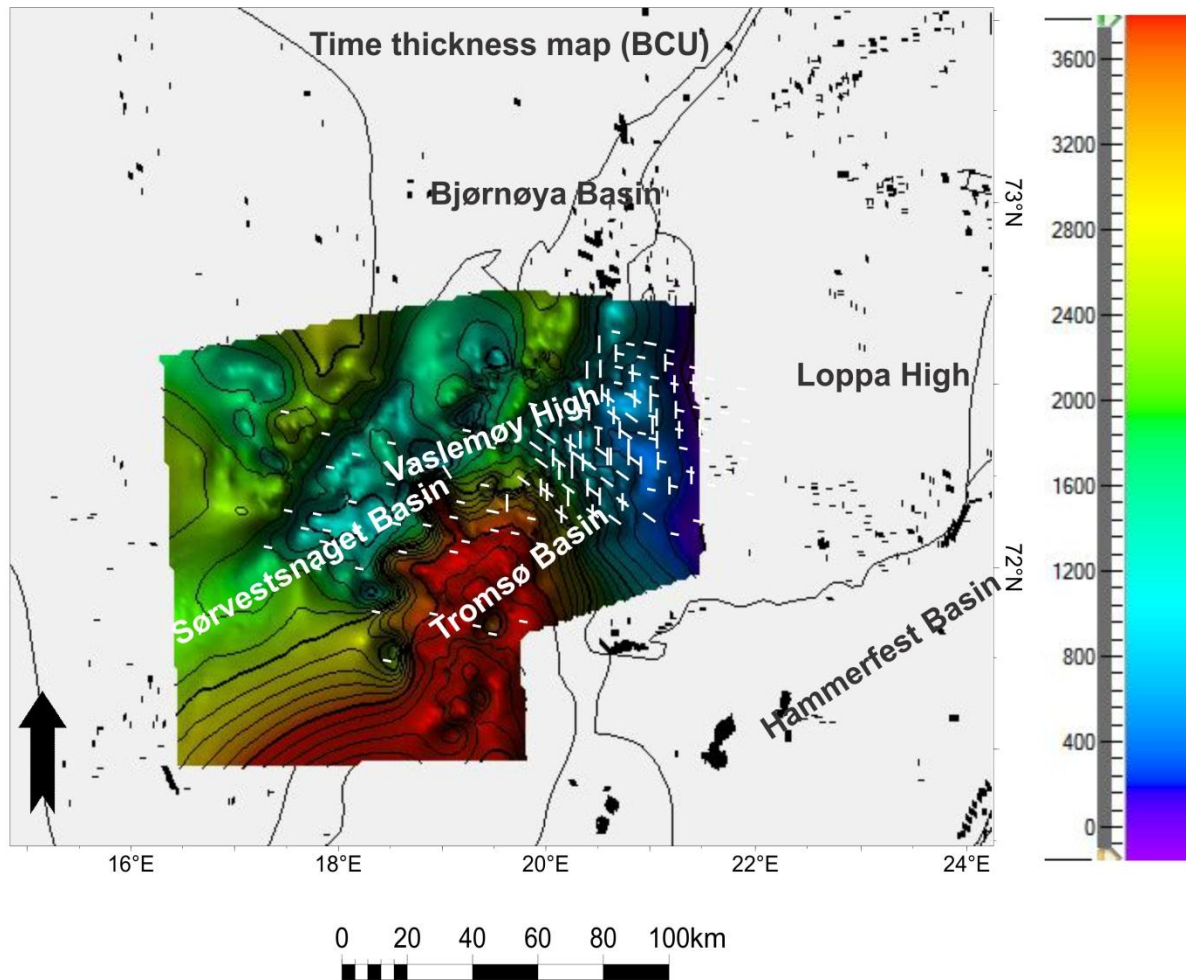


Fig 4.5: showing Time thickness map of BCU showing overall depositional pattern in study area whereas dots indicates fluid leakage features.

Cenozoic evolution in Barents Sea is closely related to the opening of the Norwegian-Greenland Sea with significant shearing along the Senja Ridge which results in forming a passive margin in the Oligocene (Ryseth et al., 2003; Henriksen et al., 2011b).

Thick and relatively complete Cenozoic succession occurs along the western margin of Barents Sea particularly in Sørvestsnaget Basin, Vestbakken Volcanic Province (fig 4.6) (Vorren et al., 1991; Rasmussen et al., 1995; Knutsen et al., 2000; Ryseth et al. 2003) that could have been caused by glacio-eustatic sealevel lowering, uplifting of the adjacent shelf area like Loppa and Stappen High and intensified erosion by glaciation process, however Cenozoic strata are absent below the base of Quarternary in part of Loppa High (fig 4.6)

(Gabrielsen et al. 1990; Faleide et al., 1993). Stappen High and Loppa High were uplifted during Paleogene appear to be possible sediment source for Cenozoic and Cretaceous sediment in Sørvestsnaget Basin and Tromsø Basin (Ryseth et al., 2003). Knutsen et al. (1992) suggest Loppa High as main sediment source based on progradational clinoformal geometry of Cenozoic sediment in SW direction whereas Faleide et al. (1993) propose Stappen High as main source for thick Eocene sedimentation in Vestbakken Volcanic Province and in the northern part of Sørvestsnaget Basin. Based on my Interpretation and thickness map of Torsk (seafloor and Torsk horizon), I agree with Knutsen et al. (1992) and Faleide et al. (1993) proposal with Stappen High and Loppa High as possible source area for Torsk Formation.

Fig 3.5 illustrates the relationship between sediment supply and shoreline. Sediment supply and shelf width can be important factor for shoreline position relative to the seismic offlap break (Ryseth et al., 2003). The flat nature of the Paleoshelf may have resulted from flooding during relative sea-level rise caused positioning of shoreline landward of offlap break (Ryseth et al. 2003). Torsk formation is interpreted to be deposited during relative sealevel fall causing erosion of Torsk formation on upper paleo-slope, shelf break and the Paleoshelf. Under these circumstance basins (Sørvestsnaget Basin) in the SW Barents Sea receiving sediment from erosion and uplifting of Stappen High and Loppa High (Vorren et al., 1991; Knutsen et al. 1992;Faleide et al. 1993; Ryseth et al.2003;Henriksen et al., 2011b)

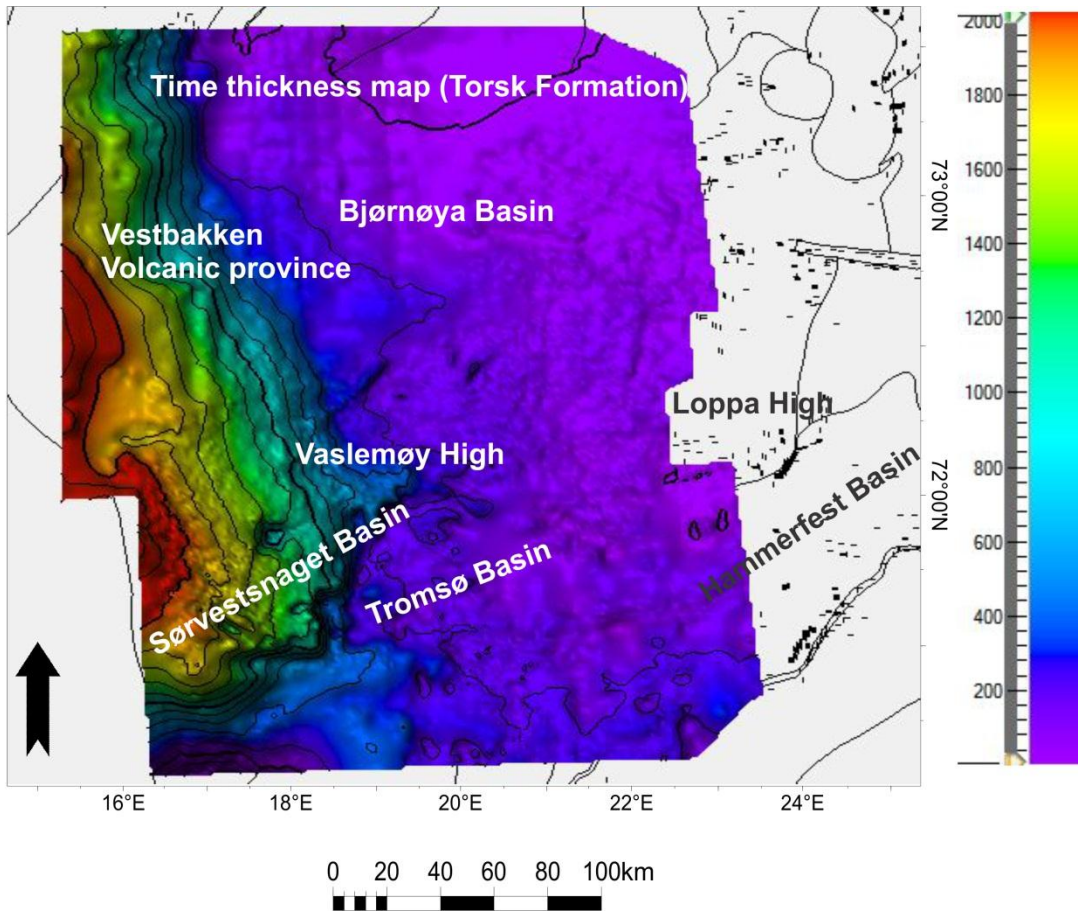


Fig 4.6: illustrating time thickness map of Torsk formation indicating the overall depositional pattern in study area. Small dots indicates fluid leakage features

4.2 Distribution of fluid flow features

The distribution of fluid flow feature is very important for the origin of the fluid flow system. The SW Barents Sea is a large hydrocarbon prone basin of the Norwegian Arctic region and houses a series of petroleum source rock of Silurian to Cretaceous in age referring to as a multi-sourced and overfilled petroleum system (Henriksen et al., 2011b; Ohm et al., 2008). It is very important to understand the petroleum system before starting discussing about fluid flow features. Fig1.13 describes the petroleum system of whole Barents Sea, based on the presence of source rock on the map, one can assume that Barents Sea is phenomenon unique area in the world with regards to hydrocarbon generation but unfortunately due to some geological condition it became increasingly challenging to get access to these hydrocarbon resource. However, a more thorough discussion of the

relationship with the source rocks in the Barents Sea is given in this chapter. The discussion here focuses solely on the distribution of fluid leakage structure, whereas the mechanisms of leakage are discussed in chapter 4.5.

Fluid flow features in my study areas can be described in terms of gas chimneys, acoustic masking, shallow gas accumulation, blow out pipe like structures, leakage of fluid along faults and fractures and high amplitude anomalies related to the accumulation of trapped gas. It has been interpreted that mostly fluids have been migrated or leaked into the shallow subsurface.

Fluid leakage in my area apparently related with the structural setting. There is clear coincidence of fluid leakage structure with the major structural boundaries indicating that major fault complexes have acted as leakage pathways from deep reservoirs (fig 3.40). The fault complexes might have been reactivated during tectonic activity or due to the loading of the Barents Sea ice sheet (Knies et al., 2009). Fluid flow features are densest along the Bjørnøyrenna Fault complex related to the opening of the North Atlantic. Also, their location towards the main depocentres of the glaciation and their N-S extension makes them more prone to reactivation than earlier W-E extending rift fault complexes which enclose close basins and basement highs. In addition to this, some fluid flow features also observed west of Loppa High, Hammerfest Basin, along the Veslemøy High and within the Sørvestsnaget Basin which is further to be discussed in the chapter 4.3 and 4.5.

In addition to this, stratigraphic development of Bottom Tertiary unit (BTU) and Bottom Cretaceous unit (BCU) have had a close relationship with fluid flow features as shown in fig (4.5; 4.6). Based on distribution of fluid flow feature in study area (fig 3.40) one can assume that fluid tends to migrate through major faults along Bjørnøyrenna fault complex and Ringvassøy-Loppa fault complex that appear to act as conduits for fluid to migrate into shallower part where it encounters BCU, Kolmule, BTU and Torsk formation. This indicates that migration of fluid must have occurred after the reactivation of faults.

The denudation of the Barents Sea has had a significant consequence for the petroleum system in Barents Sea. Total net erosion in Barents Sea varies from 0 to 3000 m. Reservoir quality, source rock maturity and hydrocarbon migration has been affected by erosional processes. (Henriksen et al., 2011a). Uplifting and erosion are closely related process which increases the risk of leakage and involve release of gas from oil due to lowering of pressure

from removal of overburden and/or tilting of reservoirs took place (Nyland et al., 1992; Dore & Jensen., 1996;Henriksen et al., 2011a; Ohm et al., 2008)

However, the pattern of net erosion in the SW Barents Sea does not show any link to the distribution of fluid leakage structure. Fig 4.7, suggesting that the amount of erosion does not have any importance. This leads me to suggest that general glaciotectonic movements and uplift have mobilized fluids along pre-existing structural boundaries. The net erosion might have had only minor effect on fluid leakage.

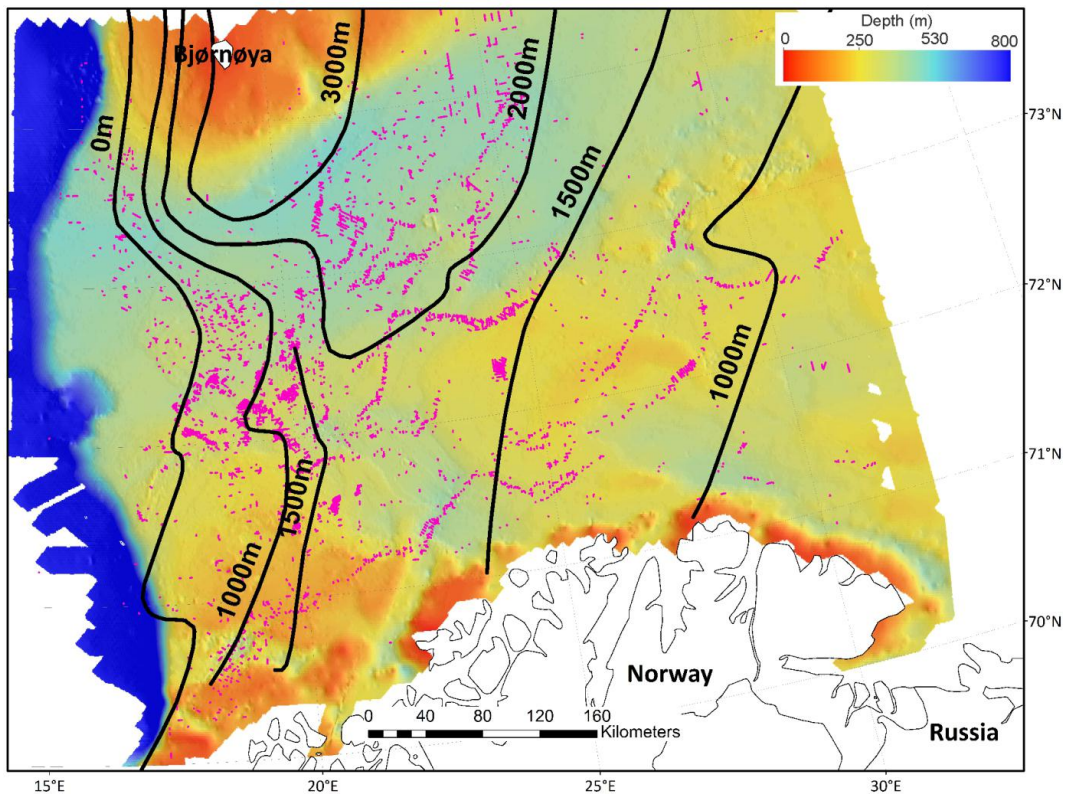


Fig 4.7: illustrating amount of erosion (black lines) has no direct relationship with distribution fluid flow process (Vadakkapuliambatta et al., (2012)

4.3 Upper Termination of Fluid flow features:

For fluid undergoing migration process there has to be two boundaries through which whole migration process goes on. These two boundaries are also called as interval pathway for any fluid to be migrated. Two boundaries are defined on the basis of origin and

termination of fluid leakage features so based on above mentioned criteria one has to assume source of fluid and the termination boundary through which migration process stop. In my study area, most of the fluid flow originated from Hekkingen source rock and it terminates at Torsk and Kolmule cap rock.

There has been some leakage of fluid into seabed suggesting presence of fault at shallow depth (fig 3.31, 3.32 and 3.33) thereby holding upward migrating fluid by means of pressure difference and sealing quality of overlying rock so in this case fault is the only pathway for migration of fluid. At certain depth where sediment lose cohesiveness and became more permeable allowing pressurized fluid to break through the sediment and migrate vertically through to the seabed.

In Hammerfest Basin and west part of Loppa High, shallow gas accumulation are located at the top of gas chimneys which could be resulted from high expansion factor of gas that are migrated from reservoir rock (fig 3.25,3.27,3.28,3.29 and 3.30)

There are several possible explanation for the Pockmarks like depression on seafloor (fig 3.31) Previously they have been interpreted as formed by Icerberg (Bellec et al., 2008) or, it could be formed as a result of gas expulsion on the seafloor (Hovland 1981, 1982).Pockmarks appears as circular, elliptical depression formed when the fluid migrate up through the sediment at the seafloor. Pockmarks may have connection with fault providing conduits pathway for fluid flow (Ligtenberg., 2005). On seismic data, it appears as depression on seafloor (Løseth et al., 2009)

There are interesting high amplitude anomalies within the gas chimneys and they appear to be presented at the top of chimneys zone (fig 3.25, 3.26, 3.28, 3.29 and 3.30) interpreted previously as gas bearing sediment (Løseth et al., 2009).These gas bearing high amplitude anomalies represent permeable layer enriched with gas or these high amplitude anomalies could be possible explained by the lithological changes. The disturbed area within the gas chimneys indicates migration of fluid flow and filling proves are currently occurring

The cross cutting high amplitude anomalies occurs top of gas chimneys could indicates presence of gas hydrate (Laberg et al., 1996) or it could be resulted from change in diagenetic property of sediment that cross cut the bedding plane. High amplitude anomalies could be caused by presence of acoustic masking (low velocity zone) which indicates

presence of free gas that are migrating upward and accumulated in shallow part of subsurface.

Seismic reflections of anomalously high amplitude are mainly common on western part of study area including western part of Loppa High and in Hammerfest basin (fig 3.25, 3.26, 3, 27, 3.28 and 3.29). High amplitude anomalies are generally regarded as direct hydrocarbon indicator as it provide indication of gas accumulation within the pore spaces of sediments as compared to surrounding reflector. It implies that gas may be accumulated within shale or silt/sandstone. High amplitude anomalies are described in terms of Bright spot, Dim spots, Flat spot, and Phase reversal on seismic data. In most cases, pronounced seismic masking characterize the area below the high amplitude anomalies which could be resulted from vertical migration of fluid that have caused the velocity reduction on seismic data

4.4 Source of fluid flow

The following discussion concentrates on explaining the potential source for fluid flow features in the study area.

The source of hydrocarbon will be discussed based on thermal gradient and potential hydrocarbon windows. The temperature ranges at which oil and gas generated varies with kerogen type, timing and several other factors (Perrodon, 1983). Typical range for oil windows varies from 65 °C to 150°C and for gas window (100°C to 200°C) and thermal gradient in Sørvestsnaget Basin based on Well 7216/11-1S is 30.5 °C /1000m (NPD).so based on these assumed values oil windows lies at the range of 2200-5000m (TWT) and the gas window at the range of 3300-6500m (TWT).

The dark marine shales of late Jurassic Hekkingen formation, deposited during restricted marine condition, are considered as the most promising source rock in the western Barents Sea (Larsen et al., 1993) and it is thought to be mature for oil and gas generation in a narrow belt at the western margin of the Hammerfest Basin and along the western fringe of the Loppa High (Doré, 1995; Henricksen et al., 2011). But on the western part of study area, it is unoften unmapped since it is too deep. Even Cretaceous sediment reach down to more than 4500-5000 ms (TWT) (Ryseth et al., 2003). Source rock will most probably be in

range of the gas window or overmature so there could be possibility that fluid migrated from source rock of early Aptian age (NPD). In addition to this the majority of well drilled in Hammerfest Basin, Troms-Finnmark Platform, Loppa High and Senja Ridge have oil shows in Lower Cretaceous strata (Knurr and Kolje formation). (Seldal , 2005)

On western part of Loppa High, Hekkingen formation is eroded due to the uplifting process so the question is from where fluid is originated? To answer this question, Snadd formation unit was mapped as it is potential source and reservoir rock (NPD) so it has been suggested that fluid might be originated from Snadd formation.

The presence of Snadd formation on western part of Loppa High can be promising source and reservoir rock (Johansen et al., 1995; NPD).The reservoir potential of Snadd formation is generally better even though it has generally high primary content of fine-grained material which could be enhances as a result of removal of overburden during uplifting of Loppa High. This has been proved by several well speculating best reservoir rock within Triassic. In addition to this, Ladinian marine and prodeltaic shale within Snadd formation has a reasonable gas/oil potential with HI values of 400- 500 mg/Gtoc. However significant source rock are also found in rocks of Olenekian to Ladinian (Henriksen et al., 2011b)

4.5 Mechanism and geological process leading to fluid flow formation

It is important to understand mechanism of fluid flow and their subsurface expressions. Fluids can be migrate as a result of diffusion process, solution of gas in pore water and along zone of weakness (Fault plane).There are certain mechanism and geological phenomenon that provides the driving force for the migration of fluids. Fracture flows are common in consolidated sediments and occur along a spatially limited set of fractures within fault zone, in hydrofractures above highly overpressured reservoirs. Fracture flow is often episodic. Fluid flow in fractured seal can be high during short-lived expulsion events and can therefore empty hydrocarbon filled trap in relatively short period of geological time (Løseth et al., 2009). Pressure buildup beneath URU would breach the sealing sequence and acts as seal bypass system (Cartwright et al., 2007) that could transport gas during short lived expulsion events.

Darcy flow is very low and almost negligible as compared with fracture flow and is used to describe linear flow within permeable sediment. Diffusion is defocused leakage mechanism that tends to lie over larger zone of hydrocarbon filled trap expressed as lateral continuous seismic anomalies on seismic data. Leakage through this mechanism have generally very low flow rate (Løseth et al., 2009)

In the nearby Bjørnøya Basin, bordering Veslemøy High to the north, most gas and gas hydrate accumulations are located immediately above or in the vicinity of large faults (fig 3.27) (Laberg and Andreassen, 1996). The Bjørnøyrenna Fault Complex, bordering Veslemøy High to the north-east and east shows similar features including indications for the presence of gas hydrates causing a BSR on seismic data (Andreassen et al., 1990; Chand et al., 2012 ; Andreassen et al., 1990). The BSR in main area is reported to result from underlying free gas which probably explains the zone of low interval velocity (Acoustic masking) beneath the BSR. A similar association was found by Andreassen et al. (1990) south of the Bjørnøya Basin, where the profound acoustic masking found above faults probably was related to thermogenic gas which had leaked along faults. The location of the faults was assumed to be the principle control on the geographical location of free gas in the area (Andreassen et al., 1990). Acoustic Masking beneath the BSR results from thermogenic gas that had been leaked from larger fault complex called Bjørnøyrenna fault complex in the area (Laberg & Andreassen .1996).

In southern Bjørnøya area, the presence of several high amplitude anomalies (fig 3.25, 3.36 and 3.27) indicates enrichment of free gas at different stratigraphic level .Interestingly there is a Triassic sequence that overlying the fault complex appears to acts as stratigraphic trap. It is interested to note that most of fluids haven't reach above the level of Torsk formation suggesting an age of fluid leakage which could happen not later than Cenozoic time.

Hydrocarbon in the fluid migration system may have been trapped in reservoir formation within Tromsø Basin and Hammerfest Basin and sealed over longer period of time. Hydrocarbon leakage into Cenozoic sediment has been documented in several areas (Solhiem & Elverhoi, 1985, 1993; Lammers et al., 1995) and probably resulted from significant erosion of the Barents shelf of up to 1 km (Nydan et al., 1992) which in turns has caused the change in pressure within the reservoir rocks and resulted in expansion of gas. Several episodes of uplifting and erosional process from Paleocene until the Plio-

Pleistocene have caused redistribution of hydrocarbon over larger distance in the Barents Sea region (Doré. & Jensen 1996). Post uplifting and erosional process led to the decrease in the temperatures that have ceased the hydrocarbon generation (Ohm et al., 2008). Other likely mechanisms leading to hydrocarbon migration can be related to the reservoir tilting and gas expansion. Differential sedimentation caused differential subsidence results in tilting of underlying reservoir rock and with the removal of overburden can caused pressure change within underlying hydrocarbon reservoir results in expansion of gas causing gas and/or oil to spill put of reservoir rock.

Fluids tend to migrate either vertically or laterally depending upon the geological setting of an area. BTU is characterized by lateral movement of fluids from Sørvestsnaget Basin to western flank of Loppa High where it is truncated by URU (fig 3.7 and fig 3.27). The major focus here is on the distribution of the vertical fluid flow features (fig 3.25, 3.26, 3.27, 3.28 and 3.29). Vertical migration pathways of fluids are mostly described as gas chimneys which are prevalent randomly in my study area (fig 3.25, 3.26, 3.27, 3.28 and 3.29). Analysis of chimney structures can, with other geological knowledge, provide relevant information regarding sealing quality of faults, indications of possible charging reservoirs and indication of possible spillage or leakage from these reservoirs (Ligtenberg, 2003). By consequence, the chimneys are the result of an overpressure that has led to the fracturing of the overburden sediments and to the propagation of the fracturing front until overpressures ceased or until another cap rock was reached. The overpressure can be caused by some of the processes outlined above.

Some of the gas chimneys are interestingly related with faults (fig 3.32, 3.33, 3.34 and 3.35) which provide migration pathways for fluids into shallower part of the subsurface and it may also be possible that faults may also be present within chimneys structure but due to the acoustic masking, identification of these faults is only possible by juxtaposition from outside the chimney structure. Some of these faults are leading into the chimneys with different orientation working as a conduits pathway with chimneys structures acts as reservoir feeder for these faults. The faults observed appear to be especially susceptible to act as vertical fluid migration pathways, due to their location in relation to the chimney structures. This could happen during the reactivation of fault during uplift and erosion of Loppa High.

In the study area, high amplitude, progradational, clinoformal geometric patterns characterized the Tertiary sediments on the western part of the Loppa High area (fig 3.22). For example, BTU is characterized by random distribution of high amplitude anomalies. BTU is the result from an uplift of Loppa High which acts as a main sediment source during Eocene to mid Miocene (Vorren et al., 1991). The distribution of high amplitude anomalies in BTU is interpreted as free gas that supposedly migrated from deeper part of the adjacent basins middle Eocene sediment consists of sandstone and shales (Ryseth et al., 2003) which could be favorable for lateral migration of fluids that provided permeable sandstones are laterally interconnected on large scale. Fluid may laterally flow at top of interconnected permeable beds or fluids may migrate vertically through faults from deeper stratigraphic levels until they joined lateral migration pathways of Tertiary sediments. Most of the fluids accumulated beneath the URU which acts as a seal for hydrocarbon migration suggesting that the migration process might have taken place after the deposition of Torsk formation. Continued accumulation of fluids beneath URU might eventually lead to overpressure and vertical migration through the glacial sediments as nicely exemplified at the Veslemøy High area (Pless, 2009)

Faults are the main conduits for fluids in many basins worldwide, especially in the deeper subsurface where sediment become more consolidated or completely vitrified (Ligtenberg., 2003; 2005). Fault cores often act as a conduit for fluid flow during deformation but then become cemented and sealed due to increasingly low permeability (Caine et al., 1996). If, however, the faults become reactivated it is more likely that they act as a conduit to fluid flow (Caine, 1996) Regional tectonics often play an important role in the leakage systems of reservoirs (Ligtenberg and Connolly, 2003). Faults are related to acoustic interference and it provides conduits pathway for fluid migration thus acting as a seal bypass system (Cartwright et al., 2007) and previous research has demonstrated a very close relationship between faults and fluid flow (Andreassen et al., 2007b; Chand et al., 2008; Chand et al., 2009). Migration along the faults seems to be an important fluid migration pathway in the study area. Faults acts as both seal and pathway for hydrocarbon accumulation. Fault zone may contains interconnected fractures but seismic data cannot image the inner details of it. The faults observed appear to be especially susceptible to act as vertical fluid migration pathways, due to their location in relation to the chimney structures. This could either have

happened through originally leaking faults or during the reactivation of faults during uplift or/and erosion, in connection with the Plio-Pleistocene glaciations.

Migration of fluid along the fault plane tends to follow columnar flow pattern suggesting concentrated flow along fault plane (fig 3.31). Whereas some of the fluid flow pathways are located in the central part of fault plane or along the weak zone within the fault plane, a change in the dip of the fault or bend of the fault could be related with diapirism process by enhancing local pressure for initiation and development of related chimneys. (Ligtenberg., 2005)

All observations are summarized in a conceptual model. The conceptual model will mainly focus on regional correlation of major interpreted horizons and their relationship with fluid flow features. The model is based on a long geoseismic profile running from Veslemøy High to Sørvestsnaget Basin, four different horizons shows the general depositional pattern on SW part of Barents Sea (fig 4.8). Torsk formation (yellow horizon) which is of Paleocene to Eocene in age shows apparent thickening in Sørvestsnaget basin as compared to Vaslemøy High. Bottom Tertiary Unit (BTU) which is indicated by pink horizons showing onlapping toward the fault at the depth of around 3.5 s (TWT). BTU on geoseismic profile showing thickening in Sørvestsnaget Basin as compared to Vaslemøy High.

Like Torsk formation, Kolmule formation shown by orange color indicates apparent thickening towards the Sørvestsnaget Basin.

Bottom Cretaceous Unit (BCU) is difficult to interpret (sky blue horizon) due to poor quality of seismic data and is shallow towards the Veslemøy High delineate the Sørvestsnaget Basin to the southeast and southwest.

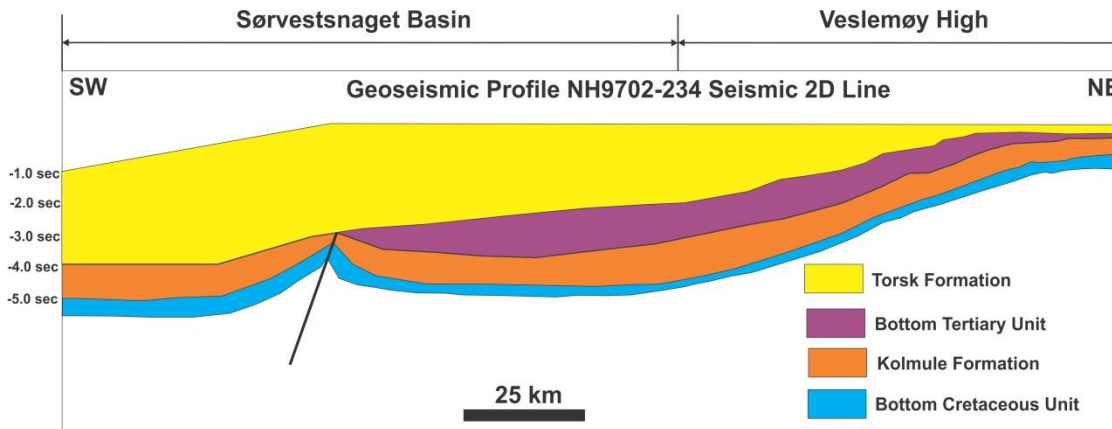


Fig 4.8: Geoseismic cross-section, Sørvestsnaget Basin and Vaslemøy High. The interpreted four horizons shows overall depositional pattern across Vaslemøy High and Sørvestsnaget Basin.

The inferred fluid leakage in the study area assumed to be closely related to the Cenozoic evolution (uplift and erosion) of the Barents Sea (fig 4.9), where gas expansion due to removal of up to 1 km of sediments from the Barents shelf and/or reservoir tilting during the late Cenozoic glaciations (Laberg and Andreassen, 1996). It is difficult to estimate whether reservoir was filled before the late Cenozoic uplift and erosion. There is hypothesis that both oil and gas were present in the reservoir at first, but due to the uplifting process oil leaked from the reservoir and as a result of that gas was expanded during this process. It could also be speculated that due to the reactivation of these fault during uplifting and erosional process, hydrocarbon leaked out of the reservoir rock and as a result of that process, accumulation of gas, high amplitude anomalies has been observed beneath the Upper Regional Unconformity (URU). Furthermore, recent published literature suggests an even more rapid deglaciation of the Barents Sea ice sheet than previously assumed (Laberg et al., 2011 and Knies et al., 2009). The rapid deglaciation would lead to a sudden pressure decrease, which enforces the theory for sudden gas expansion, causing fracturing and migration. The migrating fluids are assumed to originate from both already accumulated reservoirs (secondary migration) and generated from source rock

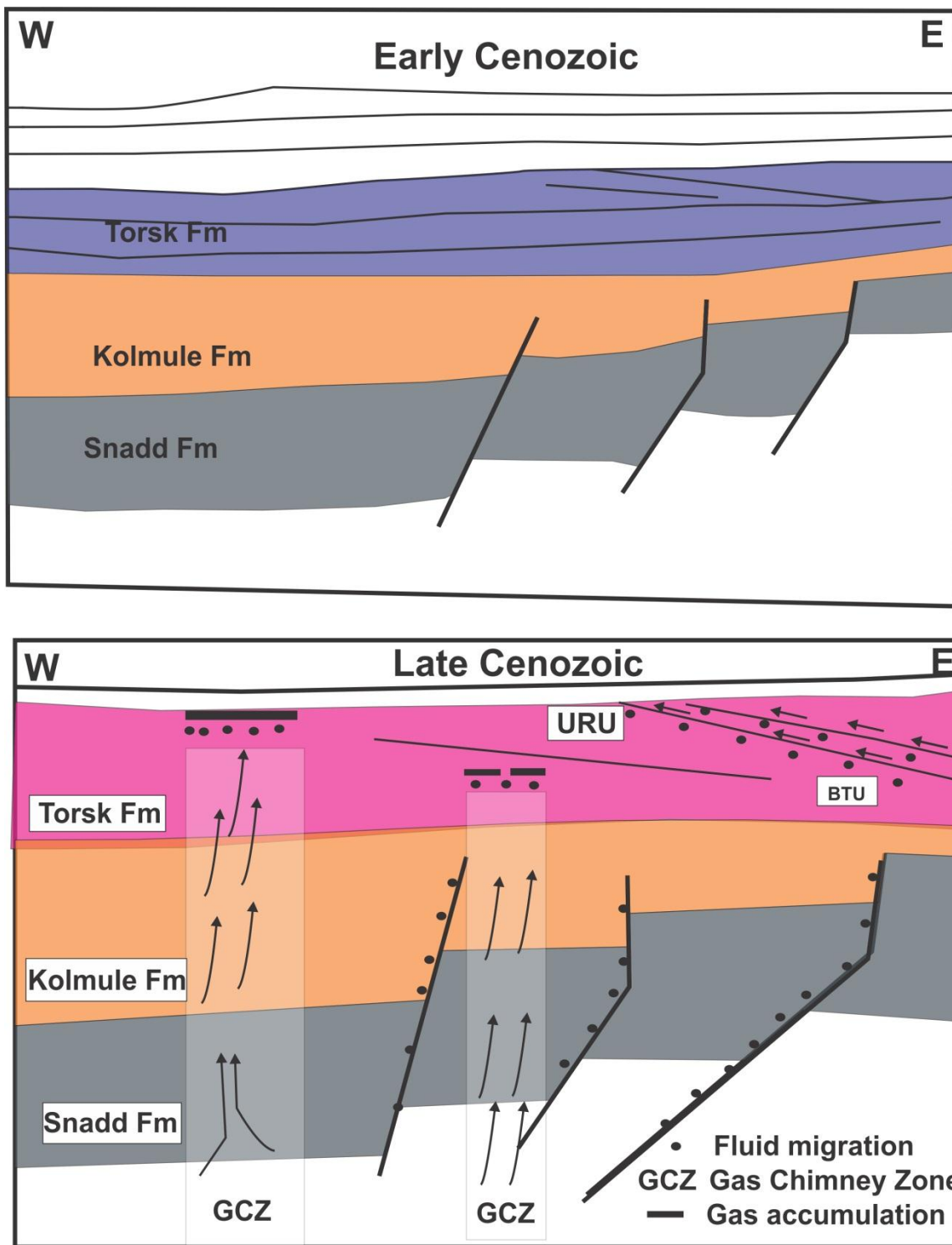


Fig 4.9: illustrating interpreted sketch of the situation within the study area in early and late Cenozoic, due to profound erosion. Not to scale. White shaded area affected by acoustic masking.

5. Conclusion

The Master thesis is based on interpretation of 2D seismic data with a focus on regional stratigraphy with relationship to fluid flow systems in SW Barents Sea. The main conclusion from this work is:

- Torsk and Kolmule formation shows westward progradational depositional pattern that could have been derived from erosion of Stappen High and Loppa High during relative sea level fall.
- Most of the major depositional unit eroded around the western flanks of Loppa High due to tectonic uplift.
- The Sørvestsnaget Basin acts as main depo-center for the majority of the eroded sediments in study area.
- Fluid flow features are abundant and widespread in SW Barents Sea with gas chimneys being the most dominant fluid flow features.
- Distribution of fluid flow features shows direct relationship with structural elements of SW Barents Sea. The geographic distribution of chimneys seems to be controlled by major fault boundaries.
- Gas Chimneys in study area mainly result from vertical migration of gas through micro-fractures which causes an irregular compressional velocity response which leads to scattering and attenuation of the reflected seismic wave causing that large areas are acoustically masked.
- None of the large chimneys terminate at the seabed. Torsk and Kolmule formations acts as a cap rock for fluid flow features whereas Upper Jurassic Hekkingen formation is the most widespread source rock in study area. In addition to this, the lower Cretaceous unit has been reported for significant oil show. Snadd formation can potentially be a source and reservoir rock (NPD)
- Shallow gas accumulations mostly occur at the top part of gas chimneys characterized by reverse polarity and high reflection amplitudes.

- BSR-like anomalies sub-parallel the seafloor occur as patchy reflections above the inferred gas leakage from deeper source. This indicates the presence of gas hydrates within sediments of the SW Barents Sea.
- Tectonic activity and glaciation process together with net erosion could have a great impact on timing and leakage of fluid flow features in study area

Reference

Abrams, A. M., 2005. Significance of hydrocarbon seepage relative to petroleum generation and entrapment: *Marine and Petroleum Geology*, v. 22, p.457-477.

Al-Zoubi, A., and Ten Brink, U.S., 2001, Salt diapirs in the Dead Sea Basin and their relationship to Quaternary extensional tectonics: *Marine and Petroleum Geology*, v. 18, p. 779–797, doi: 10.1016/S0264–8172(01)00031–9.

Andreassen, K., Hogstad, K., and Berteussen, K. A., 1990, Gas hydrate in the southern Barents Sea, indicated by a shallow seismic anomaly: *First Break*, v. 8, no. 6, p. 235-245.

Andreassen, K., 2009, *Marine Geophysics. Lecture notes for GEO-3123. University of Tromsø.*, p. 106.

Andreassen, K., Ødegaard, C. M., and Rafaelsen, B., 2007b, Imprints of former ice streams, imaged and interpreted using industry 3D seismic data from the south-western Barents Sea: *Application to Hydrocarbon Exploration and Production. Special Publication*, v. 277, no. Geological Society, London, p. 151-169

Aydin, A., 2000, Fractures, faults, and hydrocarbon entrapment, migration and flow: *Marine and Petroleum Geology*, v. 17, p. 797-814.

Bellec, V. et al., 2008. Bottom currents interpreted from iceberg ploughmarks revealed by multibeam data at Tromsøflaket, Barents Sea. *Marine Geology*, 249(3-4): 257-270.

Breivik, A.J., Gudlaugsson, S.T. and Faleide, J.I., 1995. Ottar-Basin, SW Barents Sea – a major Upper Paleozoic rift basin containing large volumes of deeply buried salt. *Basin Research*, 7, 299-312.

Brown, K.M., 1990. The nature and hydrogeologic significance of mud diapirs and diatremes for accretionary systems, *Journal of Geophysical Research*, v95, pp 8969-8982.

Brown, A. R., 1999, Interpretation of three-dimensional seismic data.

Bulat, J., 2005, Some considerations on the interpretation of seabed images based on commercial 3D seismic in the Faroe-Shetland Channel: *Basin Research*, v. 17, no. 17, p. 21.

Caine, J.S., J.P. Evans, and C.B. Forster. 1996. Fault zone architecture and permeability structure. *Geology* 24:1025–1028

Carstens H (2005) Gas found in glacial, shallow sands: *GeoExPro. Geosci Technol Explained* 4:24–25 <http://www.geoexpro.com>

Cartwright, J. & Huuse, M., 2005: 3D seismic technology: the geological “Hubble”. *Basin Research* 17, 1-20.

Cartwright, J., Huuse, M., and Aplin, A., 2007, Seal bypass systems: *AAPG Bulletin*, v. 91, no. 8, p. 1141-1166.

Chand, S., Mienert, J., Andreassen, K., Knies, J., Plassen, L., and Fotland, B., 2008, Gas hydrate stability zone modelling in areas of salt tectonics and pockmarks of the Barents Sea suggests an active hydrocarbon venting system: *Marine and Petroleum Geology*, v. 25, p. 625-636.

Chand, S., Rise, L., Ottesen, D., Dolan, M. F. J., Bellec, V., and Bøe, R., 2009, Pockmark-like depressions near the Goliat hydrocarbon field, Barents Sea: Morphology and genesis: *Marine and Petroleum Geology*, v. 26, p. 1035-1042

Chand, S., Thorsnes, T., Rise, L., Brunstad, H., Stoddart, D., Bøe, R., Lågstad, P., Svolsbru, T., 2012. Multiple episodes of fluid flow in the SW Barents Sea (Loppa High) evidenced by gas flares, pockmarks and gas hydrate accumulation: *Earth and Planetary science letters* 331-332 (2012) 305-314.

Dahl, P., 2011, Fluidmigrasjon og akkumulasjon på Loppahøyden i sørvestlige deler av Barentshavet: Unpublished cand. scient. thesis, v. University of Tromsø, p. 99.

De Groot, P., 2001. Seismic expression of hydrocarbon accumulations and seeps ESF workshop Delft, August 2001

Dengo, C.A. and Røssland, K.G., 1992. Extensional tectonic history of the western BarentsSea. In: Larsen, R., Brekke, H., Laresen, B. and Talleraas, E. (Eds.), Structural and tectonicmodelling and its application to petroleum geology. Elsevier, Amsterdam, pp. 91-107.

Dimakis, P., Braathen, B.I., Faleide, J.I., Elverhøi, A. and Gudlaugsson, S.T, 1998. Cenozoic erosion and the preglacial uplift of the Svalbard-Barents Sea region. *Tectonophysics*, 300,311-327.

Doré, A. G., and Gage, M.S 1987. Crustal alignment and sedimentary domain in the evolution of North Sea, North-east Atlantic margin and Barents shelf. In Brooks, J. & Glennie, K. (Eds), *Petroleum geology of Northwest Europe*, Graham and Trotman, London, 1131-1148.

Dore, A. G., 1995, Barents Sea Geology, Petroleum Resources and Commercial Potential: *Arctic*, v. 48, no. 3, p. 207-221.

Doré, A. G., and Jensen, L. N., 1996, The impact of late Cenozoic uplift and erosion on hydrocarbon exploration: offshore Norway and some other uplifted basins: *Global and Planetary Change*, v. 12, no. 1-4, p. 415-436

Dowdeswell, J.A.,Villinger,H., Whittington, R. J., and Marienfield, P.,1993.Iceberg scouring in Scoresby Sund and on East Greenland continental shelf. *Marine Geology*, 111:37-53.

Dowdeswell, J.A., Bamber, J.L., 2007. Keel depths of modern Antarctic icebergs and implications for sea-floor scouring in the geological record. *Mar. Geol.* 243,120–131.

Elvebakk, H., Rønning, J.S., Jochmann, M., Henningsen, T., Johannessen, E.P., Bering, D. & Elvebakk, G. 2008: Geophysical borehole logging in Dh 10-2008 at Sysselmannbreen, Svalbard. NGU Report 2008.090, 45 pp (confidential).

Faleide, J.I., Gudlaugsson, S.T. and Jacquart, G., 1984. Evolution of the western Barents Sea. *Marine and Petroleum Geology*, 1, 123-150.

Faleide, J.I., Vågnes, E. and Gudlaugsson, S.T., 1993a. Late Mesozoic-Cenozoic evolution of the southwestern Barents Sea. In: Parker, J.R. (Ed.), *Petroleum Geology of Northwest Europe*, Proceedings of the 4th conference. The Geological Society of London, London, pp. 933-950.

Faleide, J.I., Vågnes, E. and Gudlaugsson, S.T., 1993b. Late Mesozoic-Cenozoic evolution of the south-western Barents Sea in a regional rift-shear tectonic setting. *Marine and Petroleum Geology*, 10, 186-214.

Faleide, J.I., Solheim, A., Fiedler, A., Hjelstuen, B.O., Andersen, E.S. and Vanneste, K., 1996. Late Cenozoic evolution of the western Barents Sea-Svalbard continental margin. *Global and Planetary Change*, 12, 53-74.

Faleide, J.I., Tsikalas, F., Breivik, A.J., Mjelde, R., Ritzmann, O., Engen, O., Wilson, J. and Eldholm, O., 2008. Structure and evolution of the continental margin of Norway and Barents Sea. *Episodes*, 3, 82-91.

Faleide, J.I. and Petrobar Team, 2009. Crustal architecture and basin evolution in the Barents Sea. *Geophysical Research Abstracts*, Vol 11, EGU2009-12236, 2009.

Gabrielsen, R., Færseth, R.B., Jensen, L.N., Kalheim, J.E. and Riis, F., 1990. Structural elements of the Norwegian continental shelf, Part I: The Barents Sea Region. Norwegian Petroleum Directorate Bulletin, 6, 47 pp

Galbraith, M, Hall, M., 1996. Some causes of artifacts in 3-D seismic surveys: Presented at the CSEG Ann Mtg., (Expanded Abstracts, 103-104)

Gartrell, A., Zhang, Y., Lisk, M., Dewhurst, D., 2004. Fault intersection as critical hydrocarbon leakage zone: integrated field study and numerical modelling of an example from the Timor Sea, Australia. *Marine and Petroleum Geology* 21 (2004), p. 1165-1179.

Glørstad-Clark, E., Faleide, J.I. and Nystuen, J.P., 2010. Triassic seismic sequence stratigraphy and paleogeography of the western Barents Sea Area. *Marine and Petroleum Geology*.

Gluyas, J., and Swarbrick, R., 2004, *Petroleum Geoscience*, p. 147-148.

Gudlaugsson, S. T., Faleide, J. I., Johansen, S. E., and Breivik, A. J., 1998, Late Palaeozoic structural development of the South-western Barents Sea: *Marine and Petroleum Geology*, v. 15, no. 1, p. 73-102.

Henriksen, E., Bjørnseth, H.M., Hals T.K., Heide, T., Kløvjan, S.K., Larssen, G.B., Ryseth, A., Rønning, K., Sollid, K. & Stoupakova, A 2011a. Uplift and erosion of the greater Barents Sea: Impact on prospectivity and petroleum systems.

Henriksen, E., Ryseth, A.E., Larsen, C.B., Heide, T., Rønning, K., Sollid, K., 2011b, Tectonostratigraphy of the greater Barents Sea. Implications for petroleum systems: In press.

Heggland, R. (1998) Gas seepage as an indicator of deeper prospective reservoirs. A study based on exploration 3D seismic data. *Mar. Petrol. Geol.*, 15, 1-9

Heggland, R., Hovland, M., Graue, K., Gallagher, J.W., 2001. Mud volcanoes and gas hydrates on the Niger Delta Front (Abstr.). Abstract Book, Conf., Subsurface Sediment Mobilisation. University of Gent, Belgium, p. 44, September.

Heggland, R. (2003). Vertical Hydrocarbon Migration at the Nigerian Continental Slope: Applications of Seismic Mapping Techniques..AAPG conference, Salt Lake City

Hovland, M., and Judd, A., 1988, Seabed pockmarks and seepages : impact on geology, biology and the marine environment

Hugo Ahlenius, UNEP/GRID-Arendal 2012. www.grida.no

Johansen, S.E., Gudlaugsson, S.T., Svånå, T.A. and Faleide, J.I., 1994. Late Paleozoic evolution of the Loppa High, Barents Sea. Part of unpublished PhD thesis, University of Oslo, Oslo, 25 pp.

Judd AG, Hovland M 1992. The evidence of shallow gas in marine sediments. Cont Shelf Res 12:1081–1095.

Knies, J., Matthiessen, J., Vogt, C., Laberg, J.S., Hjelstuen, B.O., Smelror, M., Larsen, E., Andreassen, K., Eidvin, T., and Vorren, T.O., 2009, The Plio-Pleistocene glaciations of the Barents Sea–Svalbard region: A new model based on revised chronostratigraphy: Quaternary Science Reviews, v. 28, p. 812–829, doi:10.1016/j. quascirev.2008.12.002

Knutsen, S. M., Skjold, L. J., and Skott, P. H., 1992. Palaeocene and Eocene development of the Trosjø Basin - sedimentary response to rifting and early sea-floor spreading in the Barents Sea area: Norsk Geologisk Tidsskrift, v. 72, p. 191-207.

Knutsen, S. M., and Larsen, K.I., 1996. The late Mesozoic and Cenozoic evolution of the Sørvestsnaget Basin: A tectonostratigraphic mirror for regional events along the Southwestern Barents Sea Margin? Marine and Petroleum Geology. Vol. 14, No. 1. pp. 27-54.

Knutsen, S-M., Augustson, J.H. & Haremo, P.2000. Exploring the Norwegian part of the Barents Sea - Norsk Hydro's lessons from nearly 20 years of experience. In: K. Ofstad, J.E. Kittilsen & P. Alexander-Marrack (eds), *Improving the Exploration Process by Learning from the Past*, Norwegian Petroleum Society Special Publications, 9, Elsevier, Amsterdam 99-112

Kristensen, L., 2010, Fluid migration and shallow gas accumulation on the south-western flank of Loppa High, SW Barents Sea: Unpublished cand. scient. thesis, v. University of Tromsø, p. 119.

Laberg, J. S., and Andreassen, K., 1996, Gas hydrate and free gas indications within the Cenozoic succession of the Bjørnøya Basin, western Barents Sea: *Marine and Petroleum Geology*, v. 13, no. 8, p. 921-940.

Laberg, J. S., Andreassen, K., and Knutsen, S. M., 1998, Inferred gas hydrate on the Barents Sea shelf — a model for its formation and a volume estimate: *Geo-Marine Letters*, v. 18, no. 1, p. 26-33.

Laberg, J. S., Andreassen, K., and Vorren, T. O., 2011. Late Cenozoic erosion of high-latitude southwestern Barents Sea shelf revisited, *GSA bulletin*; doi: 10.1130/B30340.1;7

Lammers, S., Suess, E., and Hovland, M., 1995, A large methane plume east of Bear Island (Barents Sea): implications for the marine methane cycle: *International Journal of Earth Sciences*, v. V84, no. 1, p. 59-66.

Larsen, R.M., Fjæran, T., and Skarpnes, O. 1993. Hydrocarbon potential of the Norwegian Barents Sea based on recent well results. In: Vorren, T.O., Bergsager, E., Dahl-Stammes, Ø.A., Holter, E., Johansen, B., Lie, E., and Lund, T., eds. *Arctic geology and petroleum potential*. Norwegian Petroleum Society (NPF) Special Publication 2. Amsterdam:Elsevier. 321–331

Larssen, G.B., Elvebakk, G., Henriksen, L.B., Kristensen, S.-E., Nilsson, I., Samuelsen, T.A., Stemmerik, L. and Worsley, D., 2005. Upper Paleozoic lithostratigraphy of the southern Norwegian Barents Sea. Norsk Geologisk Undersøkelser, Bulletin, 444. Geological Survey of Norway, Trondheim, 43 pp. Also available in electronic version at www.npd.no (NPD Bulletin 9, 2002)

Linjordet, A., and Olsen, R.G., 1992, The Jurassic Snøhvit gas field, Hammerfest Basin, offshore northern Norway: Tulsa, Oklahoma, The American Association of Petroleum Geologists, p. 349-370.

Ligtenberg, H., and Connolly, D., 2003, Chimney detection and interpretation, revealing sealing quality of faults, geohazards, charge of and leakage from reservoirs: Journal of Geochemical Exploration, v. 78-79, p. 385-387.

Ligtenberg, J.H., 2003, Unravelling the petroleum system by enhancing fluid migration paths in seismic data using a neural network based pattern recognition technique: Geofluids, v. 3, p. 255-261.

Ligtenberg, H., 2005, Detection of fluid migration pathways in seismic data: implications for fault seal analysis: Basin Research, v. 17, p. 141-153.

Løseth, H., Gading, M., and Wensaas, L., 2009, Hydrocarbon leakage interpreted on seismic data: Marine and Petroleum Geology, v. 26, no. 7, p. 1304-1319.

Lumley, D. (1995), Seismic time-lapse monitoring of subsurface fluid flow, Ph.D. thesis, Stanford University, Stanford, California, USA.

Magoon, L.B., and Dow, W.G., 1994, The Petroleum System,—From source to trap: American Association of Petroleum Geologists Memoir 60, p. 3-24.

Marfurt, K.J., Scheet, R.M., Sharp, J.A., Harpert, M.G. 1998: Suppression of the acquisition footprints from seismic sequence attribute mapping. Geophysics 62, 1774-1778.

NPD., 1988. A lithostratigraphic scheme for the Mesozoic and Cenozoic succession offshore mid- and northern Norway. (Bulletin 4)

NPD., 1990. Structural elements of the Norwegian continental shelf (Bulletin 6)

NPD, 2012, NPD's Fact Pages. <http://www.npd.no/engelsk/cwi/pbl/en/index.htm>.

Nyland, B., Jensen, L. N., Skagen, J., Skarpnes, O. and Vorren, T. O. 1992: Tertiary uplift and erosion in the Barents Sea: magnitude, timing and consequences. In Larsen, R. M., Brekke, H., Larsen, B. T. & Talleraas, E. (eds.): Structural and tectonic modeling and its applications to Petroleum Geology, 153-162. Elsevier, Amsterdam.

O'Brien, G.W., Quaipe, P., Cowley, R., Morse, M., Wilson, D., Fellows, M., and Lisk, M., 1998, Evaluating trap integrity in the Vulcan Sub-basin, Timor Sea, Australia, using integrated remote sensing geochemical technologies. In: Purcell, EG., Purcell, R.R. (Eds.), The Sedimentary Basins of Western Australia 2: Proceedings West Australia Basin Symposium, Perth, Western Australia, 1998, p. 237-254

Ohm, S. E., Karlsen, D. A., and Austin, T. J. F., 2008, Geochemically driven exploration models in uplifted areas: Examples from the Norwegian Barents Sea: AAPG Bulletin, v. 92, no. 9, p. 1191-1223.

Perrodon, A., 1983. Dynamics of oil and gas accumulations. Elf-Aquitaine, Pau, 368 pp.

Pless, G., 2009. Occurrence of free gas and focused flow systems in the Veslemøy High area, SW Barents Sea. Unpublished Master thesis, v. University of Tromsø. p.137

Rasmussen, E., Skott, P.H. & Larsen, K-B. 1995. Hydrocarbon potential of the Bjørnøya West Province, western Barents Sea Margin. In: S. Hanslien (ed), Petroleum Exploration and Exploitation in Norway. Norwegian Petroleum Society Special Publications, 4, Elsevier, Amsterdam, 277 - 286.

Riis, F., Vollset, J. and Sand, M. (1986). Tectonic development of the western margin of the Barents Sea and adjacent areas. In: *Future Petroleum Provinces of the World* (Ed. M. T. Halbouty), Am. Assoc. Petrol. Geol. 103, 15-51.

Ritzmann, O. and Faleide, J.I., 2007. Caledonian basement of the western Barents Sea. *Tectonics*, 26, 417-435.

Ryseth, A., Augustson, J.H., Charnock, M., Haugerud, O., Knutsen, S.-M., Midbøe, P.S., Opsal, J.G., and Sundbø, G., 2003, Cenozoic stratigraphy and evolution of the Sørvestnaget Basin, Barents Sea: *Norwegian Journal of Geology*, v. 83, p. 107-130

Schlumberger, 2011, *Seismic interpretation and visualization*, Petrel 2010.

Seldal, J., 2005, Lower Cretaceous: the next target for oil exploration in the Barents Sea?: *Petroleum Geology Conference series 2005*, v. 6, p. 231-240. Selley, R. C., 1998, *Elements of Petroleum Geology* (2.ed.), no. 2. ed.

Selley, R. C., 1998, *Elements of Petroleum Geology* (2.ed.), no. 2. ed.

Sheriff, R., and Robert, E., 1995, *Exploration seismology*.

Skjold, L.J., van Veen, P.M., Kristensen, S.E. and Rasmussen, A.R., 1998. Triassic sequence stratigraphy of the southwestern Barents Sea. In: de Graciansky, P.-C., Hardenbol, J., Jacquín, T. and Vail, P.J. (Eds.), *Mesozoic and Cenozoic sequence stratigraphy of European basins*. Society for Sedimentary Geology, Special Publication, no. 60. Society for Sedimentary Geology (SEPM), Tulsa, pp. 651-666.

Smelror, M., Petrov O.V., Larssen, B.B. and Werner, S., 2009. *Atlas Geological History of the Barents Sea*. Geological Survey of Norway, Trondheim.

Solheim, A., and Elverhøi, A., 1985, A pockmark field in the central Barents Sea; gas from a petrogenic source?: *Polar research*, v. 3, no. 1, p. 11-19.

Solheim, A. and Elverhoi, A. (1993) Gas-related sea floor craters in the Barents Sea Geomarine Letts 13,235-243.

Steel, R. J. & Worsley, D. 1984. Svalbard's post-Caledonian strata - an atlas of sedimentational patterns and palaeogeographic evolution. In: A. M. Spencer (ed), Petroleum Geology of the North European Margin, Graham and Trotman, London, 109 - 135.

Stemmerik, L. & Worsley, D. 1989: Late Palaeozoic sequence correlations, North Greenland, Svalbard and the Barents Shelf. In Collinson, J.D. (ed.): Correlation in Hydrocarbon Exploration, 99-111. Norwegian Petroleum Society, Graham & Trotman, London

Stemmerik, L., 2000. Late Palaeozoic evolution of the North Atlantic margin of Pangea. Palaeogeography Palaeoclimatology Palaeoecology, 161, 95-126.

Tissot, B. P., and Welte, D. H., 1984, Petroleum Formation and Occurrence, Springer Verlag.

Vadakkepuliyambatta, S., S. Bünz, J. Mienert & S. Chand, Giant Gas Chimneys and Gas Hydrate Occurrence in the Southwestern Barents Sea. Extended Abstract, 74th EAGE Conference & Exhibition, 4-7 June 2012, Copenhagen, Denmark, 4pp

Vorren, T. O., Richardsen, G., Knutsen, S.-M., and Henriksen, E., 1991, Cenozoic erosion and sedimentation in the western Barents Sea: Marine and Petroleum Geology, v. 8, no. 3, p. 317-340

Worsley D., Aga O.J., Dalland A., Elverhøi A. and Thon A. 1986. The geological history of Svalbard-evolution of an Arctic archipelago. Stavanger: Statoil

Worsley, D., Agdestein, T., Gjelberg, J.G., Kirkemo, K., Mørk, A., Nilsson, I., Olausen, S., Steel, R.J. and Stemmerik, L., 2001. The geological evolution of Bjørnøya, Arctic Norway: implications for the Barents Shelf. *Norsk Geologisk Tidsskrift*, 81, 195-234.

Wikipedia, 2011, www.wikipedia.org.

Zhang, L., Luo, X., Vasseur., Yu, C., Yang, W., Lei, Y., Song, C., Yu, Lan and Yan, J., 2011. Evaluation of geological factors in characterizing fault connectivity during hydrocarbon migration: Application to the Bohai Bay Basin. *Marine and Petroleum Geology* 28 (2011), 1634-1647.